BIOPHYSICAL SOURCE MODELING OF SOME EXOGENOUS AND ENDOGENOUS COMPONENTS OF THE HUMAN EVENT-RELATED POTENTIAL

Thesis by

K. Jeffrey Eriksen

In Partial Fulfillment of the Requirements

for the Degree of

Doctor of Philosophy

California Institute of Technology

Pasadena, California

1984

(Submitted March 16, 1984)

ACKNOWLEDGMENTS

I wish to begin by thanking my parents, who managed to provide the proper environment for the seeding and growth of my special interests in science, singing and nature. The rest of my family deserves thanks for their uncritical support and encouragement throughout my undergraduate and graduate career.

I owe a special debt to two teachers who challenged me in high school. One was Murray Anderson, who provided me with the mathematical rigor that helped get me into Caltech and keep me here. The other was Don Campbell who nurtured in me an awareness of societal concerns. My thanks to the various professors at Caltech who introduced me to the many fascinating worlds of science and scientific research that exist here. I must have sampled them all.

I owe a special thanks to Olaf Frodsham and the Caltech Glee Clubs, the theatre arts program, and the Caltech Y. Without them, my life here would have been devoid of music, play, and companionship, and I doubt I could have succeeded in my studies.

I am forever indebted to Dr. Derek Fender for helping me return to Caltech for graduate studies, in a field of research that he pioneered and that I was and still am very interested in. I am grateful for the opportunity to work with him and only wish we could have had much more time for discussions, as his are always both stimulating and clarifying.

I wish to acknowledge the fine technical and scientific talents of Dr. Jim Ary, who could always solve, or make suggestions to solve, those problems that come up in experimental research. I also wish to thank Dr. Terry Darcey for the massive legacy of software that he wrote, which was used extensively in this thesis.

For financial support, I thank the Boeing Company who provided my National Merit Scholarship during my undergraduate career. I thank Caltech for making loan money available throughout my Caltech career. And I thank the National Institutes of Health for the National Research Service Award that supported me through most of my graduate career.

For programming and word-processing assistance, both during the last few years and especially in the final hours, I wish to thank the programming staff, especially Edith Huang and Kiku Matsumoto, who were both knowledgeable and helpful. For last minute general assistance in preparing this document, I also thank our secretary Susan Barrett.

Last, and most important, I thank my wife, Kathy, who was instrumental in providing the impetus for the final preparation of this thesis. She worked closely with me to prepare most of the figures, set the equations, type parts of the manuscript and provide stylistic critiques. I dedicate this work to her in recognition of her hard work in helping me complete it and the love and concern she holds for me.

ABSTRACT

Methods of dipole localization were applied to human scalp-recorded electrical activity associated with a simple auditory cognitive discrimination task.

Human neuroanatomy and neurophysiology were reviewed from a biophysical standpoint in order to describe the probable neurogenesis of electrical activity in the brain and on the surface of the head. Topographic electroencephalography (EEG) analysis and source localization methods were historically reviewed in detail, followed by a brief review of the history of non-invasive evoked potential (EP) and magnetic field measurements of human central nervous system activity.

Four well known simple cognitive tasks were considered that were known to elicit non-obligatory brain responses, and the odd-ball task chosen. Three subjects listened to a series of two tones, one frequent and one rare, and counted the rare tones. During task performance, 40 to 48 channels of EEG activity were recorded from their scalps.

From the EEG data, average evoked potentials (aEP) were calculated for the frequent and rare conditions. From these a difference response was calculated. All three of these EPs were plotted as equipotential maps over a schematic of a head for topographic display and the major distribution features discussed. These aEPs and maps matched those previously reported in the literature.

From estimates of the spatial electrical power over the head, four peak components were selected for analysis by equivalent source modeling (ESM). These were designated the FP40, FP100, FP200, and FP350, where FP stands for field power. ESM demonstrated that one centrally located point dipole or two bilaterally symmetric dipoles could model the empirical data quite well. These results were discussed in relation to other topographic studies, as well as

studies of intracranial recordings, lesions, and animal models. The source locations found were consistent with auditory cortical locations for the obligatory sensory peaks (FP40, FP100, FP200) and with brainstem locations as the source of the FP350 cognitive event-related peak.

TABLE OF CONTENTS

LIST OF FIGURES

NOMENCLATURE

aEP	average Evoked Potential
CNV	Contingent Negative Variation
EEG	ElectroEncephaloGram
EF	Evoked (magnetic) Field
EKG	ElectroKardioGram
EMG	ElectroMyoGram
EOG	ElectroOculoGram
EP	Evoked (electric) Potential
ERF	Event-Related (magnetic) Field
ERP	Event-Related (electric) Potential
ESM	Equivalent Source Modeling
gaEP	grand average Evoked (electric) Potential
ITI	Inter-Trial Interval
MEG	MagnetoEncephaloGram
MF	Motor (magnetic) Field
MP	Motor (electric) Potential
sEP	single Evoked (electric) Potential
SW	Slow Wave
VEP	Visual Evoked (electric) Potential

1. Introduction

Ever since their initial discovery, "brain-waves" have provided fuel for speculation. The very idea of having an objective, quantitative tool to measure what is going on in one's mind is fascinating, and a little bit scary. After all, our minds are our most private place, the only place where others cannot intrude or spy. Medical practitioners have an obvious need to examine every part of us in order to fix what has gone wrong, as do psychologists. But the potential for good can be turned around. The study of so-called brain-waves, or the EEG, has certainly not reached the stage of sophistication where it can be abused, other than by quacks. But fiction has prepared us for the eventuality. The following is taken from a well-known science fiction classic.

> Hari Seldon was the first to express what afterwards came to be accepted as truth.
>
> "Neural microcurrents," he once said, "carry within them the spark of every varying impulse and response, conscious and unconscious. The brain-waves recorded on neatly squared paper in trembling peaks and troughs are the mirrors of the combined thought-pulses of billions of cells. Theoretically, analysis should reveal the thoughts and emotions of the subject, to the last and least. Differences should be detected that are due not only to gross physical defects, inherited or acquired, but also to shifting states of emotion, to advancing education and experience, even to something as subtle as a change in the subject's philosophy of life."
>
> And now for fifty years, the men of the First Foundation had been tearing at that incredibly vast and complicated storehouse of new knowledge. The approach, naturally, was made through new techniques - as, for example, the use of electrodes at skull sutures by a newly-developed means which enabled contact to be made directly with the gray cells, without even the necessity of shaving a patch of skull. And then there was a recording device which automatically recorded the brain-wave data as an overall total, and as separate functions of six independent variables.

The first half of this extract could fit right into the next chapter of this manuscript. That is probably because the author of this book is no quack but a

respected scientist and author, Isaac Asimov [1951]. For the experimental studies presented here I wish that I actually could have had equipment like that mentioned in the last paragraph above. Instead, I was confined to 20th century methodology. However, I have had the good luck and fortune to be able to utilize the most sophisticated analysis techniques that have so far been developed for the non-invasive study of human brain activity.

Conflict in Asimov's book arises between physicists and psychologists. This thesis, however, presents an attempt to combine the techniques of both in studying simple mental processes non-invasively in normal humans. The contribution from the physicist is the electromagnetic theory that can describe the electrical events produced by biological generators. The contribution from the psychologist is the cognitive theory that attempts to describe the interplay of mental operations.

In the work to be described, the techniques of source localization will be applied to the analysis of scalp evoked electrical potentials in alert, behaving subjects. One advantage of electrical potential recording is that it can now be done quite simply and effectively, while a subject is engaged in a wide variety of tasks. This is a distinct advantage when performing some of the more complicated tasks experimental psychologists design, thus making brain potential recording a valuable adjunct to traditional behavioral studies. Some psychologists now put it on a separate but equal footing with behavioral tests. Certainly it is being used more and more in the assessment of brain function.

The source localization technique is a biophysically meaningful method for parameterizing the electrical events associated with mental activity. Up until now, it has been applied only to the study of the sensory input of the brain to locate and characterize the brain areas that have obligatory responses to

repetitive stimuli. Here I present its first use in the study of simple, non-obligatory responses of the brain that are related to mental operations of a more central nature.

Brain potential recording has had its ups and downs. In the past it has barely kept pace with other techniques used to study the brain. It does have its advantages in certain areas and thus retains its viability. Though we may never achieve the technical wizardry of Asimov's 120th century denizens, we may find in the coming years that "brain-wave" technology has finally found its prime application in the study of higher mental operations.

2. ANATOMY, PHYSIOLOGY, AND BIOPHYSICAL BRAIN MODELING

In order to address the problem of analyzing brain activity with electrical potential methods, several areas of science and engineering must be related. In this chapter I will review some areas of human neuroanatomy, neurophysiology, and biophysics that are relevant to this problem.

2.1 Relevant Functional Human Anatomy

Since we will be measuring macroscopic potentials, we have to consider the macroscopic structures of the brain. To understand the origins of the observed potentials we will also have to consider the microscopic structure of the brain. And to relate the data to brain function, we must consider the anatomy and physiology of several levels of the brain.

2.1.1 Gross View of the Brain

The upper part of Figure 2-1 shows a drawing of the human brain in its casings. The lower part of the figure shows the surface of the brain stripped of all its covering membranes. Various parts of the brain that can be seen with the naked eye are labelled. We shall be primarily concerned with the cerebral cortex, the convoluted outer layer comprising a large percentage of the total brain weight and volume. Upon closer examination, we can see that many parts of the brain can be divided into groups of cells (nuclei) and groups of cell processes (tracts), or some combination of the two. One can find neurons arranged as layers, columns, and amorphous blobs, with axial, radial, planar, and no symmetry. Figure 2-2 shows two examples of layered brain structures, the hippocampus and the lateral geniculate body. The local physical layout of brain structures will greatly affect the type of potentials generated close to and far away from those structures.

2.1.2 Cellular View of the Brain

Like most of the human body, the brain is composed of living cells. Non-cellular components of the brain include blood, cerebral-spinal fluid (CSF), and interstitial fluid, all of which are primarily the same thing filtered in different ways. Cellular components include the cells of the blood vessels and choroid plexus, the glia, and the main constituent of the nervous system, the neurons. The vascular components serve a nutritional support function, and also carry neurohormonal messages. The glia are cells intimately interspersed with the neurons which are thought to provide repair, nutrition, and physical support for the neurons. By their presence, they can affect the operation of the neurons and their resultant current distributions [Kuffler and Nicholls 1976].

The basic functional elements of the brain are the neurons. It has been estimated that the brain contains 10^{10} or 10^{11} nerve cells, or neurons. With this number of elements to deal with, it is fortunate indeed that the brain has structure to it in terms of nuclei and tracts, layers and columns. Otherwise the task of understanding would have proceeded even more slowly than it has to date. Figure 2-3 shows a sketch of various neurons that occur in layers of the cerebral cortex in man. The lower part of the figure shows expanded views of a Purkinje cell from cerebellar cortex and a pyramidal cell from cerebral cortex.

2.2 Electrophysiological Basis of Scalp Potentials

Scalp potentials are theoretically caused by neural activity reaching the surface. I will next trace the mechanisms by which this can happen.

2.2.1 Single Cell

One way of viewing a neuron is as an information processing element. This view, borrowed from computer science, has been applied for quite some time now to the nervous system as a whole. The idea still has much to recommend it,

for there are obvious and measurable ways in which the brain can be said to process information and base subsequent motor behavior on it.

Most neurons seem to be uni-directional in terms of information flow. For a neuron, information takes the form of voltage or time sequences of voltages. Hundreds or thousands of axons can impinge on a neuron, usually over the dendrites or cell body. The information from all these inputs is integrated over time and space by the dendrites and soma and thresholded at the axon, which transmits a graded output voltage or a series of frequency-modulated voltage spikes to the next neuron in the chain.

The voltages produced in and near the neuron by its normal mode of operation give rise to ionic currents that, by virtue of the fact that the brain, head, and indeed whole body is a conductor, flow throughout the surrounding tissue. The primary currents associated with neural activation are usually termed near-field, while the return currents that flow throughout the volume conductor are termed far-field. Near- and far-field current causes electric potential gradients, or voltages, that appear throughout the brain and on the scalp surface. These currents and voltages do not propagate beyond the scalp surface because of the insulating properties of air. Plonsey [1974] has developed expressions for the potentials produced by a single neuron imbedded in a volume conductor. This particular configuration is not of great utility.

2.2.2 Multi-cell

More realistic multiple-neuron structures give rise to modified currents because of constrained pathways and organized cellular orientations. These must be analyzed separately for each geometry. The structure of these groups will greatly influence the macroscopic potentials generated in their vicinity. Some examples to consider are the lateral geniculate nucleus (LGN),

hippocampus, cerebral cortex, cerebellar cortex, optic radiation, optic nerve and the red nucleus. The LGN, hippocampus, cerebellum, and parts of the cortex are all layered structures and can be expected to produce net currents primarily in a direction perpendicular to the planar layers since the cells have long processes in the perpendicular direction. The optic radiation and optic nerve are nerve fiber bundles and can be expected to produce currents in a parallel direction. The red nucleus, part of the reticular activating system, is shaped like a column, but with no particular orientation of cells. It may not produce currents in any preferred direction and thus may not be detectable in the far field. However, it could be seen as a whole entity if it acted as a current source or sink with respect to the rest of the brain for any measurable length of time.

The present view is that far-field potential gradients in the brain are produced primarily by post-synaptic potentials (PSP) and not action potentials (AP) [Wood and Allison 1981, Buchwald 1983]. Thus most scalp potentials should be a result of nerve cell and dendritic activity and not axonal activity. Part of the reason for this may be the transient nature of APs, whose potentials get spatially low-pass filtered over a very short distance. Another part of the reason may be that the currents associated with PSPs are much larger than those associated with APs.

As a general observation, a brain structure that has layering or repetition of subunits, and whose cells can be made to fire in synchrony, will produce far-field potential effects. Almost by their nature, spatially mapped sensory and motor systems have these properties. Structures that are radially symmetric, spatially unorganized, or temporally unsynchronized will not be able to produce strong far-field effects. Many non-sensory systems and structures are like this, including perhaps the reticular activation system, medulla, pons, and basal

ganglia [Truex and Carpenter 1969].

2.2.3 Scalp Potentials

Neuronal current sources can occur in any area of the brain, but whether they can be detected at the scalp surface depends principally on the anatomy of the sources and their surroundings. The folds of the cerebellum and cortex can change the source orientation drastically over a small area. The inhomogeneities between cerebral-spinal fluid, gray matter, white matter, and brain coverings can distort potential distributions. An accurate biophysical model of the brain would have to include these inhomogeneities, along with anisotropies of conductivity among various types of tissue.

The potentials produced by the activity of a particular brain structure can be said to "travel" by volume conduction to all parts of the body. This travel time is negligible in comparison to neural propagation delays [Plonsey 1969]. The skull and scalp, the latter being the tissue covering the skull, have a marked effect on the potentials that are measured on the surface of the scalp. Because the bone of the skull has an electrical conductivity about 80 times less than the brain, not much current will flow out through the skull. The current that would have reached the scalp is thus greatly attenuated and will produce smaller relative potential gradients on the surface of the scalp.

One cannot actually measure potentials, but only potential differences over space or potential gradients. The most common technique is to define one point on the body as the reference point to which the potentials at all other points are to be compared. Then several other sites are chosen as "active" measurement points, and their voltages are recorded as a function of time. Analysis of these voltage vs. time records under experimental variation constitutes the majority of the evoked potential investigations. No ideal reference point exists, however,

that can be guaranteed to be inactive in a volume conductor, as a point at infinity would. Thus recordings of potential at individual sites cannot be directly interpreted, though it is common practice to ignore such referencing difficulties.

Making inferences about the location of the source of scalp surface potential gradients is a tricky business, prone to misinterpretation. An active area of neural tissue near the surface of the brain, say in the cortex, would produce the highest current densities in its immediate vicinity, but the highest potential gradients would not necessarily appear radially outward from the source on the scalp surface. Depending on the source configuration and orientation, one or more areas of peak potential gradient could appear to the side of the radial projection of the source, and others, of varying magnitude, on the opposite side of the head.

Figure 2-4 diagrams a hypothetical situation like this using a small area of cortex near the surface of the scalp, tilted as it might be inside a fissure. Currents produced by this piece of cortex are indicated by dashed lines and the resulting isopotential contours by solid lines. It can be seen that peaks in potential gradient would most likely occur off to the side of the radial projection of the tissue on the scalp surface, thus giving the wrong impression as to its location. In the worst case, with the reference and active inputs of a potential measuring device placed as indicated in the figure, zero potential would be measured directly over the site of the active tissue!

The only way to be sure of properly locating possible neural current sources is to record from an array of measuring sites and study spatial potential differences. In practice this is not always done, with many workers still assuming that sources are located directly underneath recorded potential peaks. These problems of referencing and oversimplified localization can theoretically be

eliminated by biophysical modeling of brain activity.

2.3 Biophysical Brain Modeling

The brain is a physical system, albeit highly complex. As such, it is amenable to physical analysis. Here we will be primarily concerned with electromagnetic theory. Mechanics are not too important when speaking of the neural processing of the brain, unless the brain in question is undergoing some pretty strenuous accelerations. Chemistry is important at a low level in terms of the basic operation of the neural elements, and at a somewhat higher level in terms of gross neurohormonal effects, but it will have to be included at a later date as a refinement. No quantum mechanical effects manifest themselves in the brain, to the best of present knowledge, so only classical electromagnetics will be included here.

Plonsey [1969] has developed equations describing the potential field due to bioelectric sources in a volume conductor assumed to be linear, homogeneous, and isotropic. Using pertinent electromagnetic theory, an expression is derived for the electric scalar potential field arising from generalized impressed current sources. This expression involves complex phasor notation. Plonsey then estimates the relative size of the real and complex terms and concludes on the basis of experimental measures of biological media properties that the potential expression can be reduced to a real one. This is equivalent to stating that the biological media of concern exibit no capacitative or inductive effects. Poisson's equation is derived from this potential expression and presented as the "quasi-static mathematical formulation of the volume-conductor problem,"

$$\nabla^2 \varphi = \frac{-I_v}{\sigma} \tag{2.1}$$

where φ denotes electric potential at a field point, I_v the volume current source

density, and σ the media conductivity. This is the basic starting equation then for most biophysical models of brain and cardiac activity, including those used here. One benefit of this Poisson formulation is its parallel in the study of the electrostatic potential of charges. Solutions to problems in the latter area can thus be applied to the volume conductor case.

2.3.1 Utility of Modeling

Modeling can be described as representing an object or a process in physical or symbolic form. Modeling can be used to study and test hypotheses about complicated systems. A system may be well described, but its behavior under various conditions may be practically impossible to deduce from its description. Other systems may not be well described. Here modeling can help in first simply identifying the system parameters. Man-made structures are examples of the first type of system. A dam, for instance, can be modeled to determine if it could withstand a particular stress. The brain is an example of the latter class. Modeling the brain can allow us to test hypotheses about how the various parts of the brain are configured and work together.

Various disciplines have used a variety of methods to model the brain and its processes. Mathematical psychologists use equations to describe measurable aspects of cognitive phenomena. Psychophysicists use equations for sensory transduction, often partly based on some knowledge of neural organization. Neural modelers on the cellular level use a biophysical description of single neurons [Rall and Shepherd 1968]. Neural modelers on a higher level use very simplified models of single neurons so as to be able to link a lot of them together in a network. The modeling described in this thesis is a biophysical model on a somewhat higher level than the single neuron, representing a section of neural tissue on the order of millimeters or centimeters acting in synchrony.

As with all brain models, compromises have to be made. The modeling in this thesis is not neural modeling, as it includes no information about the structure or processing capabilities of neural elements. Rather it is a model that relates currents in the brain to mental processing.

The history of this type of modeling is short, so a full review will be attempted. First a brief description of multielectrode analysis and display will be given, followed by a history of biophysical modeling of brain macropotentials.

2.3.2 Multi-electrode Topographic Display

For experiments involving only a few measurement sites, visual inspection of evoked potential versus time plots can be sufficient for analysis purposes. Most experiments, however, should use many measurement sites across the head because of the complications of volume conduction, lack of knowledge of individual brain configuration, and lack of knowledge of the complexity of the response or phenomena being studied. Large numbers of recordings then present a problem in analysis and display.

One early attempt to deal with the vast amount of data generated in brain potential recordings was to use a type of pseudo-3D display where one axis was time and one space, or distance across the head [Rémond 1961]. A third dimension was introduced in the form of a topographic representation of the recorded potential using isopotential contour lines. This method has not been used by any other investigators. Unfortunately, it can deal with only one spatial dimension, whereas there are 2 (ideally 3) on the head.

Various display techniques have been described using two spatial dimensions over the head, and a contour, gray, or color scale to indicate potential levels [Allison et al. 1977, Buchsbaum et al. 1982, Dubinsky and Barlow 1980, Duffy et al. 1979, Estrin and Uzgalis 1969, Lehmann 1971, Petsche et al.

1974, and Wilkus et al. 1981]. Time must be indicated by a series of such maps, but our perceptual systems seem to cope with this better than if we had separated one of the spatial dimensions from the other. Motion pictures have even been made of series of maps at Caltech and elsewhere, thus re-introducing the time dimension in a natural way. Such display methods, however, begin to have a very high information content and beg for simplification. They are useful for visual topographic comparison, but not for direct quantitative comparison.

Topographic analysis of brain potentials or brain fields [Barth et al. 1982, Romani et al. 1982, Cohen and Cuffin 1983] can be likened to topographic analysis in meteorology of temperature or pressure levels over the earth's surface. These phenomena, however, have a strong 2D component, with a minor component in the third (radial) dimension in the atmosphere and less so in the depth of the earth. Brain potential analysis could more accurately be compared with seismic exploration in the depth of the earth. Measurements can usually only be made on the earth's surface of waves produced by earthquakes or simulated earthquakes (man-made explosions). Surface topography alone can be complicated and misleading to the novice. Proper analysis requires knowledge or theories of the underlying rock strata, sometimes covering the whole interior of the earth. Similarly, to properly analyze brain topographic data, it must be placed within a framework of knowledge about the interior structure of the brain.

2.3.3 Dipole Methods

One popular method for modeling brain electrical activity is to assume that localized areas of the brain can be simulated by a current dipole, consisting of a current source and a current sink in close proximity, with current flowing from the source to the sink. Brazier [1949] first published a discussion of such a

method. Wilson and Bayley [1950] first published equations describing the electric potential of a dipole in a sphere, which they based on work done almost a century before by Helmholtz [1853]. Shaw and Roth [1955ab] studied some of the theoretical aspects of these equations for use in EEG studies.

Geisler and Gerstein compared theoretical single dipole results to monkey auditory scalp potentials, and added a concentric shell around an inner sphere to model the lower conductivity of the skull. Paicer et al. [1967] reported studying a three-shell model and comparing theoretical and experimental results of median nerve stimulation using a single point dipole, which did not fit the data well. Vaughan and Ritter [1970] reported a good fit between theoretical dipole sources in auditory cortex and experimental scalp potentials, but did not say what sort of head and source models they used. Nakamura and Biersdorf [1971] talked about using dipole models, but did not indicate if they actually made quantitative calculations. Jeffreys [1971] and Jeffreys and Axford [1972ab] performed visual experiments and compared their results to a single homogeneous sphere model containing a single dipole. Thus ended the Stone Age of dipole source modeling.

2.3.4 The Inverse Problem

Up to this point everyone had based his comparisons on the solution of the forward problem, that is, calculating the potential distribution from a hypothesized source configuration and qualitatively comparing it to the empirical results. The complementary inverse solution involves calculating the source configuration from the empirical potential measurements. This problem is ill-posed mathematically, but with a few constraints can be solved uniquely. Schneider [1972] first introduced optimization methods ("steepest ascent") to source calculations, calculating the optimum dipole that fit the scalp potential

data of epileptiform EEG. He made a detailed report of how his optimization method converged for various dipole locations and orientations and initial starting conditions, something later workers have not bothered to do.

Smith et al. [1973] reported the use of the steepest ascent method with the Wilson and Bayley dipole formulation to localize sources of activity in three modalities, but their results are suspect since they only recorded from four electrodes. The dipole model has six parameters and thus needs a minimum of six simultaneous measurements at non-redundant locations to produce anything meaningful.

Henderson et al. [1975] published the next major work in brain dipole localization. They recorded from 16 electrodes widely spaced over the head and attempted dipole fits to eyeblink potentials, alpha rhythm, and visual evoked responses. In addition, they constructed a physical model of the head to test the accuracy of localizations of known sources. They used an improved method of optimization developed by Powell [1964] that is more efficient because it does not need to calculate derivatives.

Fender and his colleagues followed the work of Henderson, applying a more refined set of models to the visual evoked potential recorded from 40 or more electrodes. Kavanagh [1972, et al. 1976] analyzed the dimensionality of the human VEP using principal factor analysis. They found that 97 percent of the variance in the data taken from 38-41 electrodes could be accounted for by only six parameters. This can be taken to indicate that a dipole model at least has a good chance of fitting the data. Following this, Fender and Santoro [1977] reported the results of multipole modeling of the VEP. A sixteen-pole model usually over-fit the data. One- and two-dipole models were usually sufficient to account for the variance in the data measured on 42 electrodes.

Kavanagh et al. [1978] used both one- and three-shell models of the head with one or two embedded dipoles to fit VEP data. They introduced the use of the Marquart algorithm [1963] for parameter optimization. This algorithm gives confidence limits on the sources, which were plotted along with the dipole parameters. Over certain time intervals of the flash-evoked response the dipoles could be localized to within a cubic centimeter volume. Darcey [1979, et al. 1980ab] and Ary et al. [1981abc] followed this work with visual experiments using a more appropriate pattern-reversal stimulus presented to various parts of the visual fields of one or both eyes. They were able to differentially activate visual cortical areas and find appropriate dipole-like sources in the proper anatomical locations for certain topographically stable regions of the visual responses. Darcey et al. [1979] additionally applied these methods to simultaneous intracranial and scalp potential recordings taken from 48 electrodes.

The use of dipole source models and spherical head models for the forward problem and the addition of non-linear optimization techniques for the inverse problem was thus well established by the end of the 1970s. As is usual, the terminology in this new area has diverged and produced some confusion and misinterpretation. Sidman et al. [1978] introduced the acronym DLM (Dipole Localization Method) for dipole source modeling and it has caught on in the small literature of this area. I will prefer here to use the less loaded and more generalized term equivalent source modeling (ESM). It does not constrict the model nor imply that anything is being localized in as direct a fashion as CT scanning, for instance.

Others to use ESM to solve the inverse problem in the brain are Hosek et al. [1978] in the monkey, Sidman [et al. 1978, 1979] for early somatosensory activity, Sencaj and Aunon [1979] for visual pattern presentation, Ryding [1980]

for somatosensory activity induced by finger stimulation, and Wood and Wolpaw [1982] for auditory stimulation. None of these reports has yet matched the work of Fender and colleagues in number of electrode sites and model sophistication.

2.3.5 Refinements to Equivalent Source Modeling

Most improvements to ESM fall into two categories: more realistic head models and more realistic current sources. Of course, most improvements will involve an increase in complexity and hence an increase in the computational load of calculating the results of a model.

Refinements to the head model fall into two categories: structural anatomy and media properties. Suggested refinements to the head anatomy include adding more spherical shells, using non-spherical heads such as ellipsoids, and using piece-wise continuous models of combinations of simple shapes. These refinements can be accomplished by reference to anatomy books and tomography. Though the head is bilaterally symmetric, on any detailed scale it is a complicated structure. Thus, for better accuracy, weighted-residual methods might be utilized to discretize the shape of the brain, skull, and scalp. EKG researchers have used the weighted-residual method extensively, but only Witwer et al. [1972] have applied them to brain studies.

Further measurements of head electrical properties can be performed using both invasive and non-invasive techniques. Average properties have been fairly well established. The main problem is to individualize the model. To do this Rush and Driscoll [1968] proposed passing current through the subject's head and measuring the resultant potential distribution, from which some aspects of the electrical properties of the head can be established, especially given anatomical data from other sources.

Improving the source models usually involves adding more dipoles, as individually specified point dipoles or as parameterized two- or three-dimensional structures. In another approach, the dipole can be left behind and replaced by individual current sources and sinks, or multipoles. Sources and sinks can be made into two-dimensional structures instead of points. The possibilities are endless, but choices should be guided by known anatomy and physiology and by computational difficulty.

2.3.6 Validity of Equivalent Source Modeling

The inverse problem is mathematically ill-posed. A unique solution cannot be found unless other constraints are placed on the solution. Practically there many ways to establish such constraints. Studies of the variability of the data, such as in Kavanagh et al. [1976], can limit the maximum number of parameters to utilize. Anatomical knowledge can suggest the most likely source configurations. Intracranial recordings can be fit into the same models as the scalp data to give extra information. Very few techniques in science are completely direct and fool-proof. We are impressed by CT, PET and NMR scans, just as we are impressed by moon landings. Some wonder why the study of brain potentials cannot be straight forward, just as some wonder why, with our technical excellence, we cannot solve such problems as world hunger. Moon landings and tomography simply involve more straight forward physical phenomena. Brains and societies are much more complicated.

Even if ESM cannot always give definitive information when used alone, it is still a valuable way to summarize and parameterize multichannel recordings of brain activity.

2.3.7 Magnetic Source Modeling - A Step Backwards

Magnetic fields are also produced by biological currents. The recording of brain-associated magnetic fields in the past decade has grown exponentially, but their interpretation has not been very sophisticated. To date, every researcher has assumed a single dipole model in a single homogeneous sphere and has estimated dipole position in a manner akin to early brain potential researchers, based simply on the position of field extrema.

Modeling of brain magnetic fields and electric potentials should be put on the same level of sophistication. The models in this thesis can easily be expanded to include the magnetic fields produced by the identical sources that lead to the potentials. Simultaneous measurement of the brain's field and potential can then be used for the solution of the inverse problem. There are well-described theoretical cases in which certain source configurations will produce no measurable electric potential or no measurable magnetic field. By recording both, responses produced by either of these cases can be detected. It has already been established that the EEG and MEG contain complementary information [Cohen and Cuffin 1983]. Such additional information could be used in ESM hypothesis testing to decide between various possible source configurations that would all fit the EEG data alone.

2.3.8 What We Have Learned

Dipole modeling has proven effective and accurate for some types of responses over certain time frames, primarily early sensory-evoked potentials. Here the response has been well understood previously from other techniques, and the dipole model assumed correct if and when it matched the known anatomy and physiology. It was necessary to do this first in order to verify the applicability of the technique. Not much new scientific information has been

disclosed about the brain, except for the thesis work of Ary [1976], where different cortical generators were suggested for the source of different color responses. This thesis describes an attempt to apply these complex methods to post-sensory processes in the brain, about which little is known compared to the sensory processes.

The computational complexity and equipment requirements of the ESM method have retarded its use. On a more basic level, the apparent non-uniqueness of the inverse problem has caused a lack of faith in its validity, mainly among the clinical contingent. Nevertheless, the method can generate detailed hypotheses about the source of electrical and magnetic brain responses that can be verified sometimes by other means. Information from many other fields can be combined with equivalent source modeling profitably.

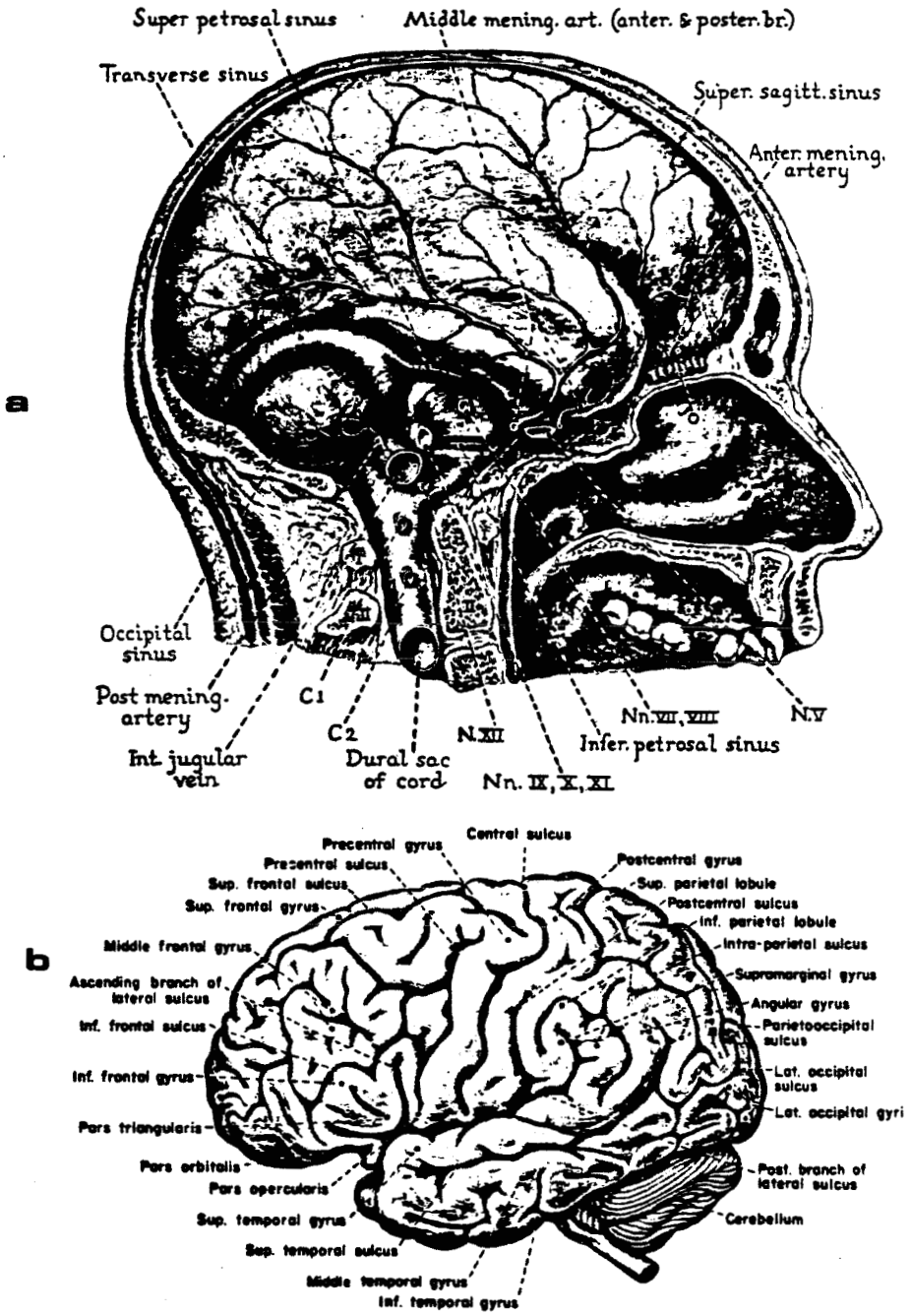

Figure 2-1. The human brain: a) in the skull, b) uncovered.

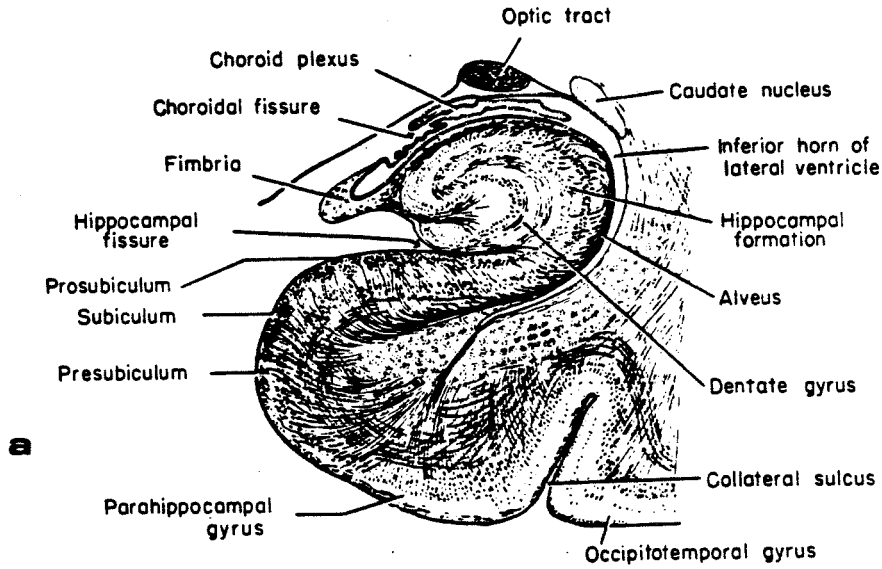

Transverse section through human hippocampus and parahippocampal gyrus

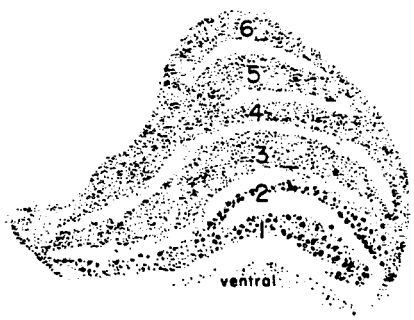

b

Ventromedial

Drawing of the cellular lamination of the lateral geniculate body. Laminae *1* and *2* constitute the magnocellular layers; the *ventral* nucleus is shown *below*. Crossed fibers of the optic tract terminate in laminae *1*, *4*, and *6*; uncrossed fibers terminate in laminae *2*, *3*, and *5*.

Figure 2-2. Layered structures in the brain: a) hippocampus, b) lateral geniculate body.

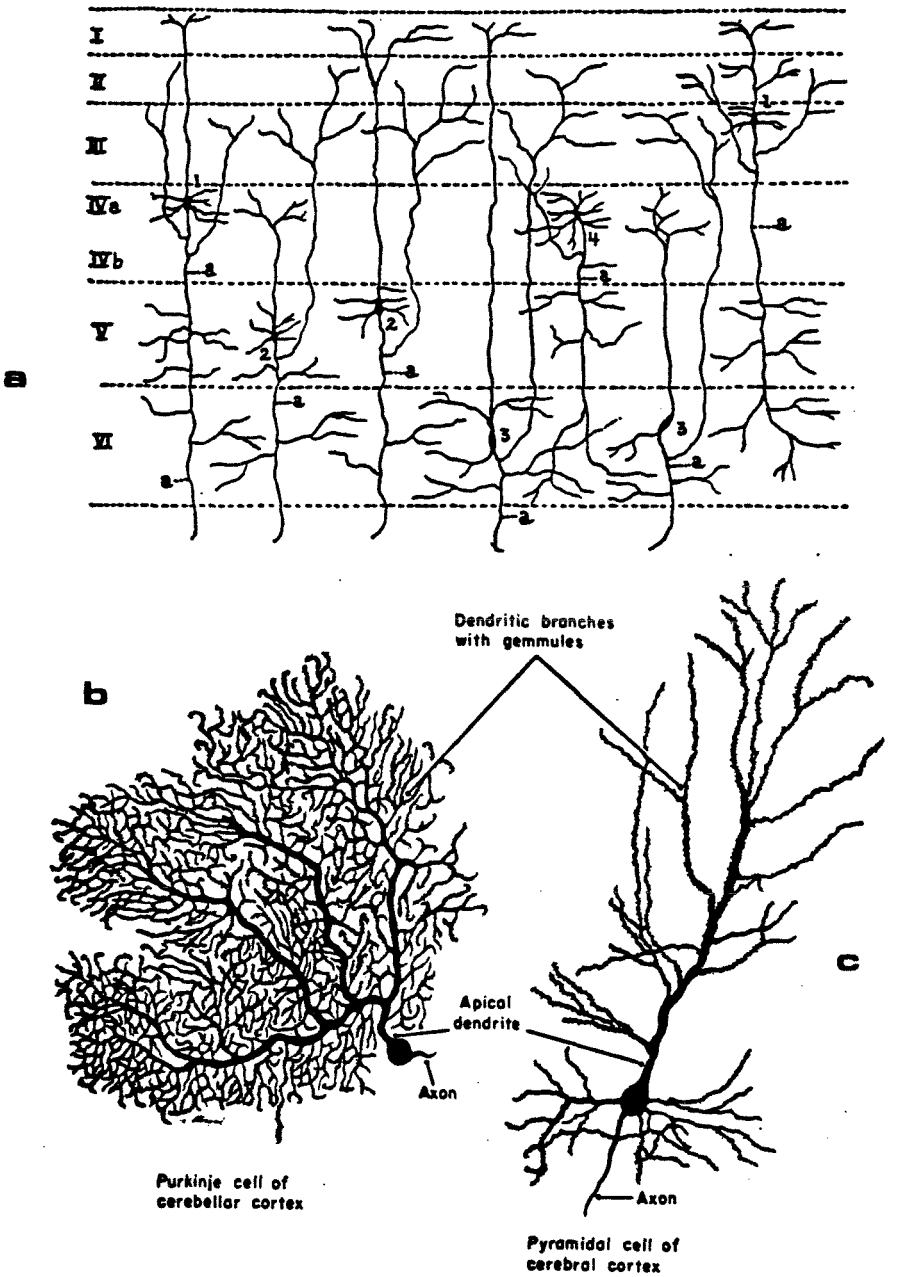

Figure 2-3. Neurons in the central nervous system: a) layered structure of the cerebral cortex, b) Purkinje cell of cerebellar cortex, c) pyramidal cell of cerebral cortex.

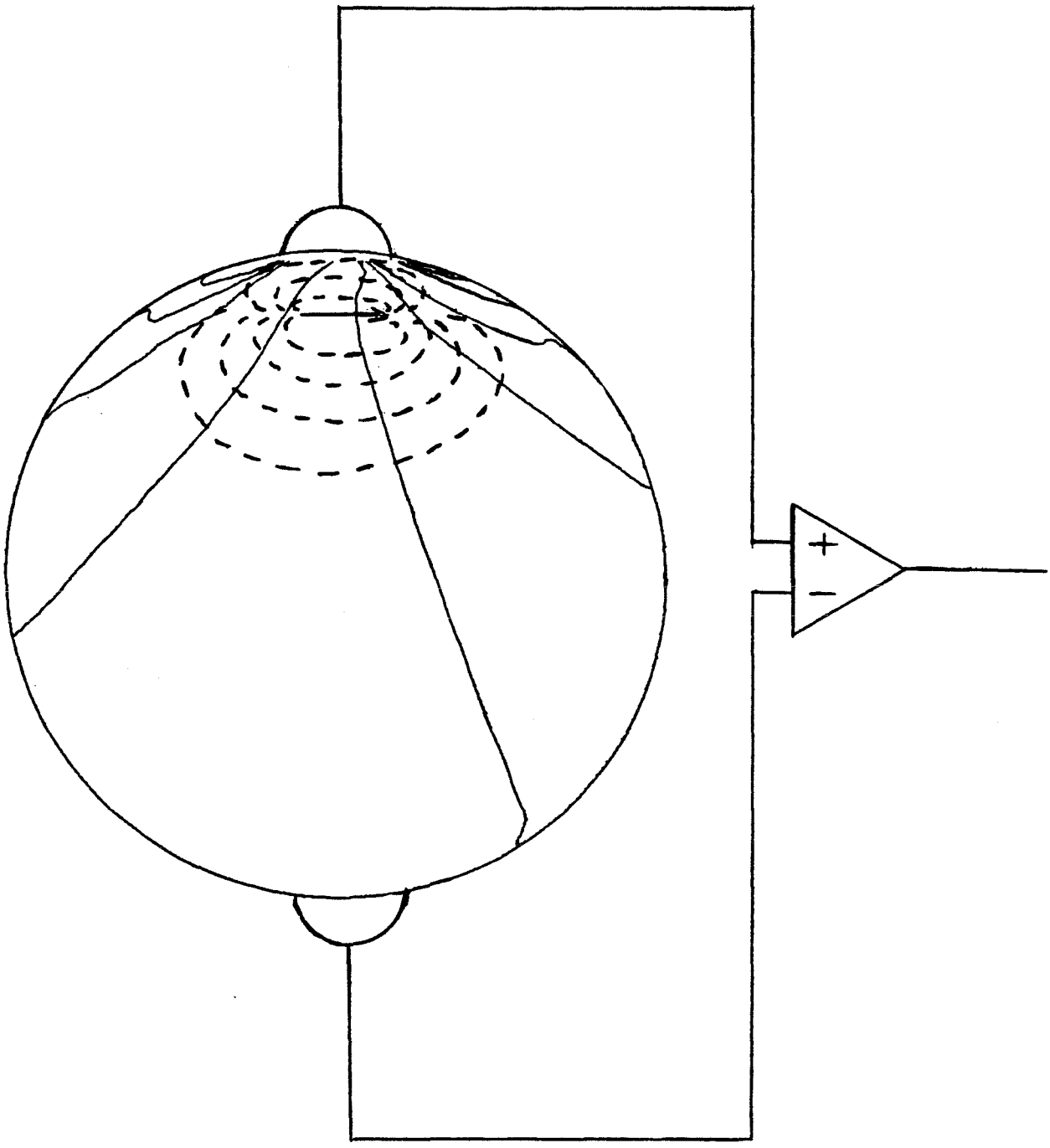

Figure 2-4. Potential gradients on the surface of a sphere caused by a small neuroelectric current source. Amplifier lead placement illustrates problems with locating the source from potential measurements.

3. EVOKED AND EVENT-RELATED POTENTIALS

This chapter will define and discuss some of the nomenclature of scalp potential studies, followed by a brief history of their discovery, development, and use. Analysis methods will be critically reviewed with an emphasis on demonstrating the improvements that can be achieved using ESM techniques. Finally, several well-studied, cognitive-related scalp potentials will be presented as likely candidates for the application of ESM.

3.1 Nomenclature

In the early days of recording brain electrical activity, the potentials were amplified and translated directly to paper in graphical form for which the term electroencephalograph (EEG) was coined. Today, the EEG refers to the ongoing potentials on the scalp, either in a hypothetical sense or in reference to a recorded or coded form of the potentials. The EEG is the basic data from which other derived measures are taken.

A section of the EEG taken immediately following a controlled stimulus given to the subject can be called a single evoked potential or sEP. Often, many single EPs are averaged together to increase the signal-to-noise ratio, generating an average EP, or aEP. It is widely agreed that the preponderance of the noise associated with sEPs is caused by intracranial, biological sources. Such noise is often assumed to be a stationary random process. If it is, adding together a set of successive sEPs will result in the noise increasing more slowly than the signal, or putative "true" EP [Ruchkin 1965].

Median or modal calculations are other possible ways of increasing the signal/noise that offer advantages under certain conditions [Walter 1971, Ruchkin 1974]. In fact, a vast range of operations that can be subsumed under the rubric of signal processing can be and are performed on single EPs. Since

the nomenclature can become cumbersome if new letters are prepended for every operation, I will use the term EP in a very general sense to indicate any time-domain representation of biological potentials associated with an evoking stimulus. It can be single, averaged, filtered, experimental, or derived from a model. Its derivation will be taken from context.

It is fairly useful to differentiate among evoking sensory modalities. I will follow the practice of prepending modality. Visual EPs, auditory EPs, somatosensory EPs, olfactory EPs, and gustatory EPs will be indicated by VEP, AEP, SEP, OEP, and GEP, respectively. Any of these evoked potentials may be derived in a variety of ways from the raw EEG. Only the modality is specified. Terminology again starts to become cumbersome when we consider multiple modality EPs, so no special names will be used for these.

If we consider a simplified model of the brain as a black box having inputs, outputs, and some kind of processing in between, evoked potential terminology usually refers to the initial input stages. The final effector outputs produce what have been termed motor potentials or MP. They are not considered evoked in general, at least in relation to the stimulus, because they are dependent upon the central processing. Just as sensory evoked potentials are associated with a sensory stimulus, an MP is associated with a motor response that can be measured and located in time. Presumably, a fixed, reflexive motor potential should be called a motor evoked potential, or MEP.

Another term has been in use almost as long as EP. Not all potentials can be considered as evoked, especially those associated with internal mental processes. Donchin [1979] has championed the use of the term event-related potential, or ERP, to refer to any potential related to an external or internal event. Psychologists are more likely to use the term ERP, while physiologists use

EP. Psychologists may also use ER, or evoked response, to refer to sensory-evoked potentials. The ERP designator is often used for later, more variable, responses of the brain, but can also be used inclusively. Hence we can have sensory, motor, or cognitive event-related potentials, the latter being related in time to some variable, internal state of the subject.

In this thesis I will use both EP and ERP interchangeably, depending on convenience and context. In order to discuss magnetic field work also, I will adopt a similar nomenclature. ERP becomes event-related field (ERF), EP becomes evoked field (EF), and motor potential becomes motor field (MF). The EEG is analogous to the magnetoencephalogram (MEG). To lump both electric potentials and magnetic fields I will use simply evoked response (ER).

3.2 History of Brain Potential Recording

3.2.1 The Electroencephalogram

Hans Berger, in 1929, was the first to record the EEG from human subjects. Clinicians initially had great hopes for using the EEG as a window on the brain. Its early promise was never quite realized, in part because of over simplification in its interpretation. The EEG has been most useful in the diagnosis of epilepsy. It also has been an aid in brain trauma diagnosis and large brain tumor detection. New analysis techniques show some promise in adding to the usefulness of modern clinical EEG recordings.

3.2.2 Evoked Scalp Potentials

The concept of an evoked potential was a natural one, arising from the scientific principle of experimental control. The first single evoked potentials were recorded by Berger during his early work. But they were, of course, only visible under very restricted conditions. The first application of averaging evoked potentials was reported by Dawson [1947]. He simply superimposed

multiple EEG traces, each time-locked to a stimulus presentation, on the same piece of film. The experimenter performed the averaging in his visual system upon examination of the exposed film. Dawson also [1951] reported the use of an analog, capacitor-based averager.

The use of EPs grew in parallel with the development of computer storage and signal digitization technology. Clynes and Kohn [1960] developed the first digital signal averager for use with EPs by converting a device used in nuclear energy research, the Computer of Average Transients or CAT. With the CAT one could record in real time up to four averaged EPs, display them on a storage CRT, and photograph the display for a permanent record. Raw data were initially stored in analog form on FM magnetic tape and could be played back on a CAT for off-line analysis. More recently, raw data have been digitized and stored on a variety of digital media. Both on-line and off-line analysis can be performed on the digital data, resulting in higher precision, reliability, and portability.

Just as with the EEG, researchers initially had great hopes for EPs as probes of the brain. They were recorded under a wide variety of stimulus conditions. Basic researchers eventually lost interest because EP results were not clear-cut and could not usually be correlated with other measures that were deemed more trustworthy. A resurgence of interest in EPs, now renamed ERPs, occurred in the 1970s. On the one hand, clinicians found new uses for ERPs, mainly based on new stimulus and data analysis techniques being applied to the right patient populations. On the other hand, psychologists discovered many cases of reproducible ERPs elicited by endogenous events. In both cases ERPs are used as a rough correlational tool, as a blind measure of something whose origin is unknown, but that correlates with experimental variables.

The study of exogenous ERPs has not led to much new scientific knowledge

about the way the brain processes sensory information, but it has led to clinical applications whose viability has then been rationalized by neurophysiological hand-waving. The study of endogenous ERPs, though, is beginning to shed new light on central processes that in the past could only be studied with behavioral methods. Some researchers are beginning to use ERPs to decide between rival cognitive theories [Hillyard and Kutas 1983]. Donchin et al. [1978] consider the study of ERPs as a separate but equal partner to traditional behavioral methods in psychological research, providing complementary information about the workings of mental processes no less valid than the information gleaned from reaction time tests and psychophysics.

3.2.3 The Magnetoencephalogram and Evoked Magnetic Fields

Cohen [1968] demonstrated that neural activity in the brain could produce measurable magnetic fields around the head resulting from alpha activity and visual evoked responses. Cohen had to place his subjects in a special magnetically shielded room to exclude the ambient natural and man-made magnetic fields that normally would swamp the incredibly small brain-evoked fields. Brenner et al. [1975] reported the successful utilization in a brain response experiment of a new, highly sensitive detector of magnetic fields, the superconducting quantum interference device (SQUID). They measured visual EFs in a non-shielded environment, demonstrating the viability of the magnetic technique in a regular university research environment.

From this point on, the use of the SQUID grew rapidly. Reports came out on the use of SQUIDS to study sleep activity [Hughes et al. 1976], somatically evoked fields [Brenner et al. 1978], auditory evoked fields [Reite et al. 1981], epileptic spike activity [Barth et al. 1982], tonotopic organization in the auditory system [Romani et al. 1982], and the source of the endogenous

magnetic P300 analog [Okada et al. 1983]. High hopes were initially placed on the theoretical localization properties of the magnetic technique. While many still hold on to these hopes, it is notable that the original reporters of human brain magnetic recordings have recently compared the EEG and MEG both theoretically and experimentally [Cohen and Cuffin 1983] and concluded that neither of the two has any strong advantages over the other. With proper quantitative biophysical analysis, though, the two can probably complement each other in their application to the elucidation of the neural generators of brain potentials and fields.

3.3 Scalp Potential Analysis Methods

This section will critically review many aspects of traditional EP measurement, analysis, and interpretation. The concept of an EP component is discussed in detail. EP parameterization is next discussed, followed by measurement practices and statistical analysis. Then the improvements in analysis of equivalent source modeling to EPs and EFs are discussed.

3.3.1 Components

A central notion in EP work is that of the component. Since an EP is composed of a time series of voltages, it naturally will have some shape to it in terms of peaks and troughs. The earliest EP researchers, noticing changes in amplitude of EP peaks, initially considered each peak as representing a separate part, or component of the response, as their amplitudes could often be manipulated independently. Underlying this idea was the hopeful supposition that a component could also be associated with a particular cortical area or brain process. Some components were named by their negative or positive peak number or peak time in milliseconds. Examples of the former are N1, P1, N2, P2, and the latter, P165, N200, and P300. Components that did not fit this scheme

well received special names, with acronyms such as CNV, MP, SW, and BP.

A refinement to the component idea was to differentiate between those peaks that seemed to be directly associated with an evoking external sensory stimulus, and those that were assumed to be correlated with an internal event in cognition or the brain. Classic examples of the former, "exogenous" components are the P100s of the VEP, AEP, and SEP. Examples of the latter, "endogenous" components are the P300 and N400 cognitive ERPs. The P100 of each sensory modality is primarily influenced by the properties of the external stimulus. The P300 and N400 are mainly affected by aspects of the subject's internal state, as set by the experimental task and the subject's moment-to-moment reactions. If we define a component as an EP peak, then almost all components will likely have endogenous and exogenous parts. The N100 peak is known to be affected both by stimulus properties and subject attention [Hillyard 1981], for instance.

The concept of a peak component is artificial and can be misleading. It is obvious that any part of an EP could be composed of the sum of many so-called components overlapping in time. Many people have recognized this and have made various attempts to identify components defined not by waveform features, but by experimental manipulation. Hunt et al. [1983] recently described a way of modeling EPs using what mathematically would be called basis functions. Donchin [1966] has long used a statistical technique to extract overlapping components on the basis of variance measures. Wood [1983] has pointed out some difficulties with this technique of "principle components analysis." However, it is still a theoretically more realistic model than simple peak components.

The differentiation between endogenous and exogenous components is also

somewhat artificial, but is based on a fairly clear differentiation between externally measurable stimuli and internal brain "events." As more experiments are done, though, it appears that most components after 50 ms or so are either endogenous or a mixture of exogenous and endogenous sub-components. The only truly exogenous components are perhaps pre-cortical in origin. The distinction is still useful in that it serves to categorize the variables that influence EPs.

Underlying the previous discussion is the assumption that the EEG and EP are actually direct measures of something like the potential at a particular spot on the scalp. But only potential differences, i.e., potential gradients, can ever be measured [Feynman et al. 1964]. The choice of reference can and usually does greatly affect the EPs. To properly interpret EPs they must be recorded referred to an inactive reference far removed from the active current sources or situated at a null point in the potential distribution. The first is hard to achieve since placing the reference electrode far away allows the pick-up of more environmental and biological noise. The second is virtually impossible to achieve over any finite time frame of interest because of the complexity of the neural generators and the varying topology of their resultant scalp potential distributions.

Even if they exist, null points are very rarely searched for in any systematic fashion. Thus most EPs are suspect in this regard, though the extent of the uncertainty is difficult to estimate. Wolpaw and Wood [1982] have recently experimented with several referencing schemes and again pointed out the problems associated with determining a proper reference. I believe that the best solution to the referencing problem is to record over a spatial array and analyze the potential gradients.

3.3.2 Parameterization Techniques

Given a time series of measurements, it is often convenient and useful to reduce the amount of data to a small set of numbers derived from the full time series. Early EP workers started this process by concentrating on the peaks and valleys of the individual EP, noting the time, or latency, and voltage value of selected positive and negative local extrema. These parameters were found to correlate with various experimental parameters and became the basis for the earliest systematic EP studies. One difficulty with measuring peak voltage values is determining the zero potential, or baseline. (The referencing problem also obviously enters into this discussion, but has been dealt with adequately above.) Technical zero, the output of the amplifier with its inputs shorted, is probably the best choice, but amplifiers do drift with time. Many chose to define the baseline as the average pre-stimulus value over a specified time.

To get around the baseline definition problem, many started to use peak-to-peak measures, with the rationale that differences between closely spaced transient components would not be affected by the slow baseline shifts that occur in some ERPs. This still assumes peaks have a connection with underlying brain phenomena, which can be true for simple exogenous ERs, but is most definitely not true for more complex endogenous ones.

Another problem stems from the reliability of the signal in the presence of noise. The most significant noise problem arises from biological sources. Even after averaging 100 to 200 individual ERs, enough noise can remain to shift the latency or value of a peak a significant amount. Area measures were thus introduced as a further way to increase the signal/noise ratio by essentially averaging over the ER time dimension (whereas the initial averaging was over the experimental, or stimulus repetition time dimension). Each throws away

information, while improving the S/N ratio. But area measures can be valid only if the peak they are based on corresponds to a single underlying process. This has rarely been established for any peaks besides the earliest brainstem responses.

3.3.3 Number of Recording Sites

Typically, only one to three active electrodes are utilized in most ERP experiments. ERP researchers actually discuss the "topography" of a response based on three midline electrodes! I will reserve the term topography to cases where data have been recorded from 16 or more electrodes in a montage that covers an area, not just a line. The realities of volume conduction, neural transmission, and inter-subject variability do not leave much hope that useful information can be obtained from a small number of measuring sites. Some phenomena are robust enough, though, to actually produce a measurable effect across subjects on electrodes placed by external landmarks and referenced in a wide variety of ways. But only very rarely have any experimenters shown that their referencing and montages are optimal for a particular task. This can only be done by recording from a large number of electrodes and then properly selecting from them. Otherwise, many non-robust phenomena can be obscured or lost.

3.3.4 Statistical Methods

Through the years, more involved statistical treatments have been applied to ERP analysis. This was only natural in order to extract more information out of poor parameterizations of indirect measurements. All statistical analysis requires a model of the phenomena being measured. In ERP work, these models are most often ad hoc, and take no stock of physics and physiology. An analogous situation would be genetics before DNA and molecular biology. Early

genetics had to rely almost wholly on statistical analysis of measurements made on individual phenotypes in order to deduce anything about the underlying genotype. The power of biochemistry led genetics far beyond what it could achieve beforehand. I feel that the power of biophysics, if properly applied, could lead neuroscience far beyond where it is today.

Spectral analysis is often used in EEG work, and sometimes in ER work, to obtain measures of the EEG or ER that can then be correlated with experimental variables. To perform any type of spectral analysis, a model is made, either implicitly or explicitly, of the system under study. In most cases, the model is simply a bunch of spectral generators, with highly constrained properties such as stationarity and ergodicity. While the brain does have components that act like spectral generators at times, such models never attempt to take into account actual physiological data concerning these generators and the spread of their signals.

Principal Components Analysis (PCA) is a powerful statistical technique first applied to human ER work by Donchin [1966]. It comes closer to modeling a real brain in that it allows overlapping components, presumably arising from different brain processes. If each component can be varied by experimental manipulation, then PCA is capable of separating these components, though a recent study by Wood [1983] indicates that the assignment of variance may be faulty. Others have tried explicitly modeling ERs as a series of overlapping waveforms [Hunt et al. 1983]. All these attempts still fail to account for physiology and thus lose much validity and power.

3.3.5 The Use of Equivalent Source Modeling

All currently known measures of brain processing are indirect, ERs included. ERs are a measure of the currents associated with brain events. I

argue that ESM is the most direct measure available of those currents, simply because the underlying model is exactly those currents. With ESM, time series of complex topographic data can be reduced to a small set of parameters with which we can define components in a more objective way than with peak area, or statistical means. Referencing problems are non-existent. Because of the large number of recording sites used, noise can be dealt with in more effective ways. Statistical methodology can still be applied, but on top of a more realistic base.

ESM is not able to stand completely on its own, because of its mathematical non-uniqueness. But no other ER analysis technique can stand alone either. For correlational purposes, ESM should stand far above other ER measurement techniques. Information from complementary fields of inquiry can be combined with ESM to provide new analytical conclusions. The main difficulties with ESM are the extra time and expense needed to record from many sites and develop the software to model and compute sources.

3.4 Endogenous Event-Related Potentials

In this section I will introduce the nomenclature of evoked potentials and event-related potentials (ERP), particularly in relation to so-called cognitive potentials. I will discuss the central notion of components as applied to brain potentials. Finally, I will summarize the main types of cognitive ERPs based mainly on the categories of tasks involved in eliciting them.

3.4.1 What is an Endogenous ERP?

Many endogenous ERP components have been labeled "cognitive." This word means many things to many people. To lay people it relates to "mental," "thinking," "conscious." or "reasoning." To psychologists, it also has many meanings, though usually well defined in relation to any particular experimental context. Webster defines cognition as "the act or process of knowing, including

both awareness and judgment." To psychophysiologists, a cognitive ERP is usually an endogenous component presumably associated with some internal cognitive state of the subject. This usage seems to lump both conscious and unconscious processes and just about anything not directly related to sensation or motor output. Such a broad definition of cognitive does not suit Webster or psychologists, so it is perhaps wiser not to use such a loaded word and stick with the descriptive terms exogenous and endogenous.

The rest of this section will introduce several well-known "cognitive" or endogenous ERPs. They will be given their usual names, with the realization that their appropriate derivation and nomenclature are more properly derived from the experimental task and subject state.

3.4.2 Expectancy and the CNV

Walter et al. [1964] first described and named an ERP called the Contingent Negative Variation (CNV). It was observed following an unconditioned stimulus (UCS) as a "slowly" growing negative (with a standard ear reference) "wave," that "resolved," or disappeared when the conditioned (CS) stimulus came along. In this classic case, the interval between the CS and UCS was one second. The CNV started about 800 ms before the UCS, grew to about 20 μV, and returned to pre-UCS baseline in about 100 ms.

The first CNV was recorded with a dc amplifier. This was not common practice, but turned out to be necessary in order to observe the low-frequency content of the response. The CNV presumably occurs in many experimental tasks but is not seen because of the higher bandpass used by most workers. Some use a higher bandpass purposefully in an attempt to exclude the CNV, but this tactic cannot be completely effective, and distorts the other slow (low-frequency) components of the response.

Naturally, subsequent workers attempted to see what effects varying the timing of the stimuli had on features of the CNV. Different modalities and response modes were tried. Evidently, eye movement artifact was problematic in the early CNV studies and led to many misinterpretations [Chapman 1969]. The need to use DC or low bandpass amplification also confused things, since there was little standardization of recording techniques. The consensus seems to be that the CNV indexes some measure of "expectancy." If this is true, then the CNV must be ubiquitous in all types of "cognitive" experiments that involve warning, repetition, responses, or subjective timing.

3.4.3 Attention and the N100

Hillyard and his colleagues [1973] have defined an endogenous response that overlaps exogenous responses at about 100 ms after a sensory stimulus, and usually is negative with reference to a subject's earlobes. Some call it N1, to indicate the first negative peak, but I will prefer the N100 designator here, indicating a negative peak at about 100 ms. The N100 was first reported as an enhancement of the exogenous N100 in an attended auditory channel. When instructed to pay attention to tones presented to one ear while ignoring tones presented to the other ear, N100s associated with the attended ear's stimuli were larger than N100s associated with the unattended ear's stimuli.

The first "attention" N100 was differentially defined between two sensory channels that were physically quite separate, i.e., the ears. Other workers have tried defining channels in other modalities, cross-modalities, and within modalities, sometimes separated physically, sometimes only by attribute. More than two channels have even been examined. Through all these variants, one form or another of N100 has been observed.

The N100 can be said to index processes that most psychologists associate

with attention [Posner and Boies 1971]. At this time, many fine points of attention are being discussed in the ERP literature in terms of various psychological theories of sensory gating, stimulus set, and response set [Hillyard and Kutas 1983]. Because of its presumed connection to peripheral gating, the N100 is thought by most to originate in sensory cortex or in the pathways to sensory cortex. Knowing the cause of the N100 could evidently help resolve some very important questions in cognitive psychology.

3.4.4 The Ubiquitous P300

Sutton et al. [1965] discovered the most famous of the endogenous ERPs when he asked subjects to guess whether single or double clicks were to appear next in a randomized sequence. When the actual stimulus occurred, it elicited a late peak around 300 ms if it was not the stimulus that the subject had guessed, or expected. A similar positive peak was later observed to follow rare events in a sequence consisting of two stimuli presented in random order, one being much more frequent than the other [Ritter and Vaughan 1969]. This latter experiment has become known as the "oddball paradigm" for the P300 response.

Auditory [Ritter et al. 1972], visual [Simson et al. 1977a], somatosensory [Wood et al. 1980], and mixed modality [Ford et al 1973] P300s have been recorded. P300-like responses have also been recorded time-locked to a missing stimulus in a sequence [Simson et al. 1976]. Squires et al. [1975] claim that there are two varieties of P300 based on semi-topographical data. Donchin has studied the P300 extensively, varying stimulus probabilities in complex ways and fitting the resultant data to ad hoc mathematical models of subjective probability.

The interpretation of the P300 has had the most extensive evolution of any of the endogenous components. Because it seems to arise in so many different

contexts, it continually has more attributes laid upon it. Sutton first linked it to the resolution of "uncertainty" in his guessing tasks. Ritter and Vaughan [1969] related it to novelty or surprise on the basis of the oddball paradigm. Kutas et al. [1977] thought it indicated stimulus evaluation or response selection. There has been a long controversy over the relationship of the P300 to the CNV. Initially, some workers thought that the P300 was the result of the resolution of the CNV upon stimulus evaluation [Chapman 1969]. Studies by Donchin et al. [1975] and others have since demonstrated many differences between the two in terms of experimental manipulation and topology. However, Simson et al. [1977b] present arguments that both could still have the same neural origin.

Because it peaks over the parietal region when measured with various standard reference sites, the P300 was originally supposed to originate in parietal, or associational cortex. This supposition did not conflict with the interpretation of the P300 as an index of stimulus evaluation. However, later experiments using intercranial recordings in man [Wood et al. 1980] have suggested a role for deeper, non-cortical brain structures such as the hippocampus and amygdala.

3.4.5 Semantic Incongruity and the N400

A more recently discovered endogenous ERP is the N400 elicited by the occurrence of semantically incongruous words in a sequence of words that normally form a sentence. Kutas and Hillyard [1980abc] presented seven word sentences, each word spaced one second apart, to subjects while recording EPs. One quarter of the sentences ended with an inappropriate word that produced a nonsense phrase. When the sentence ended appropriately, a P560 was seen at the vertex electrode. But when the sentence ended inappropriately, an N400 potential peak was observed.

Though the N400 has been replicated and seems to be a robust phenomenon, too little information about its variability is available to make inferences about its localization and function. Full topographic studies are still lacking.

4. EXPERIMENTAL DESIGN

The goals for this thesis are to choose an experimental task that elicits a robust endogenous component, to repeat the experiment within and across subjects a sufficient number of times to ensure reliability, and to apply the techniques of source location to the data thus gathered to characterize the ERP in terms of the time courses of the sources that represent the components of cortical activity associated with the task.

In choosing an experimental task, I considered those that had well-studied cognitive or endogenous components in order to facilitate comparison to a previous body of knowledge. Candidates considered were the odd-ball task, the attention-shift task, the expectancy task, and the semantic-incongruity task. The odd-ball task produces a high amplitude P300 in a majority of subjects. The attention task enhances or reduces the N100, which also overlaps sensory components. The expectancy task produces a long duration, slow negative shift contingent upon an expected event (CNV). The semantic task generates an N400 at the end of a series of words presented to a subject.

4.1 Sensory Aspects

Since I intend to apply the techniques of source location to what are most likely overlapping neural processes in the brain, I desire a task where the putative sensory and motor components can be minimized or eliminated.

The CNV is generally thought to be very long-lasting, which in ERP terms is a second or more. In the classical experiment [Walter et al. 1964] it presumably starts upon detection of the warning stimulus and resolves after the imperative stimulus. The CNV thus overlaps both of the exogenous responses to the stimuli.

Exogenous components that last well past 100 ms are produced in all modalities. The attention-related endogenous N100 will thus always overlap

some sort of sensory response. In fact, the N100 is often defined operationally as a difference potential, the N_d [Hillyard 1981]. While it is my intent to develop the capability to analyze overlapping components, it is preferable to be able to separate the components by other means as a verification. The N100, as the CNV, is virtually impossible to separate from exogenous components by experimental manipulation.

The odd-ball P300 occurs only after a surprising or unexpected sensory stimulus. By reducing the length or intensity of the stimulus, exogenous sensory components which normally end by 250 ms can be reduced in amplitude, leaving an almost uncontaminated P300. Of course, if the stimuli are reduced to near threshold, the task becomes more one of signal detection and the whole scenario changes. A P300-type response can also be emitted by the absence of an expected stimulus in a repetitive string of identical stimuli. This kind of P300 may have different properties from the evoked one, however.

The classical P300 is thus easy to separate from exogenous components. Upon closer examination, many workers have discovered earlier components associated with the P300. An N200 has often been reported and can be seen most clearly by taking the difference potential between the rare and frequent responses. The P300 is probably best defined as a difference, but the rare and frequent stimuli will produce slightly different exogenous components that may obscure the true odd-ball difference potential. Goodin et al. [1978] use the difference between attending to and ignoring the stimulus sequence, thus controlling stimulus parameters. Their odd-ball difference potential evidences a P165 peak as well as the N200 and P300 peaks. So while part of the odd-ball response may be separable in time from exogenous components, other parts are probably not.

In the semantic task the N400 should be easy to analyze separately from exogenous components because of its relatively long latency. It has not been examined as thoroughly yet as the P300, and it could possibly have other associated early components that overlap the exogenous responses to the eliciting words. No one has computed the semantic incongruity response as a difference so far, either. Another component of interest is the P560 following a semantically correct sentence. This is even further removed from the exogenous components.

In conclusion, we see that parts of the responses to the odd-ball and semantic tasks can be separated in time from the earlier sensory responses, especially by reducing stimulus intensity, since the sensory responses are primarily independent of the stimulus parameters. The expectancy and attention tasks do not allow this.

4.2 Motor Aspects

The expectancy task is classically performed with a motor response to the imperative stimulus. Motor-related brain potentials thus complicate the CNV. In their original paper, Walter et al. [1964] reported that subjects could produce a CNV without an imperative stimulus, suggesting that it was the intention to produce a motor response that caused the CNV. The CNV has caused much controversy over the last 20 years concerning its relation to or identity with motor and other endogenous components. I will assume that the CNV is not easily separable from associated motor components by experimental manipulation.

The attention-shift task is usually presented as two separate odd-ball tasks, one to each ear. Attention is focused by requiring a motor response to the odd stimuli in the selected channel. While the motor response could be replaced by

mental counting as in the P300 odd-ball task below, the attention task is more involved in that it switches between one channel and the other. The motor requirement is probably necessary here, to force a mental set to one channel or the other.

It is possible to perform the odd-ball task without motor involvement by mentally counting the occurrences of the rare stimuli. A difficulty with doing this is the lack of an alternative measure of stimulus detection or recognition, such as a motor response would give. In lieu of this, the subject is asked to report a total count at the end of a session. This necessitates paying attention at least to the rare stimuli in order to obtain a correct count. The subject is given feedback on the accuracy of the count, so that vigilance can be controlled. Of course, only runs with accurate subject counting and presumably detection and recognition of the rare stimuli are used for the analysis proper, though data on subject errors are also intrinsically useful for further study.

The semantic task usually is performed without a motor response. Thus it is the best choice if we are to avoid any motor contamination. The odd-ball task runs a close second since it can be readily accomplished without a motor response. The attention task comes in third since it probably works better with motor involvement. The CNV finishes last as it appears to be intimately connected with motor behavior.

4.3 Operational Aspects

Because of the vast amounts of data collected in a 40-48 channel experiment, it is necessary to consider the length of time needed to produce a desired brain response and the amount of data of which the response consists. The CNV can last from 1 to 2 seconds, and typically uses intertrial intervals (ITI) of 3 to 10 seconds. Also, the CNV is best recorded with dc amplifiers which

involve contact-potential problems at the electrodes. The available EEG amplifiers are AC coupled with a bandpass of 0.5 to 100 Hz, which pretty much rules out any possibility of recording the CNV with the present equipment.

The N100 is a short latency potential, and the complete response in an attention-shift experiment should last 250 to 300 ms. ITIs can be as short as 200 ms. Even with a 400 ms minimum ITI, a subject would have to sit only one-tenth as long as for a CNV experiment to get the same number of repetitions. Of course, there is still the problem that the attention-related N100 can be observed only as a difference potential.

The so-called P300 can last as long as 600 ms, and ITIs can be as short as that. Thus it would take more subject time and data collection per trial for the odd-ball task compared to the attention task. But the collection time is much greater because the rare stimulus occurs only about 20 percent of the time, and the ITIs must be randomized in duration to produce a strong P300, thus increasing the length of the mean ITI.

The N400 is longer than the P300 but requires many stimuli in a single trial. Kutas and Hillyard [1980abc] used seven-word sentences with one second between words, while Herning et al. [1983] were successful with four-word sentences. And as with the P300, only a small percentage of the sentences can be semantically incorrect, making the semantic task the longest running and data-intensive of the four tasks considered.

From a data collection standpoint, the attention task would take the least amount of time, followed closely by the odd-ball task. The semantic task would take a much greater amount of time, as would the expectancy task. The latter would be out of the question without first converting the preamplifiers to the direct coupled mode.

Based on the above considerations, I chose to examine the P300 and associated components elicited by the odd-ball task. It is relatively easy to separate from sensory or exogenous components. Motor contamination can be controlled or eliminated. Data collection is manageable with the use of fairly short ITIs. Finally, the odd-ball task is quite simple to implement.

4.4 Controls

There are a myriad of experimental controls that would need to be done in a full study of the odd-ball task, both to ensure data integrity and to reduce the variability of the responses. Many of these could not be performed here, but a fairly complete exposition of them will be presented.

4.4.1 Other Modalities

I selected the auditory modality for the initial odd-ball experiments because it is the easiest to work with. Visual and somatosensory stimuli are just as successful in eliciting the odd-ball ERP, but the stimulating apparatus needed is more involved. Visual ERP experiments also have to contend with controlling and measuring fixation, extraneous eye-movements, and concomitant noise. Even so, it would prove useful to perform odd-ball experiments in other modalities to confirm or refute the currently accepted notion that the odd-ball ERP is independent of modality.

4.4.2 Noise and Artifacts

The intent of an ERP experiment is to elicit brain responses and record them for later analysis. Other potentials, however, can arise from various sources in the equipment and in the subject. These all are considered to be noise and must be controlled or eliminated. Amplifier and electrode noise are not usually a problem with modern equipment, and with the system used for this experiment I can always discard the data from a few channels if they are in

any way suspect. Each channel can be viewed during the experiment as well as afterwards in voltage-time plots and equipotential maps in order to look for unwanted noise of any sort.

Biological noise from the subject comes in two varieties. One is intrinsic brain noise caused by all the other ongoing processes in the CNS during a task. This type of noise is recorded along with the ERPs and dealt with later during the averaging process. The second is from sources outside the brain, such as muscle activity and associated movement of body parts, especially the eyes. Muscle tension produces its own electrical activity that will spread by volume conduction to all conducting parts of the body. Movement of the eyes, which have a standing potential gradient, generates the EOG electro-oculogram which also can appear on EEG electrodes, especially in the frontal area.

Movement-related noise can be reduced three ways: by experimental design, by proper subject instruction and behavior, and by special data processing. In choosing the auditory odd-ball task I have eliminated motor responses and task-relevant eye movements. The subjects are told to minimize all movements while performing the task. Of course, independent measurement of a subject's behavior should always be made in order to verify that the subject has indeed performed as instructed. Ideally, non-physiological measures of eye and head movement should be made. Lacking these, voltage-time records and equipotential maps should be examined to discern if eye and muscle artifacts appear in the raw or averaged data.

4.4.3 Randomizing Intervals

It was discovered early on in the study of sensory-evoked potentials that the brain could lock onto repetitive stimuli and produce certain potentials, such as alpha bursts, that went away when the ITIs were randomized in length. From

a systems-engineering standpoint, the brain was thought to be driven by the periodic input. Academic researchers, and eventually clinical workers as well, adopted the practice of randomizing the ITIs in evoked potential experiments. Psychophysiologists soon discovered that many endogenous potentials were affected by the exact probability structure of the preceding stimulus sequence. Randomization of ITIs then became not a means to remove artifacts but an experimental variable in its own right.

For the odd-ball task, the ideal ITI sequence would probably follow a Poisson distribution, where the next interval could be any length and would bear no relationship to any previous interval. This is impractical in that very long intervals would result. The next best solution would be to select the ITIs from a uniform distribution with a fixed lower and upper bound, thus preventing overlapping responses and unduly long intervals.

4.4.4 Counting

To reduce motor artifacts and motor-related brain potentials, I decided to have the subjects simply attend to the sequence of rare and frequent tones. To control attention and verify that they were actively participating, I asked them to keep a mental running count of the number of occurrences of the rare tones and report it at the end of each run, while ignoring the more frequent tones. Their report could be checked against the actual count immediately after the run and fed back to them.

A difficulty with such mental counting is that it may produce its own ERP signature which, if time-locked to the stimulus presentations, would appear in the averaged ERPs. Of course, such internal counting would probably be highly variable in time and differ in strategy from subject to subject. In performing the task myself I find that I repeat the previous count whenever I hear a frequent

tone and increment it when a rare tone occurs, with a lot of extraneous talking to myself in between. The most proper way to deal with this difficulty would be to perform an experiment to try to characterize mental counting alone, using internally and externally timed sequences.

4.4.5 Reverse Tones

If the odd-ball task were to be done with tone 1 always being the frequent tone and tone 2 always being the rare one, a bias would result because of the difference in exogenous responses to the two slightly different tones. It is necessary to reverse the rare/frequent designation of the two tones on half of the runs to determine if the difference in stimulus attributes obstructs the analysis of the endogenous components. If it does, then it will be essential to examine the odd-ball difference potentials calculated from the same tone used in different runs as the frequent or rare stimulus.

4.4.6 Ignore Condition

Besides controlling the stimulus attributes to reduce the variability of the exogenous components, it is necessary to control the task to reduce the variability of the endogenous components. If the endogenous components are truly caused by attending to the tones, then it should be possible to suppress them by engaging the subject in some other primary task while the tones are ignored. Goodin et al. [1978] utilized this control, presenting subjects with identical sequences of tones while they either attended to the tones or read a book. The endogenous odd-ball components did not appear when the subject was reading, but the exogenous components remained, presumably because the brain has no power of suppression at this level.

4.4.7 Rare/Frequent Probability

Aspects of the odd-ball task ERP are affected by the relative probability of occurrence of the rare and frequent tones. As may be expected, the P300 mostly disappears when the odds reach .50/.50. As the probabilities become more skewed, the amplitude of the P300 rises monotonically [Duncan-Johnson and Donchin 1977]. I chose a ratio of .20/.80 as a compromise in order to produce a robust P300 component in a reasonable number of trials, and because most other workers use that ratio. It would be very interesting to vary the ratio to .50/.50 as a control and to other values to see how the odd-ball ERP changes configuration with stimulus probability.

4.4.8 Pure Exogenous Component

Even though the odd-ball task does not seem to elicit any endogenous potential in response to the frequent tone, it is not possible to be certain without a control for comparison. By generating a sequence of identical tones with the same temporal attributes as the two-tone, odd-ball experiment, and having the subjects listen to it attentively while counting or not counting the tones, and while reading, makes it possible to ascertain what the pure exogenous auditory-evoked potential is like and compare it to the frequent tone ERP from the odd-ball task.

4.4.9 Varying Stimulus Intensity and Pitch

Two additional variables affect the odd-ball ERP: detectability and discriminability. In the auditory modality detectability is primarily affected by stimulus intensity, usually measured in decibels (dB). If the intensity is reduced to near threshold the nature of the task changes to include signal detection. New ERP components appear which confound the surprise ERP component evoked by the odd stimuli. Thus the desire to reduce the exogenous components

must be weighed against the need to restrict the task definition.

Discriminability is mainly affected by the auditory stimulus attributes of intensity and pitch. Pitch also affects detectability, but usually two tones are selected that are near the peak of detectability so that pitch will not be a variable in this regard. Pitch separation, though, can affect the odd-ball ERP. Widely separated pitches are more easily discriminable and elicit a strong P300. As pitch separation decreases, the task becomes more difficult and the response becomes more complicated, just as when detectability decreases. The classical odd-ball ERP is produced when the two stimuli are easily detectable and discriminable. It would be useful to vary these two parameters and study their effects on the sources of the ERP.

4.4.10 Addition of Motor Response

To simplify the analysis, I chose to do the odd-ball task without a motor response. One complication of this was discussed above. Yet another control would be to require a button-press to the rare stimulus as Ritter and Vaughan [1969] did, but this would bias the response, since the motor-related brain potentials would be different for the two stimuli. One could require a different button-press for the frequent tone, but then we would not expect quite the same odd-ball ERP since the subject could not ignore the frequent tones as much as in the mental counting odd-ball task. Nevertheless, such a control should be run, along with a separate motor task where the subject just presses the buttons in various combinations, both self-paced and in response to repetitive cues. Presumably, after the motor components are subtracted, the remaining ERP differences should look like those from the mental counting variant. Any residual differences might reflect responses from mental counting and motor preparedness.

4.5 Conclusion

After consideration of the goals of this experimental work I have chosen to use the auditory odd-ball task to elicit exogenous and endogenous components of the human ERP. It meets requirements of robustness, ease of implementation, moderate data collection, and controllability in relation to other well-known tasks that also produce endogenous components.

5. METHODS

This chapter specifies the exact experimental and analytical methods used in performing the odd-ball tasks chosen for this thesis.

5.1 Experimental

The experimental aspects of these experiments involve subject selection, stimulus parameters, electrodes, amplifiers, referencing, and digitization and storage of data.

5.1.1 Subjects

Three subjects were used, referred to here by the designators S1, S2, and S3. Their ages ranged from 24 to 33 years at the time of the experiments. All three were male; two were graduate students and one a post-doctoral fellow at Caltech and were highly motivated and cooperative. Basic audiological testing revealed that S2 and S3 had normal hearing for their age. Subject S1 was found to have a deficit in his left ear above 2 or 3 KHz. Subjects were volunteers and not remunerated for their participation. Guidelines established by the Caltech/JPL Committee for the Protection of Human Subjects were followed throughout to ensure the safety and privacy of all the subjects.

5.1.2 Stimuli

The only necessary stimuli were two tone bursts. One was set at 800 Hz and the other at 1200 Hz. For subject S1 the tone bursts were produced by a Wavetek signal generator and gated to last 50 ms. For subjects S2 and S3 the tones were produced by an Apple II+ microcomputer equipped with a D/A converter. The amplitude, duration, frequency, and waveform envelope were controllable by the Apple. A 50 ms tone burst length was selected, with a 5 ms ramp at the beginning and end, these being the most commonly used parameters found in

the literature. The tones were presented to the subjects though 8-ohm stereo headsets. For subjects S2 and S3, the intensities of the tones measured at the eardrum were 45 decibels sound pressure level (dB SPL). For S1, the tones were estimated to be 60 dB SPL.

The tones were presented in random order based on the pseudo-random number generator built into the Apple operating system. The selection of tone 1 or tone 2 for each trial was done at run time such that the probability was 0.2 (0.8) for the rare (frequent) tone. Each tone presentation constituted one trial, with the ITI varying randomly with uniform distribution between 1 and 2 seconds. No constraints were placed on the sequence of tones, such as trying to eliminate two rare tones in succession, as some researchers are inclined to do. No other sounds, such as masking noise, were presented to the subjects. They sat in a sound-attenuating room inside another quiet room in the basement of a quiet building.

5.1.3 Data Collection

Figure 5-1 shows a schematic diagram of the experimental setup and equipment used for subject stimulation and EEG data recording. Details of the operation of this equipment for the odd-ball experiments are explained below.

5.1.3.1 Electrodes The system used for multi-electrode placement had been previously developed at Caltech by Fender and colleagues [Fender and Santoro 1977, Ary et al. 1981a]. It consisted of custom-fit plexiglas helmets with equi-angularly spaced holes where electrodes could be applied in consistent locations from day to day. The electrodes were brass cylinders coated with Ag/AgCl, with cupped ends for holding electrode gel. To apply the electrodes the helmet was donned and adjusted to skull landmarks, primarily the inion at the back of the head. The helmets are very close-fitting and do not rotate on the head in a side-

to-side manner, hence the inion positioning was sufficient to allow the application of the helmet in an identical position from day to day. Each electrode site was prepared through the 1.7 cm diameter access hole by parting the subject's hair and abrading the scalp with a dab of Hewlett Packard Redux Paste electrolyte gel. After each site was prepared, a rubber grommet was placed in the access hole and an electrode with its cupped end full of more conductive electrolyte gel was inserted through the center of the grommet and pressed against the scalp.

The montages for the electrodes were laid out to give as wide a coverage of the head as possible. This was deemed necessary because of the unknown topography of the odd-ball endogenous potentials and the probable involvement of widely separated areas of the brain. Indeed, the only time one should not use such a montage is when the phenomenon is known to have gradients in a proscribed area and one wishes to study that area in greater spatial detail. ESM generally works better the more widely separated the measuring sites. Figure 5-2 shows the montages used for each subject. S1 had 40 active recording sites, while S2 and S3 had 48.

After all the electrodes were in place, the ac impedances were checked using a modified Grass Model EZM1D Electrode Impedance Meter that applied a 30 Hz square wave to each electrode in turn, with the return current path through the parallel combination of the remaining electrodes. Impedances were minimized as much as possible by twisting the electrodes down in the grommets against the scalp until the subject expressed discomfort. High impedance electrodes were removed and the site prepared again. Impedances generally ranged from 2 to 15 K ohms for S1 and also for S3, but with a few at 20 K ohms. Subject S2 evidently had highly resistive skin, registering impedances from 5 to 30 K ohms and several up to 40 K ohms.

The whole process of electrode application and testing took about two hours. In most cases the impedances were also measured after the experimental session and were found to be the same or less than before the experiment was run.

5.1.3.2 Amplifiers and Referencing All EEG signals were amplified by custom-built amplifiers based on a Burr-Brown hybrid technology instrumentation op-amp. All their gains were set to 45000 (+-1%) prior to each experimental run by adjusting the output amplitude of a 20 Hz sine wave. The amplifiers had switch-selectable bandwidths of 0.5 to 30, 60, or 90 Hz. For S1 the 30 Hz bandwidth was used. This was changed to 90 Hz for S2 and S3 in an attempt to get a better idea of the higher frequency spectral components of the responses. Filtering was later performed on the data of S3 in order to compare it to S1's. Figure 5-3 shows the amplitude and phase characteristics of a typical amplifier used in these recordings.

Several features of the amplifier system are provided for subject protection. The input stages, connected directly to the subject, are battery powered so that if any faults occur in those sections the voltage applied to the subject is limited. The whole input section is optically isolated from the output section by integrated circuit devices rated with a 500 volt breakdown potential. The power supply for the output stages is rectified from line voltage protected by ground-fault interrupters.

Differential amplification is necessary to reject common-mode signals that can be of higher amplitude than the signal (EEG) itself. In most operating environments 60 Hz signals are induced into the body from line currents or motor-run equipment. These noise signals will appear on all leads connected to a subject and can be greatly attenuated by the process of differential

amplification. Though the subject and amplifiers were in a double Faraday cage, 60 Hz line current still could be picked up with certain configurations of the leads. The ongoing EEG was examined on all channels continuously during the experiments to check for noticeable 60 Hz interference, and none was found.

To achieve differential amplification, two additional electrodes must be attached to the subject besides the 40 or 48 active electrodes. A reference electrode is used to establish a baseline against which all the active electrodes are measured, recalling that only potential differences can be measured. The ground electrode is used to establish a baseline against which the reference and active electrodes are measured in turn, thus subtracting out the common mode voltage appearing on the ground electrode. The locations of the ground and reference electrodes for each subject are indicated in Figure 5-2. The placement of the reference is not critical to the analysis here because reference-free methods, namely topographic descriptions and ESM, will be used in the interpretation of the results.

5.1.3.3 Digitization and Storage The amplified EEG signals were brought outside the Faraday cage and, along with a stimulus indicator signal produced by the Apple, fed to a custom-built data acquisition system (DAS). The DAS multiplexed all of these signals sequentially every four ms through a variable-gain buffer amplifier and performed a 12-bit analog-to-digital (A/D) conversion. The buffer gain was set to 2.0 for all of the experiments described here. Only the higher order 8 bits were saved and stored on digital magnetic tape. The total conversion time was fixed at 10 μ s per channel, for a total time of 400 or 480 μ s required per time frame, depending on the subject. Thus the total elapsed time between sampling the first and last channel was 0.39 or 0.47 ms, or about 10 percent of the interval between successive time samples. No correction was applied to the data to compensate for this slight time shift between sampling

successive channels.

5.1.3.4 The Run of the Experiment After all electrodes were in place and their impedance checked, the subject was seated in a chair in front of a table inside the Faraday cage. Electrode cables were attached to the amplifiers along with the ground and reference electrodes. The headphones were placed on his head avoiding disturbance of the EEG electrodes. At this point the subject's EEG was visually examined by means of a multiplexed oscilloscope display system and electrodes that gave obviously bad signals were corrected. Once it was established that the EEG was nominal the subject was given instructions to keep his eyes open and to fixate on a small red light seen through the shielded window of the Faraday cage. He was instructed to listen to the tones coming from the headphones and to keep a running mental count of the number of occurrences of the rare one of the two. A test run was conducted to check the equipment and familiarize the subject with the task. The test run also provided the definition of the rare and frequent tones. The subject was told to minimize movements, especially of the eyes and facial muscles.

When the subject was ready, the light was turned out in the Faraday cage and the door closed. For each run the subject first indicated his readiness; then the experimenter started an Apple program that controlled the DAS and selected and presented the stimuli. The DAS sampled and stored data continuously during each run. At the end of each run the Apple printed the complete tone sequence used and the total number of frequent and rare tones. The experimenter then opened the door of the cage to ask the subject how many rare tones he had counted. Two 5.5 minute runs were recorded for S1, with tone 1 as the rare tone in both. Six 3.0 minute runs were recorded for S3, also with tone 1 as the rare tone in all runs. Six 3.0 minute runs were recorded for S2, with tone 1 being rare for the first three and tone 2 being rare for the second

three. Subjects S2 and S3 had breaks between their two sets of three runs in which two 30 second recordings of ongoing EEG were recorded, one with eyes open and one with eyes closed. Each subject was in the Faraday cage about 30 minutes total.

After data collection was completed the electrode impedances were checked for stability and the batteries were checked to see if they were still providing the necessary potential to the voltage regulators of the input stage. The subject was relieved of his electrodes and given the option of washing his hair. Data tapes were removed from the DAS and taken to an IBM 370 computer for copying.

5.2 Analytical Methods

A flow chart of the data analysis is shown in Figure 5-4. The same basic analysis was performed on all three subjects. Additionally, S3's data were low-pass filtered after averaging in an attempt to remove high-frequency noise. The details of each step in the data processing are explained below.

5.2.1 Averaging

It is commonly assumed that a single EP is the sum of some signal arising from brain regions excited by the eliciting stimulus and some noise unrelated to the stimulus coming from different brain regions. This relation can be expressed analytically as an algebraic sum

$$EP(n) = s(n) + e(n), n = 0, 255 \qquad (5.1)$$

where EP is an evoked potential sequence, s is the signal of interest, and e is the error term or noise. In an evoked potential experiment such as this the signal of interest has a maximum value of about 10 μV, whereas the signal actually recorded has a maximum value of about 100 μV. In most cases it is impossible to discern the EP in the noise without some form of signal processing

to increase the signal/noise. The typical method for accomplishing this is to average multiple segments of the EEG waveforms time-locked to the external stimulus. If, as commonly assumed, the EP signal is not variable in time and the background EEG noise can be modeled as a random process with zero mean, then the signal/noise can be improved by a multiplicative factor proportional to the square root of the number of repetitions averaged [Ruchkin 1965]. For example, averaging 100 repetitions would thus increase the signal/noise by a factor of ten.

Both of the previous assumptions are known to be false. EPs, and especially the later components, are not the same every time they are elicited. The EEG is not stationary over the period required to record even a few EPs. But there is a dearth of viable alternatives to time-domain averaging. One major problem is that the EEG and EP have quite similar spectral characteristics, making it difficult to apply frequency-domain methods to increasing the signal/noise. Slight differences in the characteristics of the EEG and EP have been used in schemes to filter the background EEG from the EP signal of interest [McGillem and Aunon 1977] but were considered too untried for application here.

Data tapes were taken to a VAX 11/780 system for off-line analysis with Fortran programs. The first step in the analysis was to extract the stimulus channel from each run and identify all the points where sections of the data should be extracted for averaging the rare and frequent responses. Then the data were passed through a second time to actually perform the averaging. A section of data 256 frames long was averaged for each stimulus, with 25 pre-stimulus frames and 231 post-stimulus frames. This process is formalized by

$$aEP_{ic,is}(n) = \frac{\sum_{ir=1}^{Nreps} EP_{ic,is,ir}(n)}{Nreps_{is}}, \qquad \begin{bmatrix} ic = 1, Nchan \\ is = 1, Nruns \\ n = 0, 255 \end{bmatrix} \tag{5.2}$$

where *aEP* is the average evoked potential sequence, *ir* the repetition index, *Nreps* the number of stimulus repetitions, *ic* the channel or electrode index, *Nchan* the total number of channels, *is* the experimental run number, *Nruns* the total number of runs, and n the time index. The resulting average evoked potentials (aEP) for the rare and frequent tones then ranged from -100 ms before the stimulus to 920 ms after the stimulus, each time frame being separated by 4 ms. The pre-stimulus period was desired to determine whether there was any stimulus artifact or leftovers from the previous response, and to establish a potential baseline. The post-stimulus period was long enough to capture the section of the EP in which we are interested. Using exactly 256 frames was, of course, a concession to the efficient computation of digital signal-processing algorithms.

The aEPs were stored on disk and magtape. Multiple aEPs from separate runs but identical stimulus conditions were averaged together, weighted by the number of stimulus repetitions of each. This process can be represented by

$$gaEP_{ic}(n) = \frac{\sum_{is=1}^{Nruns} aEP_{ic,is}(n) \cdot Nreps_{is}}{\sum_{is=1}^{Nruns} Nreps_{is}}, \qquad \begin{bmatrix} ic = 1, Nchan \\ n = 0, 255 \end{bmatrix} \tag{5.3}$$

where *gaEP* is the resultant grand average evoked potential and the rest of the variables are the same as before. This could not be done for S1, only one of whose runs was actually useable. For S2 and S3 six runs were averaged together, producing two grand average EPs (gaEP), one to the rare and one to the frequent tones. The next step was to subtract the DC amplifier offset from each channel. The offset was determined as the average value of the signal over

the 25 pre-stimulus values. This calculation is expressed as

$$gaEP_{ic}(n) = gaEP_{ic}(n) - \sum_{in=0}^{Npre-1} gaEP_{ic}(in), \qquad \begin{bmatrix} ic = 1, Nchan \\ n = 0, 255 \end{bmatrix} \tag{5.4}$$

where $gaEP'$ is the adjusted grand average sequence, in a dummy time index, and $Npre$ the number of pre-stimulus samples.

5.2.2 Difference Potentials

To more clearly define the changes in the EPs between the rare and frequent cases, the difference potential was calculated as the rare gaEP minus the frequent gaEP. This is formalized as

$$dEP_{ic}(n) = rEP_{ic}(n) - fEP_{ic}(n), \qquad \begin{bmatrix} ic = 1, Nchan \\ n = 0, 255 \end{bmatrix} \tag{5.5}$$

with d, r, and f standing for the difference, rare, and frequent experimental conditions. The resulting difference EP was taken as the operational definition of the odd-ball ERP. The interpretation of such a calculation is somewhat controversial. Its use here is defended in Chapter 7.

5.2.3 Lowpass Filtering

Digital lowpass filtering was performed on S3's averaged data in an attempt to remove high-frequency noise that was discovered after the experiment was run and for comparison to S1's data that was recorded at a lower bandpass. A finite-impulse response filter of 51 sample points with a frequency cut-off of 30 Hz was convolved with the three gaEPs of S3 before they were average referenced.

5.2.4 Average Referencing

Software average referencing was next performed on the three resultant EPs for each of the three subjects. At each time frame the average value of the

voltage over all the electrodes was calculated and then subtracted from each electrode at that time frame. We can represent this by

$$xEP_{ic}(n) = xEP_{ic}(n) - \frac{\sum_{jc=1}^{Nchan} xEP_{jc}(n)}{Nchan}, \qquad \begin{bmatrix} ic = 1, Nchan \\ n = 0, 255 \\ x = d, f, r \end{bmatrix} \tag{5.6}$$

where x represents the experimental condition. The result of this operation is to equalize the areas of positive and negative potential over the head for each frame. Assuming uniform spatial sampling the spatial potential gradients remain the same, but the ESM algorithms work more efficiently with the constant spatial component removed. The resulting equipotential maps are also easier to interpret.

5.2.5 Spatial Power

When only a small number of electrodes are used in an experiment it is possible to break up an EP into a series of peaks and valleys that can be discussed and analyzed separately. The segmentation may not necessarily agree with any underlying brain processes, but it is a convenience none-the-less. With many electrodes, no one of them can be singled out as representing the typical response, yet the need for a summary of the response is even more desired. One such summary statistic is the spatial field power [Lehmann and Skrandies 1980], defined at each time frame as the sum of squares of the potentials over all the electrodes, or

$$SFP_x(n) = \sum_{ic=1}^{Nchan} \left[xEP_{ic}(n) \right]^2, \qquad \begin{bmatrix} n = 0, 255 \\ x = d, f, r \end{bmatrix} \tag{5.7}$$

with *SFP* being the spatial field power sequence. It represents a measure of the strength and complexity of the potential gradients at an instant in time, but has no simple relationship to the actual underlying sources of the potentials.

Spatial field power curves were calculated for each condition of each subject. Plots were made for each subject, normalized to the maximum power among that subject's three basic xEPs. Comparisons among subjects were not justified, since each had unknown anatomical and physiological parameters that would affect the strength of the potentials at the scalp surface.

5.2.6 Equipotential Plotting

In order to visualize the spatial potential distribution at particular times of a response, contour plots were made of the potential over the surface of the head. Figure 5-5 shows examples of such equipotential maps. They cover an area of the head encompassing all the measuring sites used, which are in turn marked with x's. To achieve smooth and more realistic contours, missing potential values are estimated by local spatial averaging and assigned to the unused electrode locations. Then bi-cubic spline fitting is used to define a finer mesh of potential values between the standard electrode positions. Two extra positions between each electrode are used, thus tripling the linear sampling and increasing the spatial sampling density nine times.

Equipotential maps were only plotted for times when the spatial power was above a criterion value. Maps of low level responses are noisy and, while very interesting to look at, contain little useful information and lead to confusion.

5.2.7 Equivalent Source Modeling

5.2.7.1 Forward Solution The main intent of this thesis was to apply ESM to the EPs from the odd-ball task. To this end a homogeneous model of the head was used, consisting of a unit sphere of conductivity σ with imbedded point dipoles, surrounded by a non-conductive medium to simulate the air. The coordinate system used for this model is shown in Figure 5-6. The potential for any point on the surface of this head was given by the same equations used in Kavanagh et

al. [1978]. Multiple-dipole source configurations were calculated by summing the potentials produced by each component dipole at each electrode site. This is valid because the principle of superposition holds. The voltage at a particular location on the surface of the model head is given by

$$V_{ic} = f(d_1, d_2, d_3, \ldots, d_m) \tag{5.8}$$

$$= f(d_1) + f(d_2) + f(d_3) + \cdots + f(d_m)$$

where V_{ic} is the voltage, f the potential function, and d_m a dipole with six parameters representing its location and moment.

5.2.7.2 Inverse Solution The central technique of the variant of ESM used here is the actual equivalent source localization. A simplex algorithm [Nelder and Mead 1965] was used for all source localizations in this thesis. Given an initial guess for a dipole configuration, this algorithm varied the parameters of the dipole(s) until an optimal least-squares fit to the measured experimental data was obtained. Either 6 or 12 parameters were varied, representing one or two dipoles. The convergence criterion was set empirically to achieve accurate localization in a reasonable number of iterations. The following function was thus minimized at selected time frames

$$ERR_x = \sum_{ic=1}^{Nchan} \left[V_{ic} - xEP_{ic} \right]^2, \qquad x = d, f, r. \tag{5.9}$$

The results of each equivalent source localization were thus 6 or 12 numbers defining the location, strength, and orientation of the one or two dipoles that best fit the experimental data for that time frame.

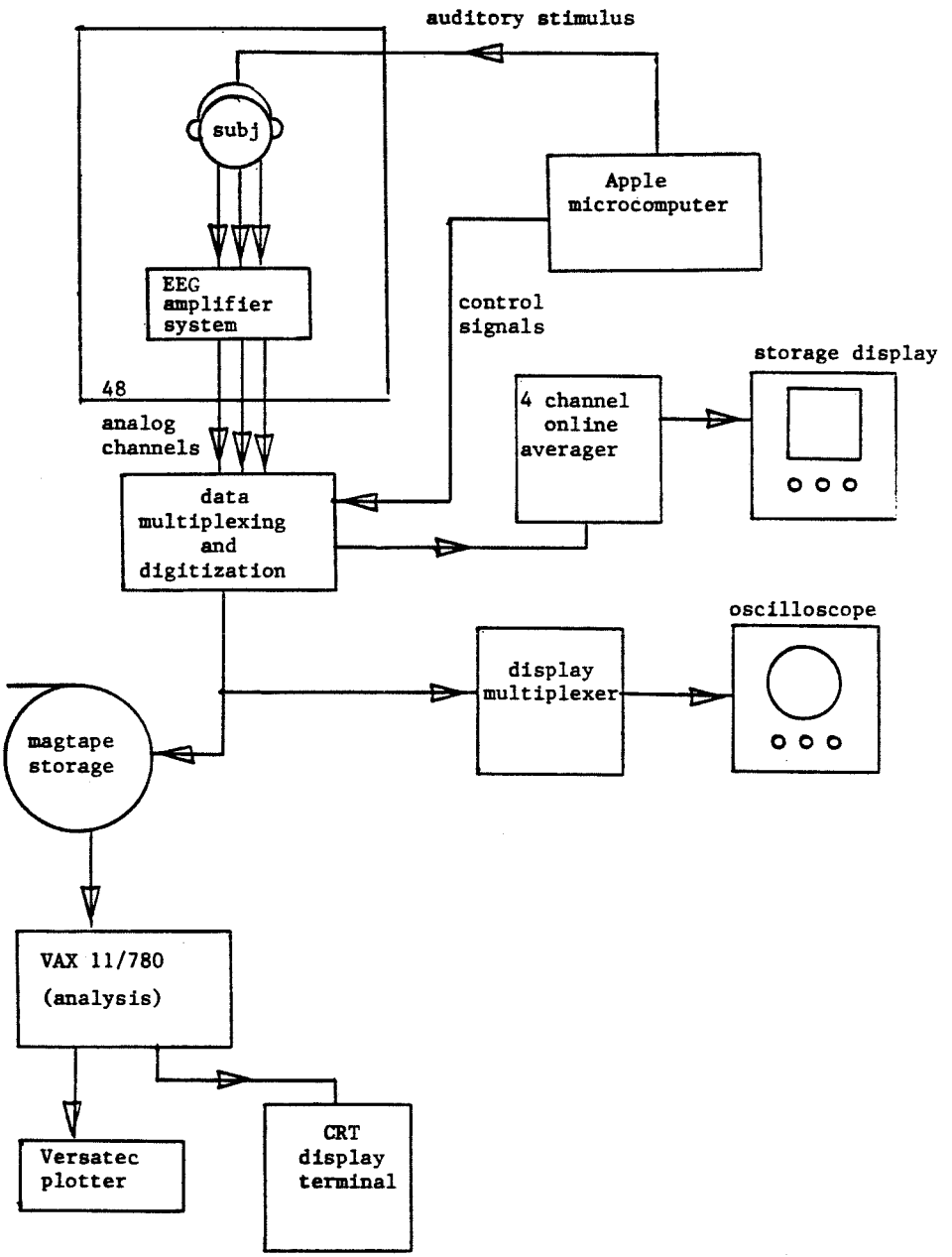

Figure 5-1. Schematic diagram of experimental equipment.

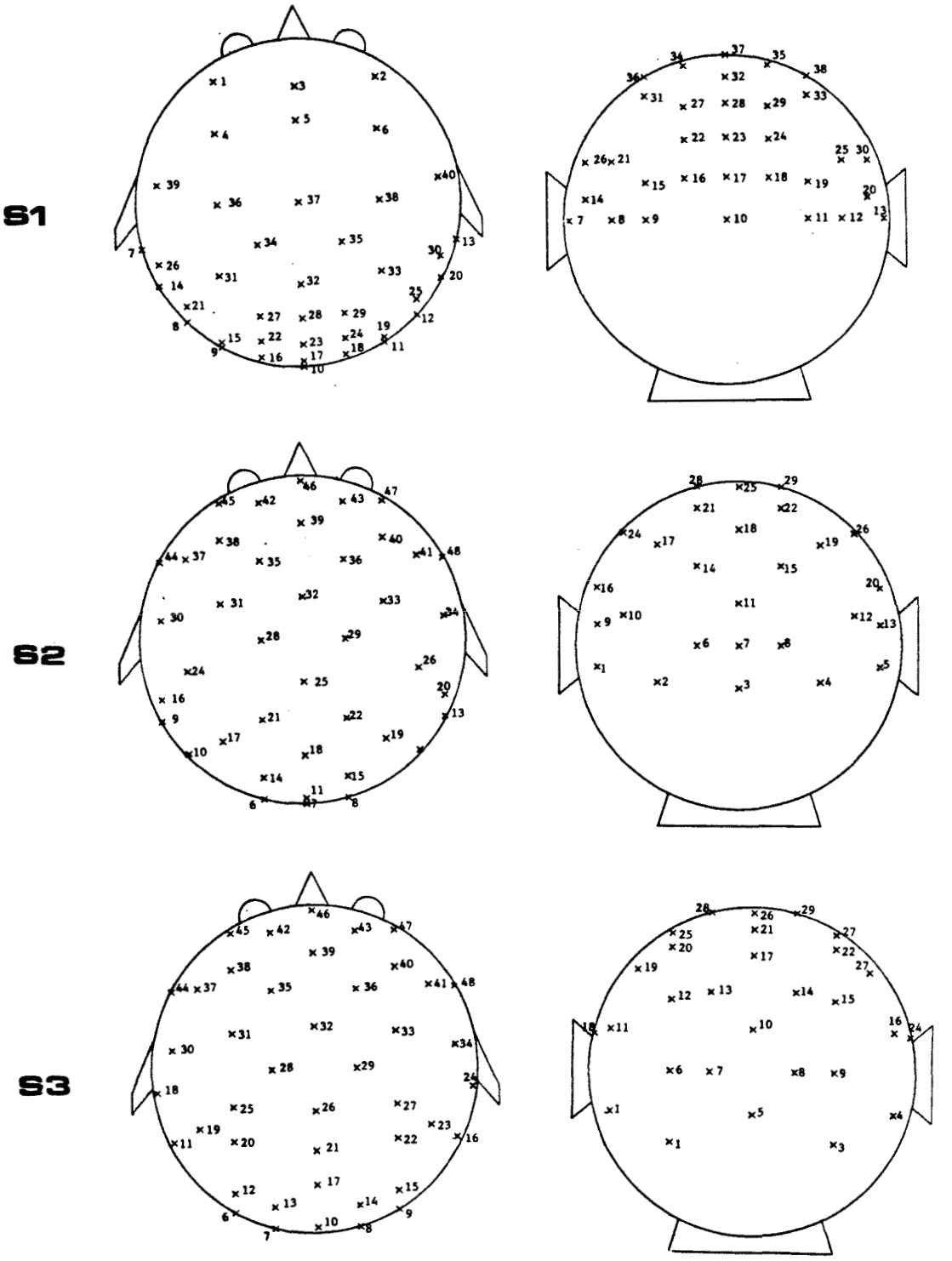

Figure 5-2. Electrode montages for three subjects.

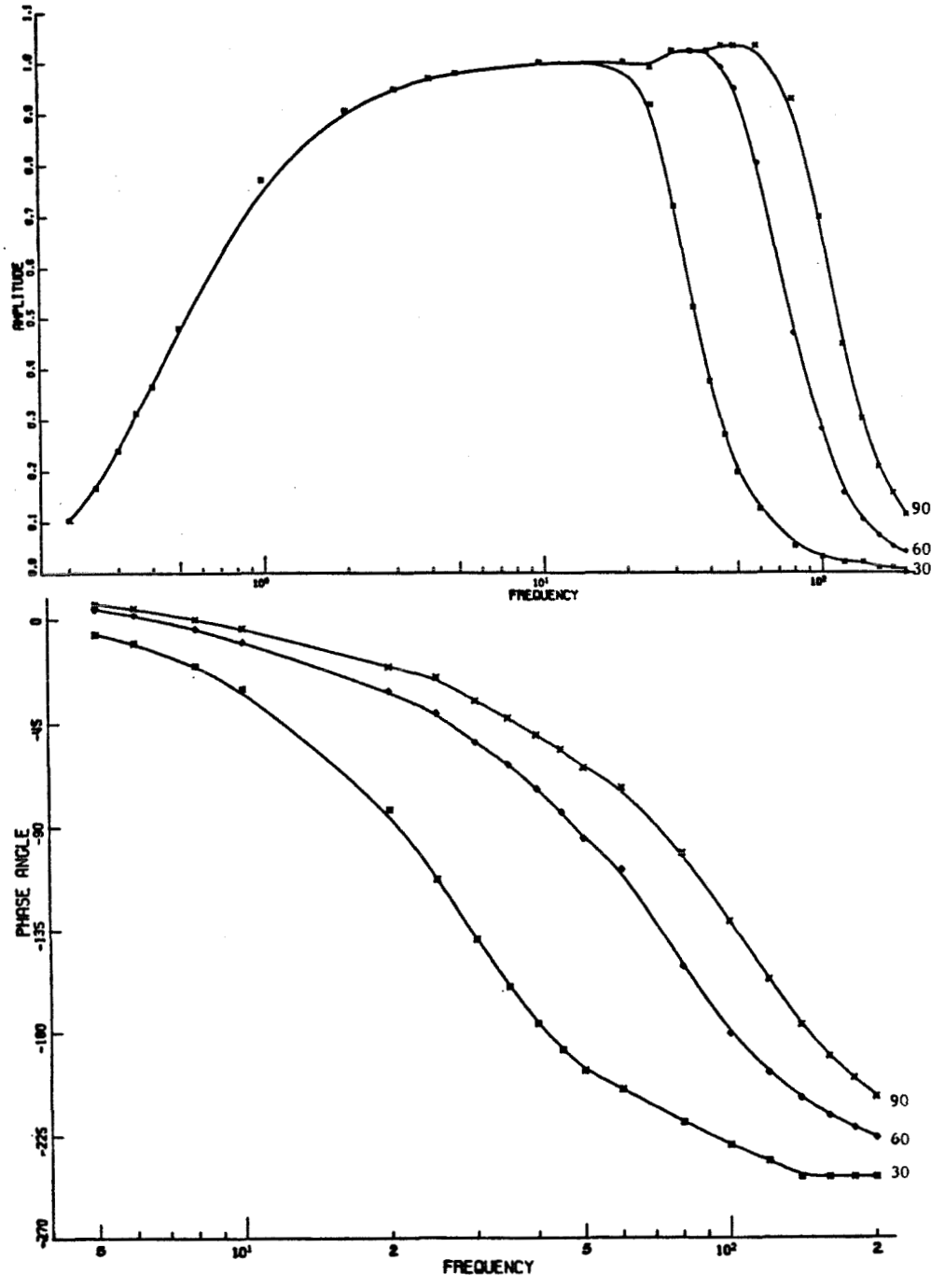

Figure 5-3. Typical EEG amplifier gain and phase.

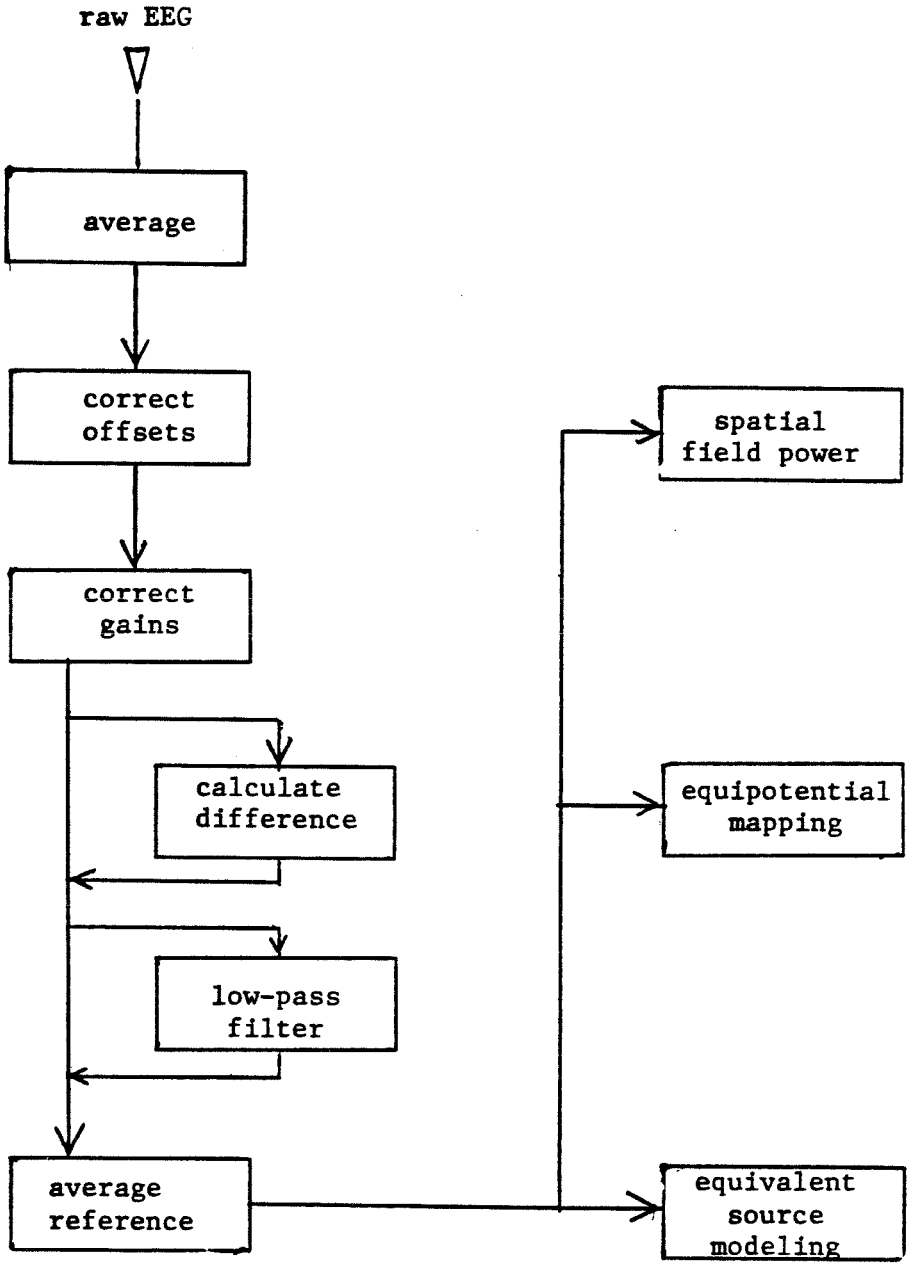

Figure 5-4. Data analysis flow chart.

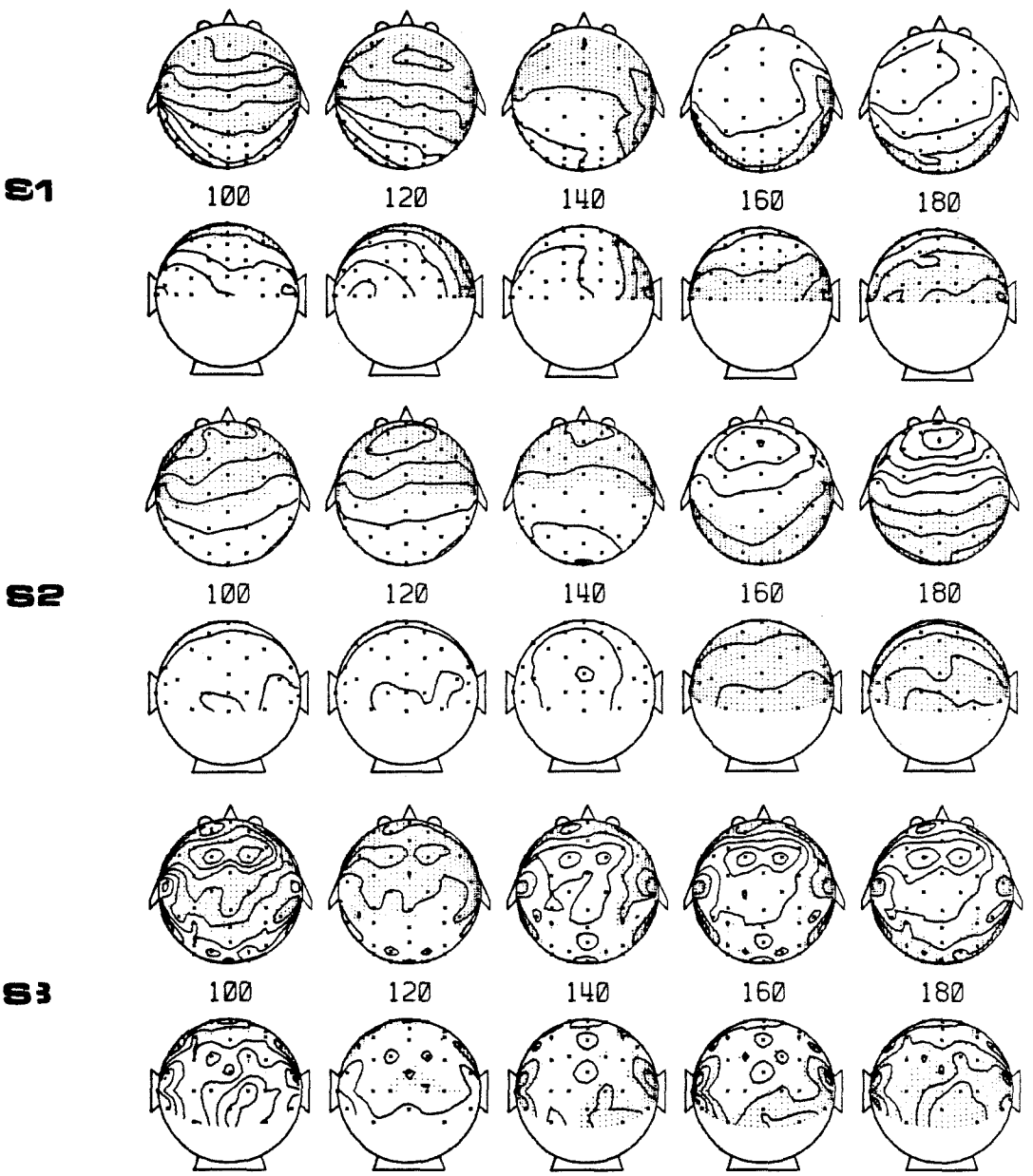

Figure 5-5. Examples of equipotential maps.

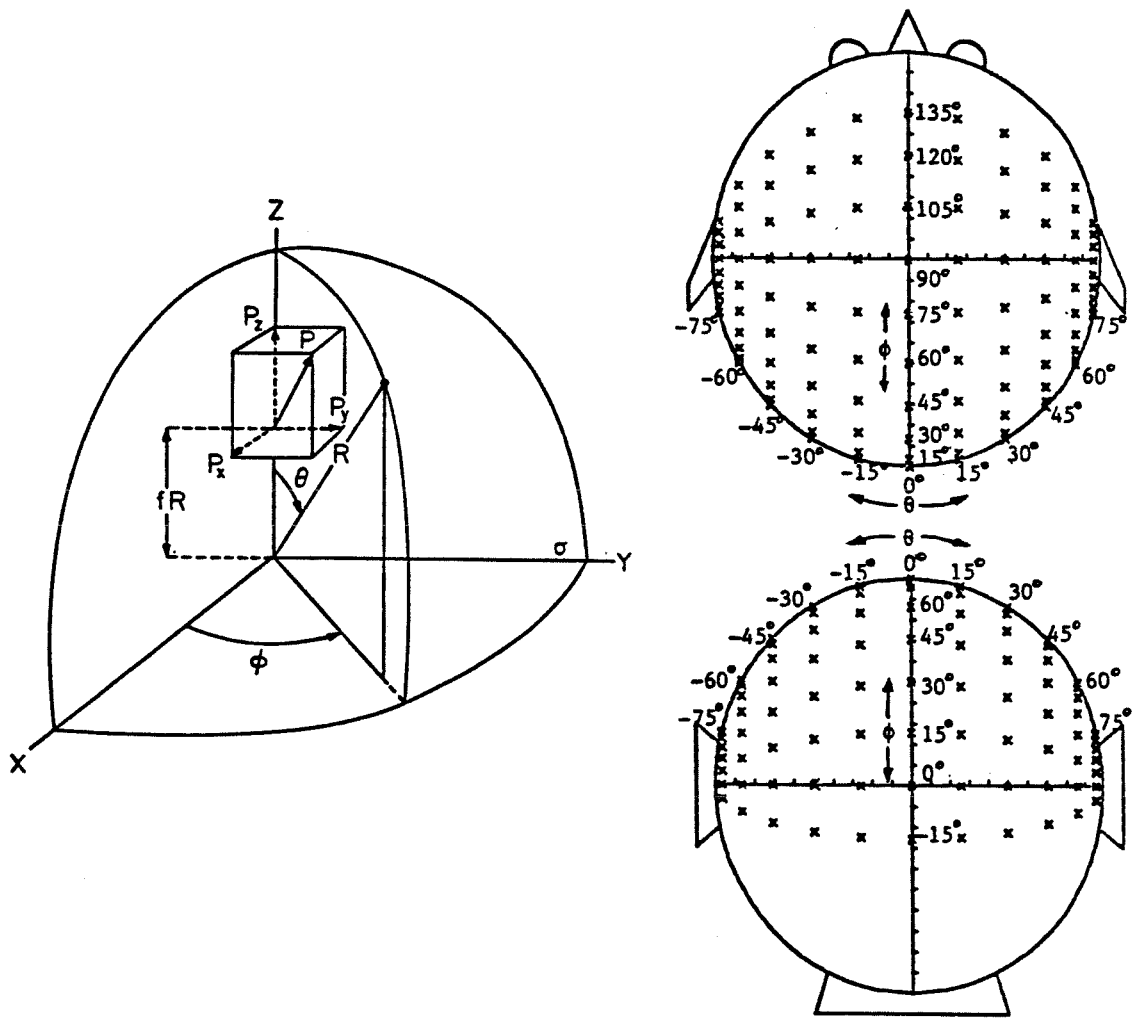

Figure 5-6. Coordinate system used for mathematical model of the head.

6. RESULTS

In this chapter I present some of the data obtained during the odd-ball experimental task and the results of topographic and source localization studies. First I summarize the stimulus sequences as they actually occurred. Next I review the raw data that were collected for each subject. Then I present the averaged EPs for each subject under the frequent and rare conditions and the difference potential calculated from these. I next show a selection of equipotential maps for each condition and each subject. Finally, I offer the results of one and two dipole modeling of the sources of these EPs.

6.1 Stimulus Summary

Only the first of the two runs for S1 was recovered, due to equipment malfunction. It was a continuous recording of 86372 time frames, or about 345 seconds. A total of 242 stimuli were delivered, 197 frequent and 45 rare. The measured rare/frequent probability ratio is thus .19/.81. The ITIs ranged from 0.99 to 1.86 seconds, with a mean of 1.40 seconds. To check the uniformity of the ITI sampling distribution, they were sorted into ten bins of equal duration over the inclusive range. The tabulated bin values are: (24, 30, 24, 28, 26, 20, 27, 22, 21, 19).

S2 completed six runs, the first five of which lasted 177 seconds on average, the sixth lasting 124 seconds. A total of 668 stimuli were delivered, 524 frequent and 144 rare, for a probability ratio of .21/.78. The ITIs ranged from 1.03 to 1.99 seconds, with a mean of 1.50 seconds. The sampling distribution is represented by the following values: (59, 66, 72, 85, 66, 52, 64, 65, 78, 55).

S3 also completed six runs averaging 177 seconds. He heard 708 tones in all, of which 548 were the frequent and 160 the rare tone. The measured probability ratio is .23/.77. The ITIs ranged from 1.03 to 1.99 seconds, with a

mean of 1.48 seconds. Bin values for the ITIs are: (68, 69, 79, 86, 67, 69, 66, 67, 77, 54). Comparing the distribution of ITIs from the three subjects, I detect biases in the sequence, with a peak in the fourth bin. I judge the bias to be negligible in terms of the goals of this thesis, which do not include an in-depth study of stimulus probability.

All three subjects had no difficulty counting the number of rare stimulus occurrences, missing the correct value by no more than one either way.

6.2 EEG Data

Examples of the raw EEG data recorded from each subject are shown in Figure 6-1. It is readily apparent from the lack of higher-frequency components that the data for S1 were recorded at a lower bandpass than the data for S2 and S3 (30 vs 90 Hz). S2 has very obvious alpha (8 to 13 Hz) waveforms with a frequency of about 10 Hz and amplitude of about 40 μV peak-to-peak, while S3 has alpha of lesser amplitude. S2 had a difficult time staying alert during the experiment, as is evidenced in the alpha activity scattered throughout all of his data, and as was verbally verified after each run. Indeed, during the experiment I could watch S2's alpha on most of the channels displayed on the display multiplexer. Overall, the subjects had an ongoing EEG of about 100 μV peak-to-peak.

6.3 Average Evoked Potentials

After offset adjustment, gain adjustment, low-pass filtering, differencing, and average referencing, I obtained aEPs such as displayed in Figure 6-2 for the frequent case. These have the highest signal/noise of the three cases since they have approximately four times as many repetitions. The channels plotted do not necessarily represent the same relative electrode locations on each subject. The positions of the electrodes can be determined from Figure 5-2.

The aEPs for S2 still retain alpha residual, even after well over 500 repetitions are averaged. A small amount can also be seen in S3's aEPs, along with some higher-frequency components in the beta range (13 to 22 Hz). S1 has some beta-range noise as well. If the relative amounts of alpha and beta activity are used as a measure of subject attentiveness, then S1 can be judged the most cooperative and S2 the least.

6.3.1 Spatial Field-Power

Comparing this set of aEPs we can see that they each have three major peaks following stimulus onset (indicated by the vertical line). These three peaks change polarity from positive to negative to positive on some electrodes, and from negative to positive to negative on other electrodes. On closer examination, though, it can be seen that these peaks occur at slightly different times on different electrodes. How can we summarize the time course of these aEPs if they each have different features? The spatial field-power curves in Figures 6-3 through 6-5 represent one way.

A quick glance at the three subjects' power curves reveals quite a bit of complexity in the responses and a lot of variability among subjects. I have split the analysis interval into four sub-intervals: 0-250, 250-400, 400-650, and 650-920 ms. These were chosen based on the observation that the power curves for all subjects under all conditions fall close to zero between them. For clarity, I will use the terms FREQ, RARE, and DIFF to refer to the frequent, rare, and difference cases throughout this chapter.

Each power calculation will be discussed in detail below, but a few general features will be mentioned here. The only interval where all three subjects have similar power curves is the first one, before 200 ms. Here each subject has two large peaks in the FREQ and RARE cases and negligible power in the DIFF

response. Most subjects' responses fall away in the last interval, except for the DIFF response of S3.

6.3.1.1 Frequent Tone Response The upper portion of Figure 6-3 shows the field-power curve for S1. It consists of three major peaks at 88, 208, and 320 ms, with a small but definite earlier peak at 40 ms. The pre-stimulus power is negligible, as is the power after 376 ms. The three main peaks obviously correspond to the three major peaks of the individual aEPs.

The FREQ tone response for S2 is shown in Figure 6-4, consisting of three major peaks at 116, 184, and 288 ms that seem to correspond to the three major peaks of S1. A peak at 40 ms is also evident and seems to stand out from the pre-stimulus baseline. The pre-stimulus noise has been mostly eliminated by the averaging of 524 responses. An additional peak at 412 ms may be caused by the alpha generator. This can be surmised from an examination of the aEPs for various channels over the head, in particular channels 40 through 48 (see Appendix A). This subject evidently produced alpha bursts after, or in conjunction with, the typical auditory-evoked responses.

S3's FREQ response power curve is shown in Figure 6-5. It starts with a definite 40 ms peak, corresponding to those of S1 and S2. The next two peaks at 104 and 188 ms correspond to S1 (88 and 208 ms) and S2 (116 and 184) also. The next two peaks, at 372 and 484, do not correspond to either S1 or S2. In addition, S3 has appreciable field-power from 665 to 920 ms, whereas neither S1 or S2 do.

Figure 6-6 compares the FREQ power curves for all subjects. In this and the two subsequent figures the spatial field-power curves have been individually normalized to help in a relative comparison. One might think that the absolute field-power values should be retained for direct comparison of brain activity

power between subjects, but such a comparison would be unreliable without knowledge of the individual electrical parameters of each subject's head.

In summary, the FREQ field-power curves show similar early peaks for all three subjects at about 40, 100, and 200 ms. After 250 ms, though, each subject shows a different structure in his response. These differences presumably reflect the different cognitive strategies used by each subject in performing the odd-ball task with concomitant mental counting.

6.3.1.2 Rare Tone Response S1 shows a most complex RARE response power curve in Figure 6-3. However, some of the complexity may be artifactual. Only 45 stimulus repetitions were averaged and the pre-stimulus and near-stimulus power is appreciable, thus indicating the presence of significant noise throughout the RARE aEPs. The 40 ms peak found in the FREQ case is now probably buried in this noise. The first strong peak occurs at 88 ms, corresponding exactly with the FREQ case for the same subject. A knee at 120 ms is more prominent than the knee seen on the FREQ power curve. The second peak occurs at 180 ms and a third at 264, unlike the FREQ response. However, it is possible that the 180 peak is just the FREQ 208 peak that has been shifted by the inclusion of extra cognitive processing. A fourth double-capped peak at 348 ms matches the 320 peak of the FREQ response. A completely new broad peak then occurs, from about 400 to 700 ms, that has no analog in the FREQ case. It has three sub-peaks, but these may be artifacts that were not completely averaged out. Examination of the aEPs for S1's RARE case (see Appendix B) bears this out on channels 1 to 10, especially.

On the basis of S1's RARE and FREQ responses it is obvious that some differences in processing are occurring between the two cases as early as 200 ms, maybe even 150 ms. Certainly there is substantial extra activity after 400

ms in addition to the changes from 150 to 350 ms.

The field-power curve for S2's RARE response, in Figure 6-4, shows no more complexity than his FREQ response. The 40 ms peak is barely visible. A double capped peak at 104-124 ms directly matches the FREQ 116 peak. The 192 ms peak directly matches the FREQ 184 peak, and ditto for the 280 RARE and 288 FREQ peaks. The 412 ms FREQ peak is replaced by a small 368 ms peak. S2 is not unusual in his low response. Many have been reported in the literature. Most researchers admit to subject selection in order to get high amplitude responses.

S3's RARE response is shown in the middle of Figure 6-5. The ubiquitous 40 ms peak is quite evident, followed by an 88 ms peak that matches the 104 ms FREQ peak. The next peak at 156 ms matches the 188 ms FREQ peak in duration, though the peak maximum has shifted considerably, perhaps representing a difference in exogenous response to the slightly different tone frequencies. The rest of the power curve is complicated, as it is for S1, but not as high in power. Pre-stimulus noise is not completely averaged out. Nevertheless, a peak at 312, a broad peak at 500, and two very late peaks at 740 and 868 ms can be discerned.

Figure 6-7 compares the RARE response field-power curves for these three subjects. All three subjects have two major peaks at corresponding latencies near 100 and 200 ms, as in the FREQ case. Any earlier peaks get lost in the noise, since the number of repetitions averaged is only about 20 percent of the repetitions for the FREQ case. Only S3 still shows a strong 40 ms peak. In the second interval, from 250 to 400 ms, each subject might be said to have two peaks, but their relative latencies and power level vary widely among the subjects tested here. The third interval has the most widely varying structure. S1 has a high, broad peak with three sub-peaks. S2 has a negligible response. S3 has a low, broad peak with one or two sub-peaks. The fourth interval also shows

a lot of inter-subject variability, with S1 registering something near the noise level, S2 again registering essentially nothing, and S3 registering two very late peaks.

6.3.1.3 Difference Response The field power curves for each subject's DIFF response are shown on the bottom of Figures 6-3 through 6-5. A full discussion of the validity and interpretation of DIFF potentials will be postponed until the next chapter. For the present simply consider the DIFF response to be an aid in delineating what has changed between the RARE and FREQ responses. It is important to note that the DIFF power curve is not the difference between the RARE and FREQ power curves. As was explained in the previous chapter it is the power of the aEP calculated by subtracting the FREQ aEP from the RARE aEP.

For S1, differencing uncovers a peak at 216 ms in the first interval, with a smaller one possibly at 164. In the second interval a very large power peak occurs at 332 ms, possibly preceded by a small one at 268. This large peak is used to normalize the FREQ and RARE power curves for this subject. In the third interval the DIFF response is essentially equal to the RARE response, since the FREQ response is negligible. Thus we see the same broad peak that we saw in the RARE case. The fourth interval seems to contain just noise.

S2 has a very low-power DIFF response, but it is above the pre-stimulus noise level. The first interval has peaks at 72, 144, and 196 ms, though these are noisy. Interval two has the largest peaks, at 276 and 368 ms. This low DIFF response may be attributed to this subject's inattentive state during the course of the experiment, though he did meet the (rather simple) behavioral criterion of correct counting of the number of rare tones.

In S3, some pre-stimulus noise is found, but a peak at 208 ms in the first interval rises above it. Differencing uncovers a large power peak in the second

interval of S3's response. A peak rises at 272 ms followed by the knee of the large peak at 320 and 380 ms, respectively. The third interval contains a definite peak at 488 ms, matching ones at 500 ms in the RARE, response and at 484 in the FREQ response. The fourth interval contains a broad peak which covers the whole interval, and two sharp sub-peaks at 744 and 864 ms. These last two are obvious in the RARE response but grow in importance when the FREQ response is subtracted.

Comparing the DIFF response across subjects in Figure 6-8, we see quite a bit of variability. Interval one perhaps contains one peak that corresponds across subjects, at (216, 196, 208) ms for (S1, S2, S3). Interval two is the most consistent across subjects with a large (relative within each subject) peak at (332, 368, 380) ms and possibly another sub-peak at (268, 276, 272) ms. In interval three S1 has a large response, while S2 and S3 have much smaller ones. In the fourth interval S1 has a minimal response, S3 a very large one, and S2 a medium one that somewhat parallels S3's.

6.3.1.4 Summary of Spatial Field Power Analysis All subjects had two large power peaks in the first interval of their FREQ and RARE responses, with a much smaller earlier peak appearing most of the time, also. In their DIFF response, two subjects had large peaks in the second interval, while S2 had a small peak that was nevertheless well above the pre-stimulus noise. Based on analysis of the spatial field power curves, I have decided to concentrate subsequent analysis on the three peaks in the first interval of the FREQ response (40, 100, and 200 ms), and the major peak of the second interval of the DIFF response (350 ms). These are most consistent across subjects and correspond to the time intervals that most other experimenters have concentrated on in the past.

6.4 Equipotential Maps

Though field power curves are a convenient way to summarize an EP, especially when 40 or 48 channels have been recorded, they are a gross over-simplification of the data. All spatial and polarity information is lost. Equipotential mapping is probably the most useful and least biased way to display the information from multiple electrode studies. The amount of information contained in a series of them is vast, so only selected maps will be presented here. I will present maps for each subject and each condition spaced at 40 ms intervals and compare them over the same four intervals selected for the discussion of the power curves.

6.4.1 FrequentTone

S1's maps are shown in Figure 6-9. They are normalized over S1's entire FREQ response to show ten contour levels at the maximum field power, which occurs at 88 ms. In the 0-250 ms interval the field pattern is negative on the back of the head and positive elsewhere at 40 ms, then inverts by 80 ms. It inverts again by 200 ms. In the 250-400 ms interval, the pattern again inverts and then decays away into the noise. Notice that, while the field power is essentially gone by 380 ms, the decaying field pattern is still discernible in the 400 ms map.

S2 shows a similar response in the first inverval in Figure 6-10. At 40 ms the back of the head is negative and the front positive. At 120 ms the pattern is reversed and reverses again at 200 ms. In the second interval it again reverses as it did for S1, but decays much more rapidly and is followed by a same-polarity pattern at 400 ms that then fades into the noise.

The maps for S3 bring to light difficulties that have been so far hidden in the aEPs and power curves. Much spatial noise is obviously present compared to

the maps for S1 and S2. I will suggest four possible origins for this noise, to be discussed partly as I go along and also in a special section in the next chapter. These are 1) EEG amplifier problems, 2) involuntary muscle artifacts, 3) eye-movement artifacts, and 4) intrinsic neural noise including alpha, beta, and epileptiform activity.

Ignoring the spatial noise for the moment, I will first discuss the major topographic features of S3's maps in Figure 6-11. In the 0-250 ms interval, the 40 ms map is comparable to the other subjects in being negative on the back of the head and positive on the front. This inverts at 80 ms and again at 200 ms, thus being comparable with the other subjects. In the 250-400 ms interval the front and right of the head are positive while the top and back are negative. The area around the left ear is positive, however. In the 400-650 ms interval this same pattern decays and then partly re-appears at 600 ms. In the 650-920 ms inverval a stable pattern varies slightly in spatial power with the front negative and the back positive.

Now I will consider the possible sources of spatial noise in S3's equipotential maps. The most obvious difference between his and the other subjects' maps is the occurrence of lots of little circles around various electrode positions. Something that could produce this effect is inequality of the amplifier gains among all the channels. The amplifier system was deteriorating at the time this third subject was run, and stability of the gains was a known problem. Hence, calibration tests were recorded between sets of experimental data. Unfortunately, too large a calibration signal was used, or perhaps feedback in the amplifier system artificially increased the gains. The calibration runs were only partially useable. The gains of some channels were indeed too low, but the relative gains of the rest of the channels could not be determined. The partial information was used to correct the gains that were too low, but with minimal

effect on the equipotential maps.

A second source of noise could be caused by muscle potentials. Muscle artifact should show up as spatially constrained, high-gradient activity on the equipotential maps. Such activity is indeed seen on many of S3's maps around the ears. Note in particular the 80 ms map. The present mapping software does not permit side views of the head, which would make observing the potentials around the ears easier. Many researchers have noted myogenic contamination while recording auditory EPs [Bickford et al. 1961], in particular around 90 ms.

Another extra-cranial source of spatial noise could be eye-related. Eye and facial muscle contractions could give rise to localized high-gradient noise in the frontal area. Eyeball rotation could give rise to lower-gradient noise with the highest gradients also in the frontal area. Frontal spatial gradients can indeed be observed in S3's maps from 80 to 520 ms, and possibly around 800 ms.

The fourth possible noise source that I consider covers all the inter-cranial activity that does not directly relate to the sources of the task-related brain activity, but may be affected in some way by the task. This includes but is not limited to the alpha, beta, and pathological activity generators. Inspection of some of the raw, unfiltered EEG for S3 reveals beta, gamma, and perhaps higher frequency components on occipital, frontal, and right frontal areas. This signal component is another likely source of the frontal and right-frontal spatial noise seen in the maps. Occipital spatial noise can be seen also at 80, 600, and 840 ms, for instance.

These noise sources are all plausible. If they are accounted for, then the three subjects can be seen to have similar responses to the FREQ tones during the 0-250 ms interval, and different responses at later times.

6.4.2 Rare Tone Response Maps

Figure 6-12 shows selected maps from S1's RARE response. In the 0-250 ms interval the topography is fairly similar to the FREQ case, except for some negativity to the front at 200 ms, thus driving the positive spatial peak toward the top of the head. The 250-400 ms interval is marked by changes in the top and frontal areas that eventually lead to a reversal of spatial polarity between 400 and 440 ms. The 400-650 ms interval has high spatial power but the pattern remains stable throughout. In the 650-920 ms interval there is still measurable power, but the pattern is not well organized.

S2 shows little change between his FREQ response to his RARE response in Figure 6-13. In the first interval he displays the same two polarity inversions with similar topographies. The second interval is marked by additional negativity across the back of the head. The third and fourth intervals have very little power.

The RARE response maps for S3 are plotted in Figure 6-14. As for the other two subjects, very little change can be seen throughout the 0-250 ms interval between the FREQ and RARE responses. In describing the rest of the topography I ignore the probable noise around the ears and in the frontal areas. The 250-400 ms interval is marked by rapid change, but with a basic pattern of top positivity and peripheral negativity. The 400-650 ms interval is stable topographically, with the opposite polarity of the previous interval. The 650-920 ms interval is also stable, with frontal positivity and occipital negativity.

Among the three subjects, the first analysis interval is topographically quite consistent for the RARE response. The second interval is also fairly consistent, the field distribution being positive on the top of the head and negative around the back, side, and front. Upon direct visual comparison, the maps for the third

interval also look similar across subjects, with the back positive and the front negative, though S?'s topography is low-power and rotated in the left-right axis. Finally, some similarities can even be seen in the last interval, though not as much as in the three earlier intervals. Here the top is negative, and positive areas appear in the front and/or back depending on the subject and exact time frame.

6.4.3 Difference Response Maps

DIFF maps were plotted based on the potentials obtained from subtracting the FREQ aEPs from the RARE aEPs on a point by point basis. For the present discussion it will be useful to consider the following working hypothesis. Assume that the FREQ response is a result of source configuration A, and that the RARE response is a result of source configuration A and B. Physically, we assume that linear superposition holds, so subtracting the former from the latter would result in a set of aEPs reflecting only source configuration B, or the additional neural generators associated with the extra processing involved upon detecting the RARE tones.

Because of the small number of repetitions in the RARE case, S1 has substantial noise power near near stimulus onset. Hence I will only consider maps for times where the spatial field power rises above this noise. In the first interval, the map at 160 ms in Figure 6-15 has frontal positivity and occipital negativity. This pattern is inverted at 200 ms and then begins to diminish in power and shift at 240 ms. In the second interval the frontal region remains positive and the back negative until 400 ms, when the pattern rotates and reverses. The pattern then remains fairly stable throughout the third interval, though it is skewed to one side. During the fourth interval the activity is down in the noise.

Though very low in field power, S2's DIFF response maps are almost as clean as S1's, as shown in Figure 6-16. In the 0-250 ms interval, the topography first demonstrates a slow rotation from back to front from 80 to 160 ms, then a reversal at 200 ms, ending with the front positive and the back negative. This pattern remains fairly constant through the 250-400 ms interval, with the positive region slowly moving backwards. The 400-650 ms interval first shows two quick reversals around 480 ms and then continues with small front-back and back-front rotations keeping the top or back negative.

Figure 6-17 shows S3's DIFF response maps. During the first interval, the maps are down in the noise. The second interval maps all have the top positive, with negative areas moving in and out of the periphery. In the third interval the positivity rotates around to the back leaving the front negative from 440 through 560 ms, then inverts at 600 ms and continues unchanged throughout the rest of of the third interval and all through the fourth.

Comparing the maps of all three subjects in the 0-250 ms interval I find that S2 differs from the other two subjects, and they are not all that similar. S1 has a strong parietal-occipital potential peak at 200 ms that may match an occipital peak at 240 ms for S3. S2, on the other hand, has a strong frontal potential peak at 200 ms. In the 250-400 ms interval all subjects do have a similar topography, with the back negative and the top and front positive. The 400-650 ms interval shows quite a bit of similarity, too, having the top negative and the back positive. Even the 650-920 interval shows a fair amount of similarity with the front positive and the back negative.

6.5 Equivalent Source Modeling

Field power curves and equipotential maps represent two extremes in data presentation. The first is a condensation to one dimension, the second a full

display of complex and probably redundant information. Equivalent source localization can be viewed as a procedure for parameterization of multichannel data that uses a small set of values to specify the many spatial measurements within some error criterion. The previous qualitative description of equipotential map topography could be accomplished more succinctly with a time series of equivalent sources. I shall instead present a set of sources calculated at times previously selected from the field power curves. Since the traditional positive and negative terminology is not appropriate, I will adopt the letters 'FP' for component designation, as the components considered here were derived from field-power curves.

6.5.1 FP40 FREQ Component

All three subjects have an FP40 peak exactly at 40 ms in their FREQ response. The left-most column of Figure 6-18 compares the maps for each subject. The second column shows the location, orientation, and strength of the best-fit single dipole. The third column maps the field resulting from the dipole in the second column. The fourth column shows the parameters of the two-dipole best-fit solution. The last column maps the field resulting from the two-dipole fit.

Just looking down the first column of experimental data it is obvious that all subjects have a similar topology, though S1's is rotated backwards a bit and skewed to one side. This skew may be a result of a differential hearing loss, which will be discussed later. The single-dipole fits match the experimental data fairly well, based on visual inspection of the maps. The two-dipole fits match the data somewhat better, though not dramatically. For S1 the two dipoles are bilaterally symmetric and in locations not inconsistent with auditory pathways. For S2 the two dipoles do not match expectations for auditory sources, but the

fit may be bad here because of the small spatial gradients involved. For S3 the two dipoles are almost co-linear, indicating that the fit is no better than the one-dipole fit.

A few comments are in order that will apply to the rest of the discussion of source localization. First, only the homogeneous head model has been used. If the more proper inhomogeneous shell model of the head were used instead, the sources would be located more eccentrically, and more physiologically reasonable fits might be achieved. Second, only point dipoles are being used as source models here. More realistic extended sources would also lead to more eccentric source locations. No one would argue that bilateral sources are active at 40 ms, and equivalent source modeling should reflect this. The use of extended sources would most likely result in a two-dipole, bilaterally symmetric source configuration that would fit the data better than one- or two-dipole point sources.

The simplex algorithm used for optimizing the dipole fits is not guaranteed to find the global minimum over the whole parameter space. The final result depends somewhat on the initial guess, the convergence criteria, the initial parameter displacements, and machine round-off error. More optimal results can be obtained by trying multiple guesses, decreasing the convergence criterion, increasing the parameter displacements, and using higher precision machine arithmetic, but convergence time is increased accordingly. Practically speaking, a compromise has to be reached.

Another tactic that can be tried with multiple sources that are presumed to have certain spatial relations is to build those relations into the model. This has the effect of reducing the number of model parameters. For instance, if two dipoles are known to be bilaterally symmetric, a six-parameter model specifying

two mirror-image dipoles can be used instead of a full 12-parameter model for two unconstrained dipoles. Or a nine-parameter model can be used, with three parameters to specify mirror-image locations and three parameters for each dipole's orientation and strength, if they are thought to be unrelated. After reducing the number of model parameters the search space can be increased and a more global minimum with a better fit can possibly be achieved.

6.5.2 FP100 FREQ Component

Figure 6-19 compares the FP100 peak component across the three subjects. The maps of the experimental data in the first column show a similar topography for all subjects with frontal negativity and occipital positivity. One central dipole fits the data quite well for each subject. The two-dipole fits reduce the residual as they are bound to do. Visually, two dipoles fit the maps better than one for S1 and S2. Bilaterally symmetric sources are found for S1 and S2, while S3 has a source in the occipital area that could be an alpha generator. The deeper source for S3 matches the left dipole of the other subjects. Note that the process of dipole localization acts as a form of spatial low-pass filtering on S3's maps, allowing an easier comparison of his results with the other two subjects'.

6.5.3 FP200 FREQ Component

The FP200 component in Figure 6-20 is an inversion of the FP100 component, which in turn was an inversion of the FP40 component. All three subjects again show the same general topography of frontal negativity and occipital negativity. Visually, the FP100 and FP200 look like a true inversion, the topographies being very similar except in polarity. The FP40 and FP100 do not look as similar.

One dipole fits the data fairly well for all three subjects, though S3 is problematic, as usual. Two dipoles fit the topography better for S2 and S3. S1 has two bilaterally symmetric sources, just as he did for the FP40 and FP100 components. The two-dipole fit for S2 is probably spurious, since the resultant dipole would match the one-dipole fit. For S3 one dipole is located very near the ear, indicating a myogenic noise source. The other is near the vertex.

6.5.4 FP350 DIFF Component

The major component of interest for this thesis has been what the ERP literature refers to as the P300 component. Here I have the same component, but defined in terms of the field power calculation on the DIFF potential between the two experimental conditions. For S1 and S2, this peak is the highest power peak for the duration of the response, and for S3 it is the highest in the first 700 ms. Visually inspecting the equipotential maps for each subject's DIFF response it is apparent that this FP350 component is stable for a considerable period. For S1 it lasts from 276 to 344 ms, for S2, from 332 to 396 ms, and for S3, from 268 to 384 ms, though it is harder to judge this last one.

Since the DIFF potential has controversial aspects to it, I will precede its discussion with a comparison of the FREQ and RARE cases from which it is derived. Figure 6-21 shows the results of source localization on the FREQ FP350 for each subject. Topographies are different for each subject, as is the spatial power level. One-dipole fits are fairly good, with two dipoles better for S2 and S3. The two-dipole fit for S1 is probably spurious. One dipole for S3 is very near the right eye, indicating EOG artifact.

The dipole localizations for the RARE FP350 are shown in Figure 6-22. Unlike the FREQ response at these time frames, the RARE response is similar across subjects, being positive on top and negative on the back and front. This

topography has been found by most other researchers for the P300 [Simson et al. 1977a, Vaughan and Ritter 1970]. One-dipole fits are fairly good. Two-dipole fits are all better looking, but are physiologically unreasonable.

Figure 6-23 shows the DIFF FP350 for each subject. The topography is essentially the same as for the RARE case, with more spatial power and noise for S3. As for the RARE case, the one-dipole fits are reasonable, the two-dipole fits are all better but unrealistic. What has been accomplished, then, by subtracting the FREQ response? For one thing, the power of the odd-ball response has been increased. This can be seen for S1 and S3 in the power curves, and for all three subjects by the length of the single-dipole fits in the second column of Figures 6-22 and 6-23. Numerically, the single-dipole amplitudes increase by factors of 1.11 for S2, 1.45 for S3, and 1.89 for S1.

By subtracting I have shown that the RARE and DIFF topographies are quite similar to each other both within and between subjects. The FREQ topographies are so for neither. These results are consistent with the hypothesis that in the FREQ case source configuration A is active, while in the RARE case source configuration A and B are both active. Configuration A is different for each of the subjects here. Configuration B is similar for these three subjects and of much greater power than A. Configuration A masks B partially in the RARE case. This masking can be removed by subtracting the FREQ potential from the RARE potential and analyzing the difference. Configuration B is associated with the odd-ball, surprise response to the RARE stimuli. Configuration A is associated with the presumably different processing each subject uses in rejecting the FREQ stimuli. Later components may reflect subject-specific processing of the RARE stimulus, i.e., mental counting.

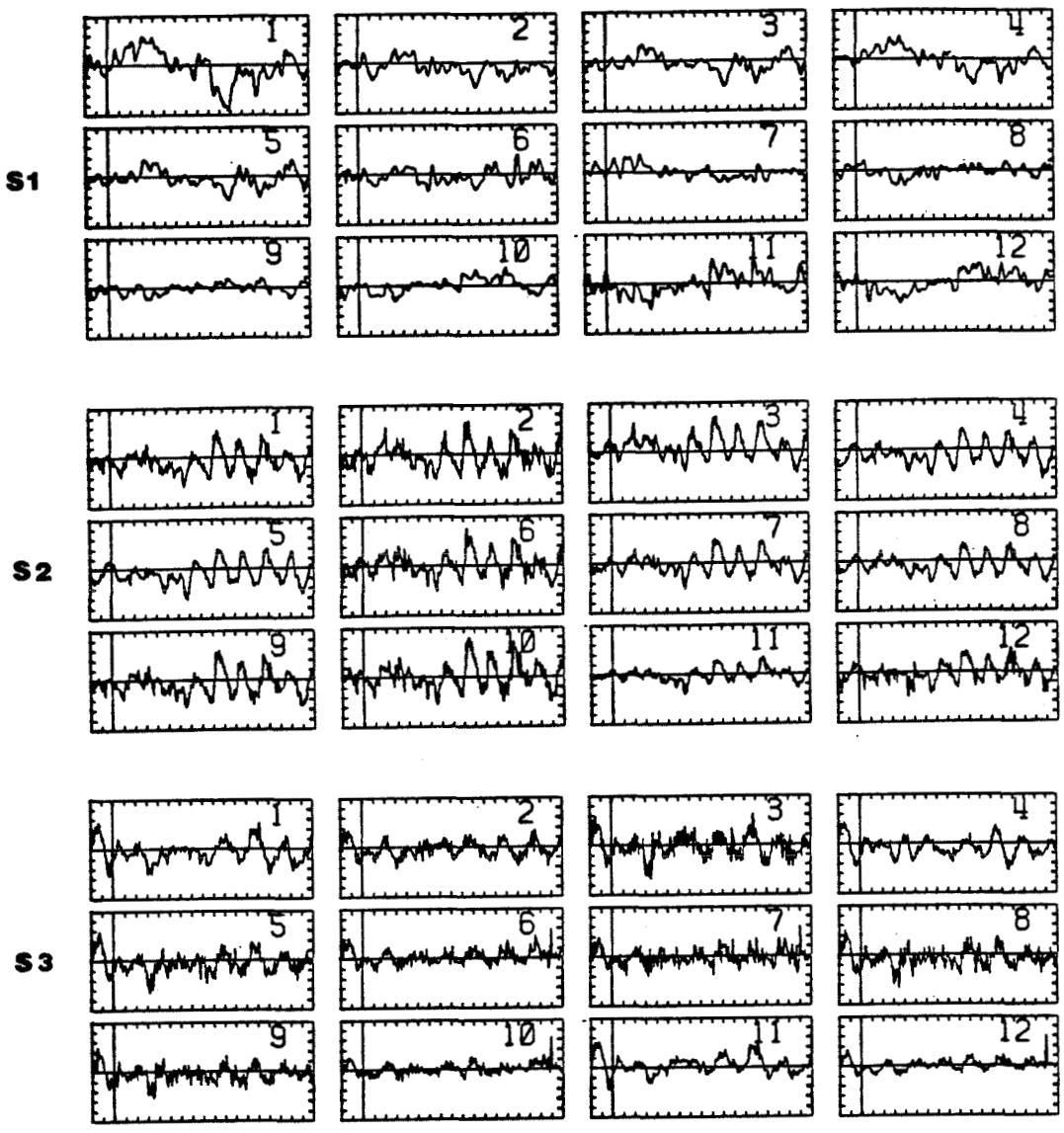

Figure 6-1. Selected raw EEG data for three subjects. Numbers on each plot refer to electrode placements diagrammed in Figure 5-2. Horizontal tiks = 51 ms, vertical tiks = 10 μV.

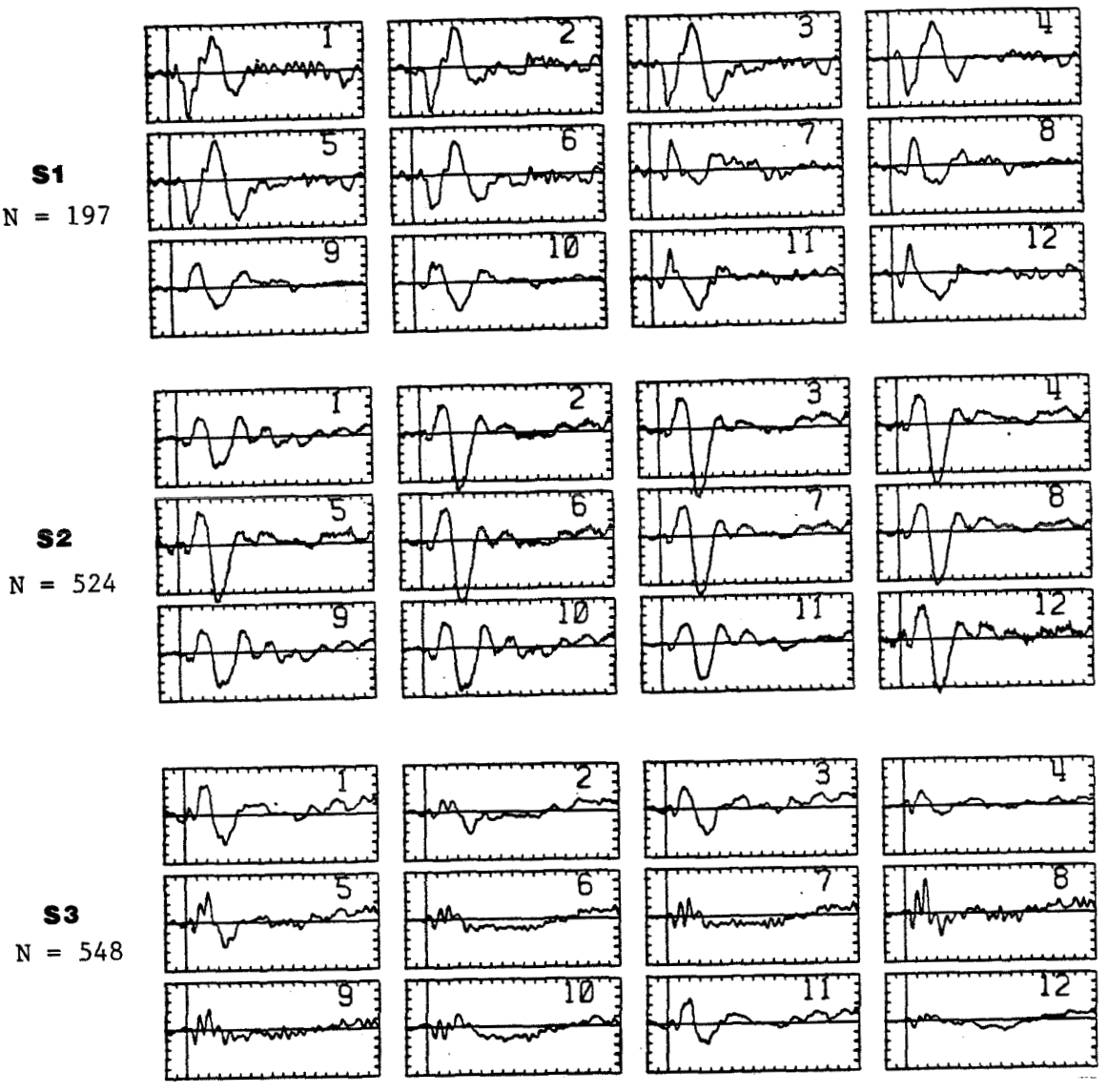

Figure 6-2. Selected average evoked potentials for the FREQ condition. Numbers on each plot refer to electrode placements diagrammed in Figure 5-2. Horizontal tiks = 51 ms, vertical tiks = 1.0 μV. The number of stimulus repetitions averaged is indicated as N.

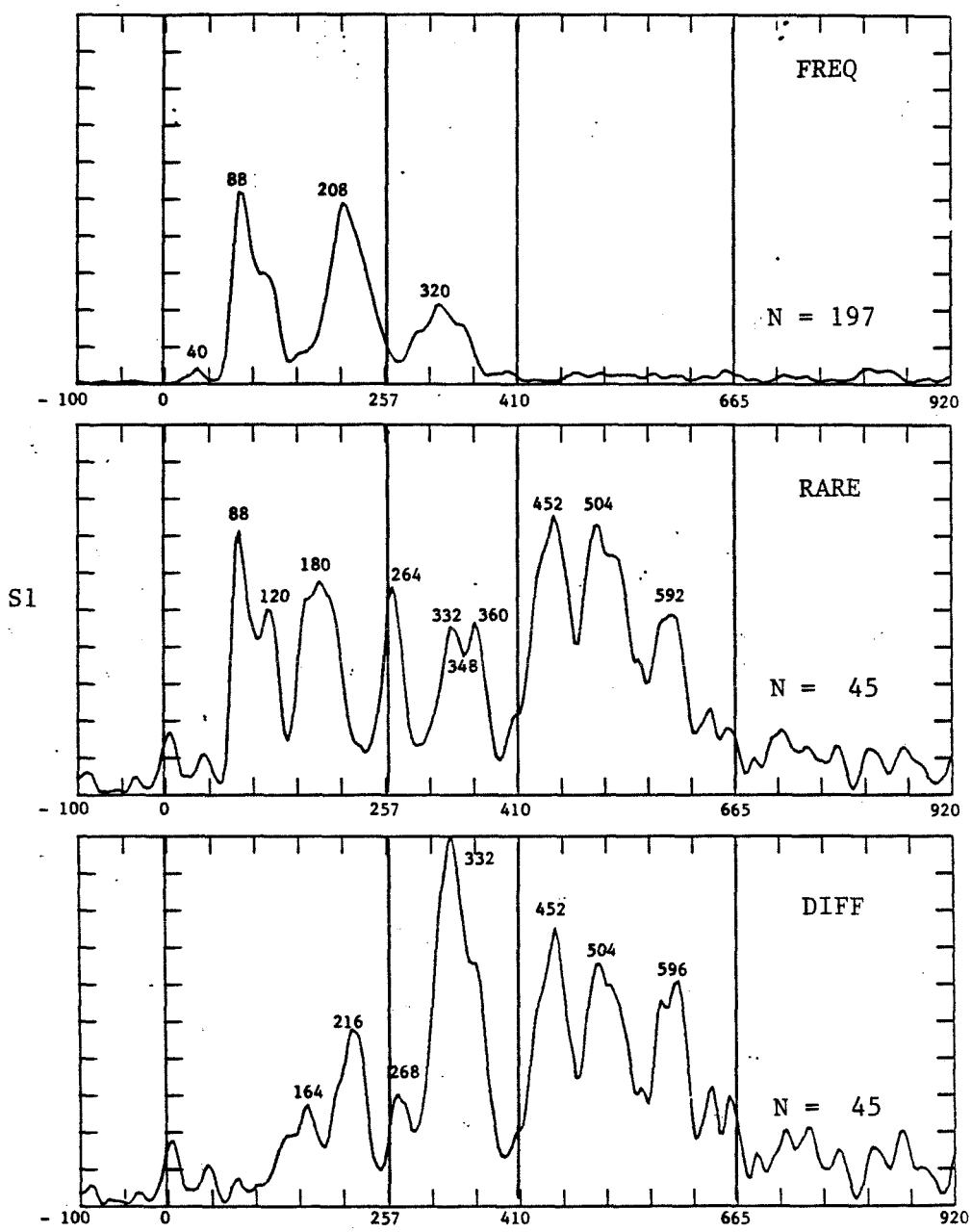

Figure 6-3. Spatial field power curves for S1 for three experimental conditions. Horizontal tiks = 51 ms, vertical tiks = 10 percent of maximum field power for the DIFF response. The number of stimulus repetitions averaged is indicated as N.

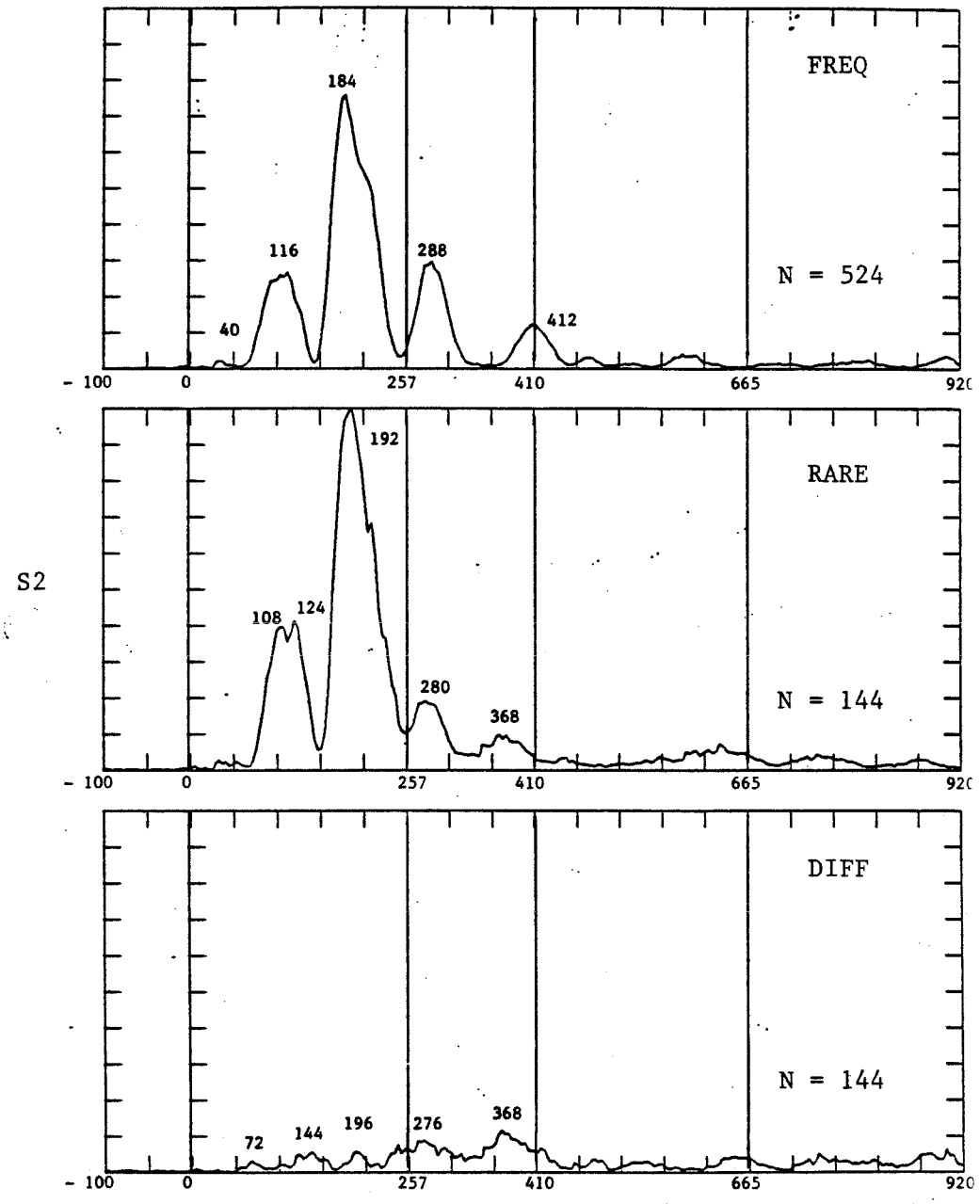

Figure 6-4. Spatial field power curves for S2 for three experimental conditions. Horizontal tiks = 51 ms, vertical tiks = 10 percent of maximum field power for the RARE response. The number of stimulus repetitions averaged is indicated as N.

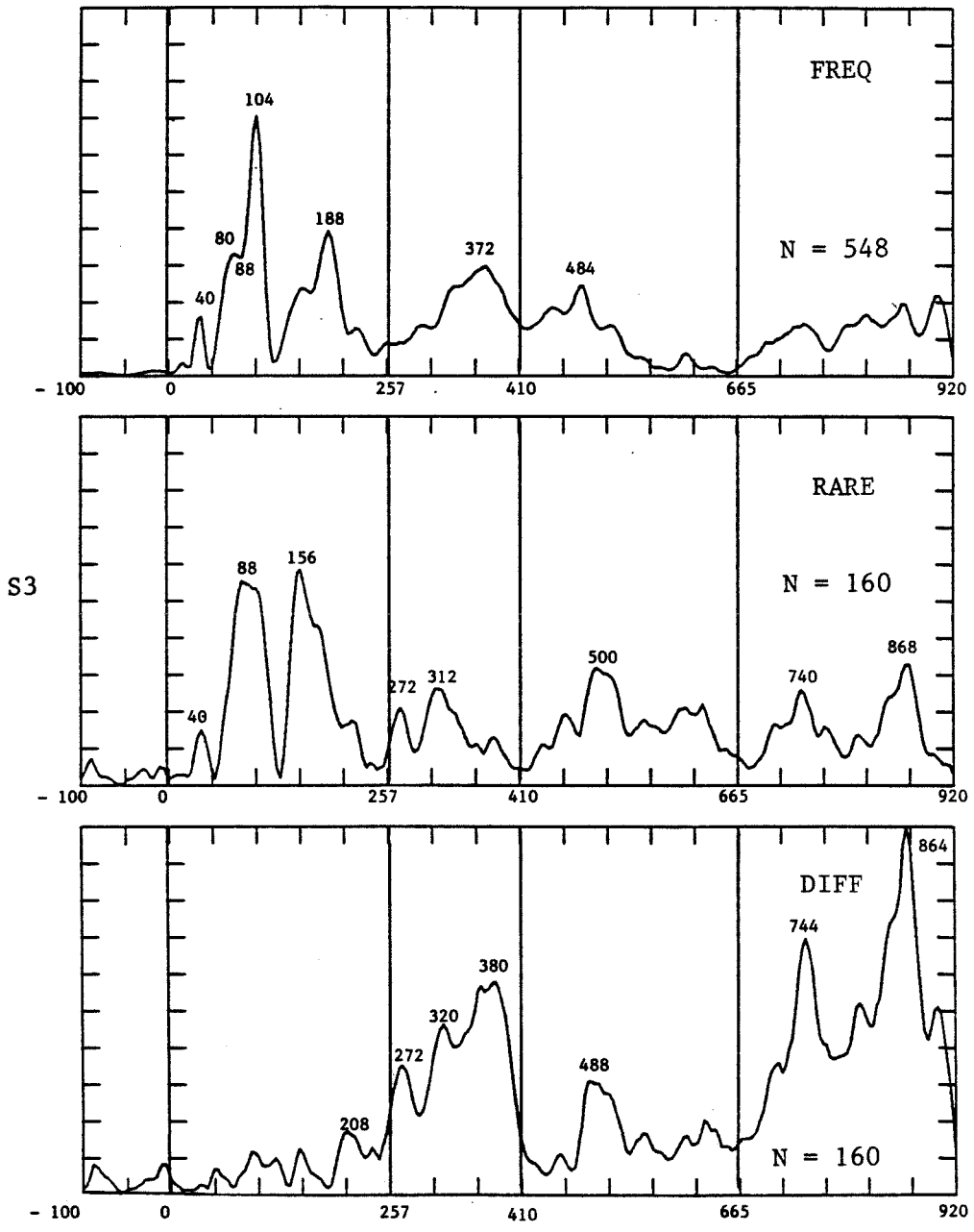

Figure 6-5. Spatial field power curves for S3 for three experimental conditions. Horizontal tiks = 51 ms, vertical tiks = 10 percent of maximum field power for the DIFF response. The number of stimulus repetitions averaged is indicated as N.

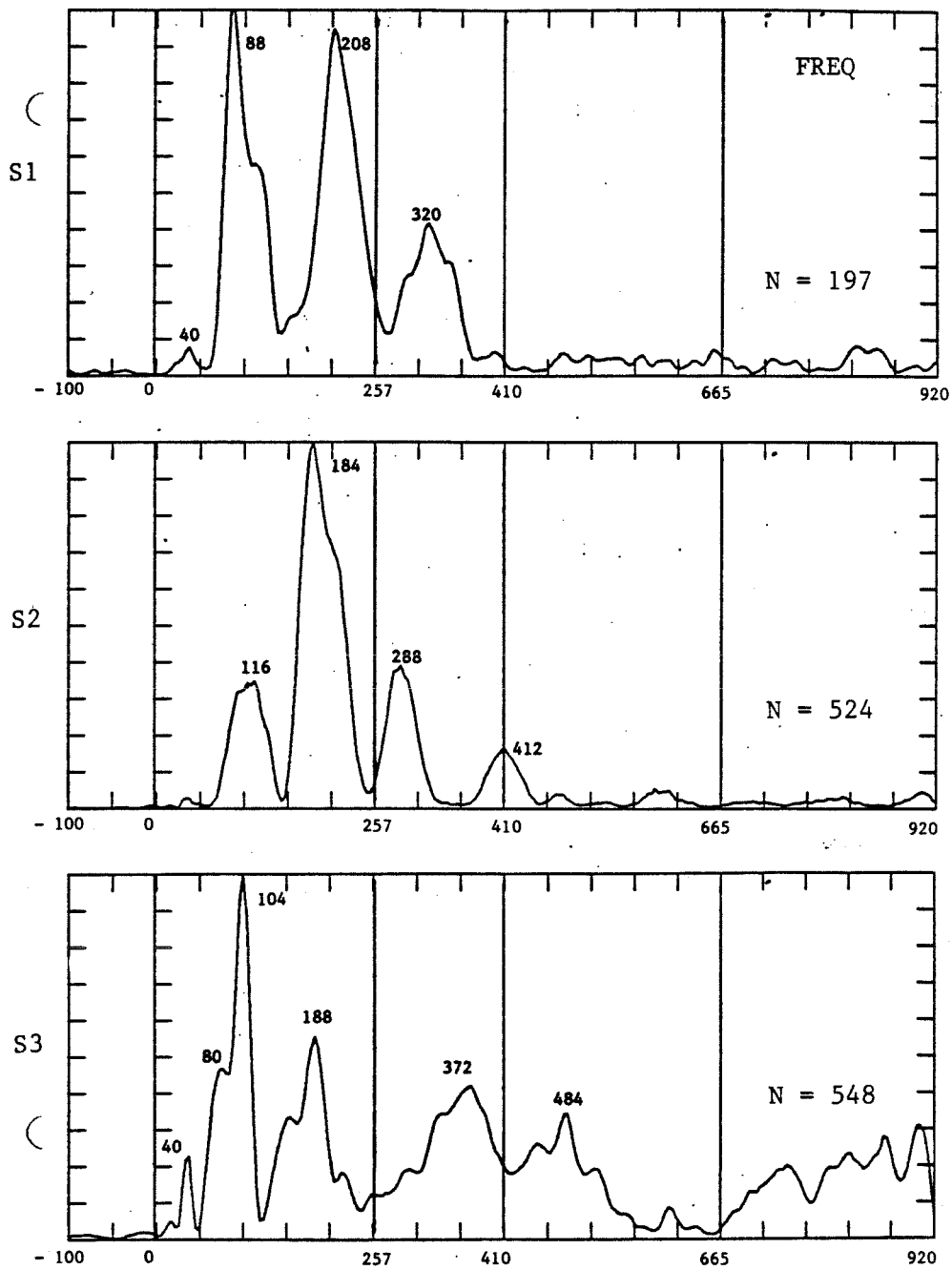

Figure 6-6. Spatial field power curves for three subjects for the FREQ condition. Horizontal tiks = 51 ms, vertical tiks = 10 percent of maximum field power for each curve. The number of stimulus repetitions averaged is indicated as N.

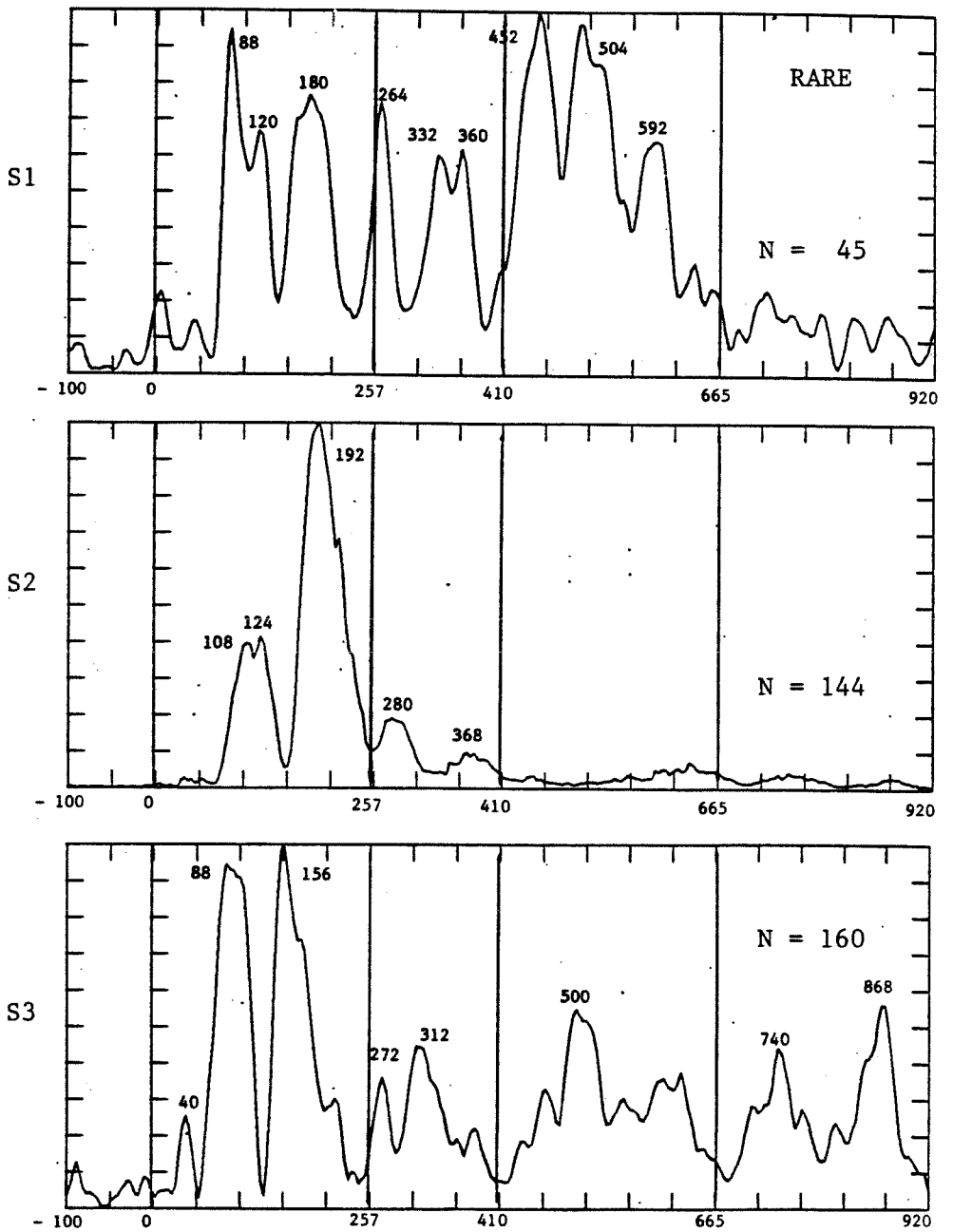

Figure 6-7. Spatial field power curves for three subjects for the RARE condition. Horizontal tiks = 51 ms, vertical tiks = 10 percent of maximum field power for each curve. The number of stimulus repetitions averaged is indicated as N.

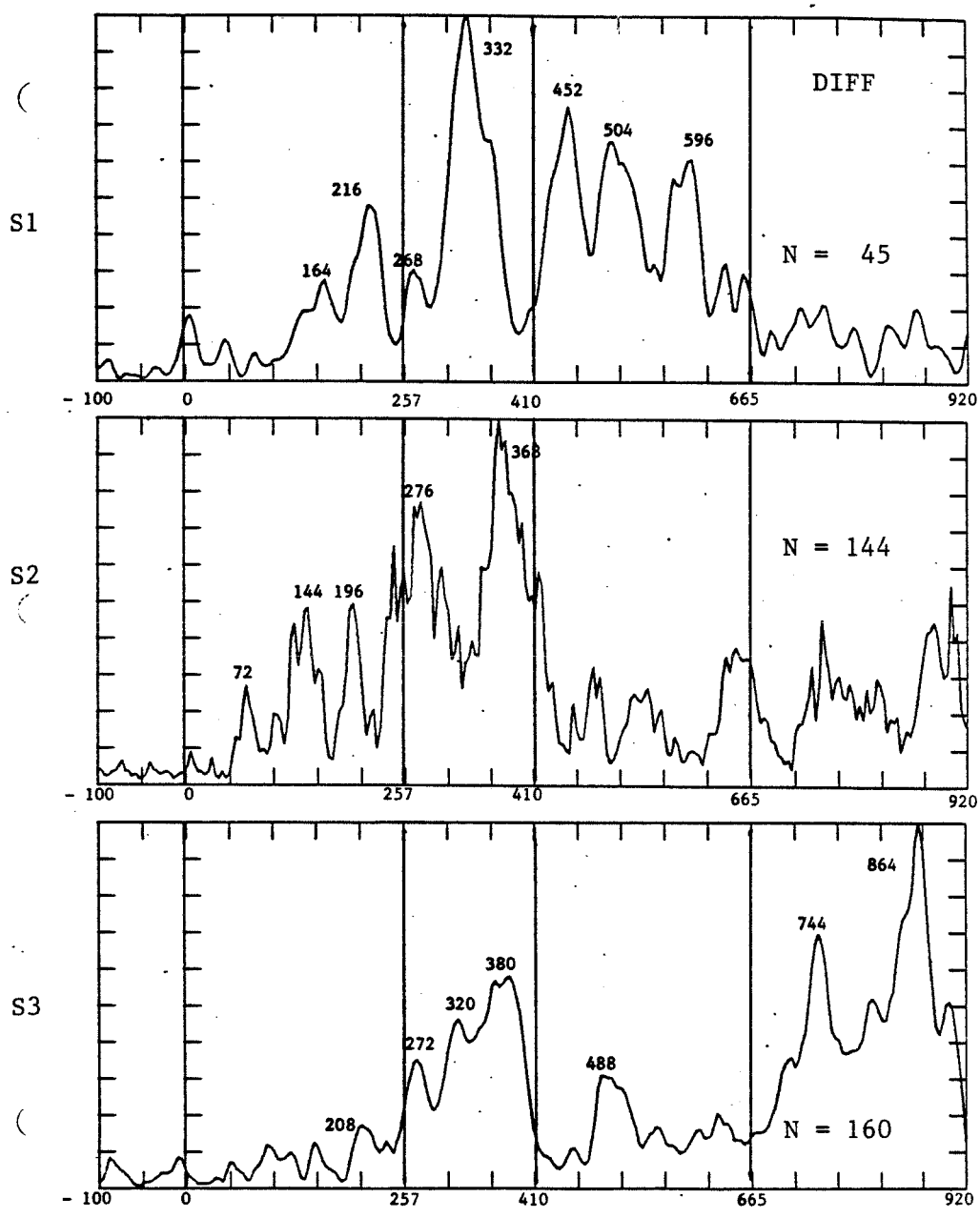

Figure 6-8. Spatial field power curves for three subjects for the DIFF condition. Horizontal tiks = 51 ms, vertical tiks = 10 percent of maximum field power for each curve. The number of stimulus repetitions averaged is indicated as N.

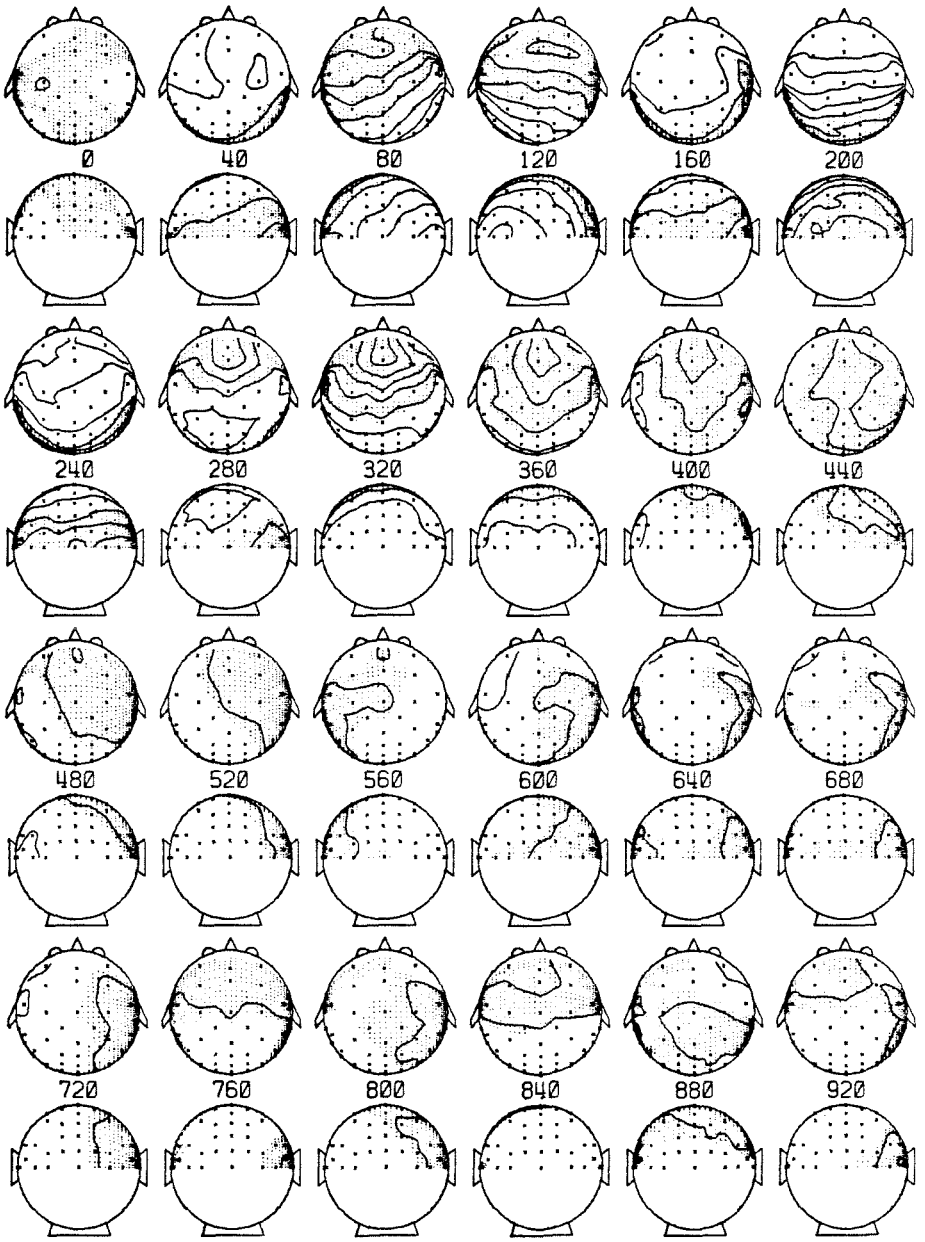

Figure 6-9. Equipotential maps for S1 for the FREQ condition. Top and back views of head spaced every 40 ms with time frames as indicated. Each map is normalized to produce ten contour lines for the maximum field power of this subject under this condition. Shaded areas are negative. Times are in ms. N = 197.

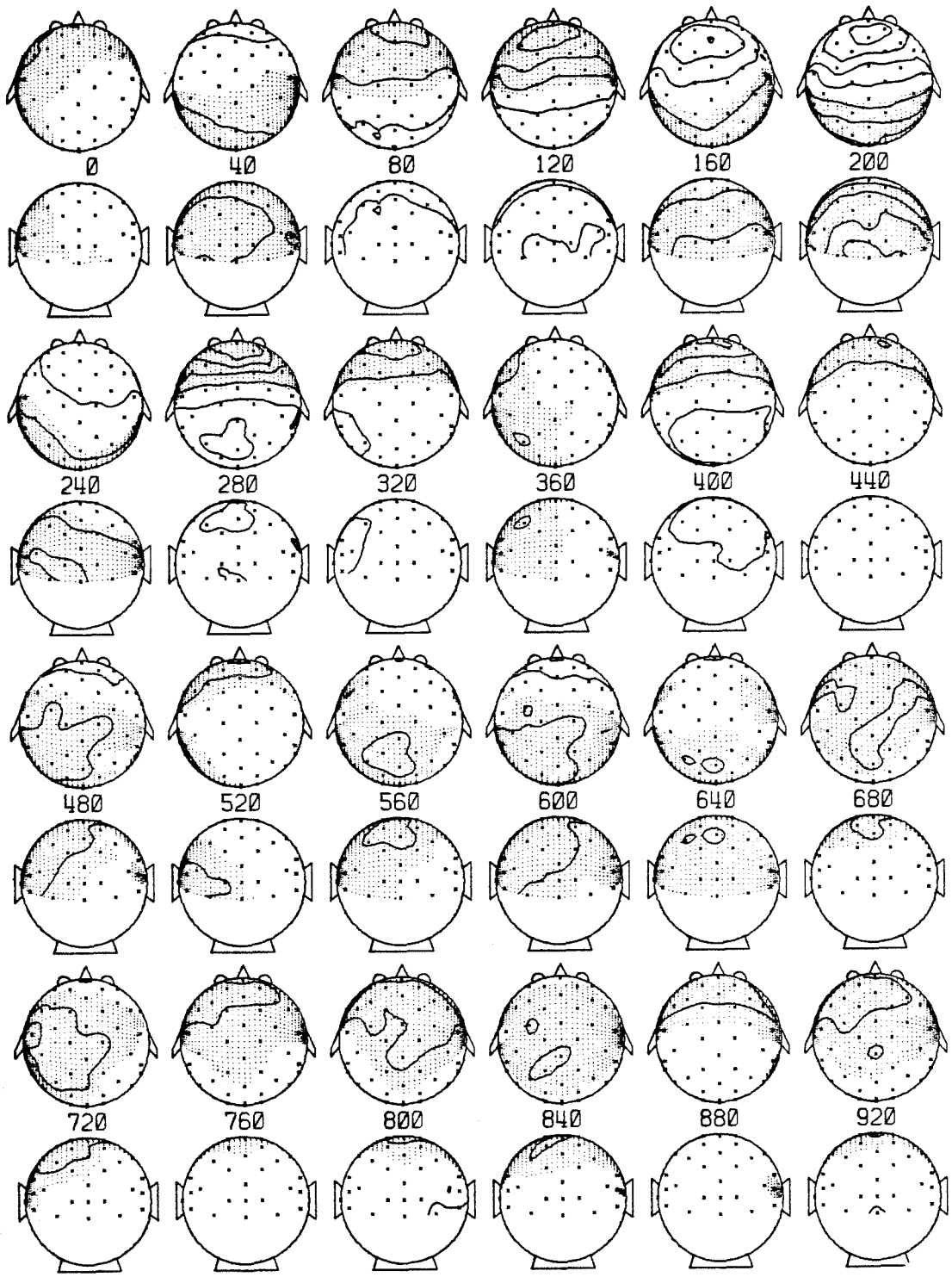

Figure 6-10. Equipotential maps for S2 for the FREQ condition. For explanation see Figure 6-9. N = 524.

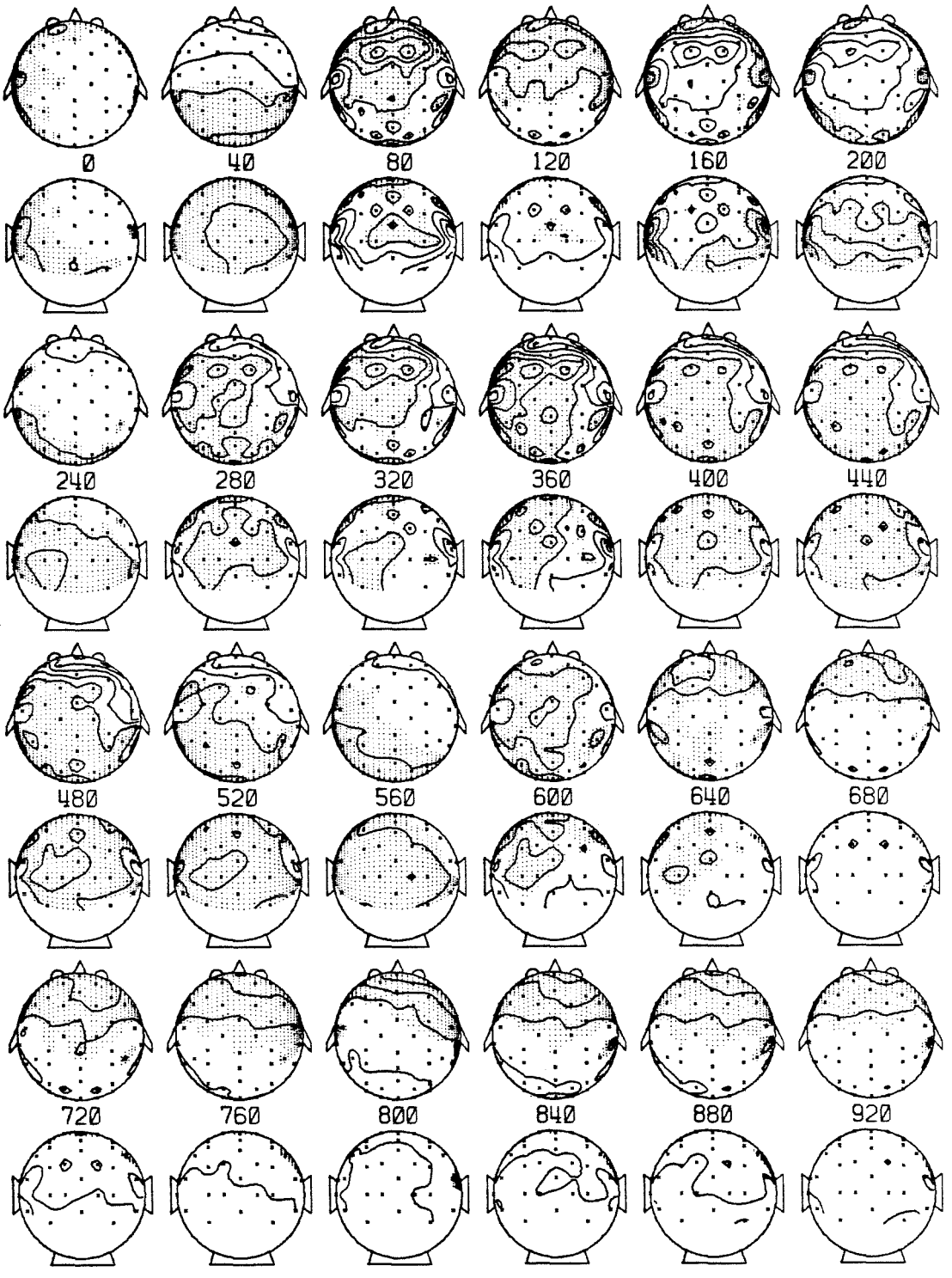

Figure 6-11. Equipotential maps for S3 for the FREQ condition. For explanation see Figure 6-9. N = 548.

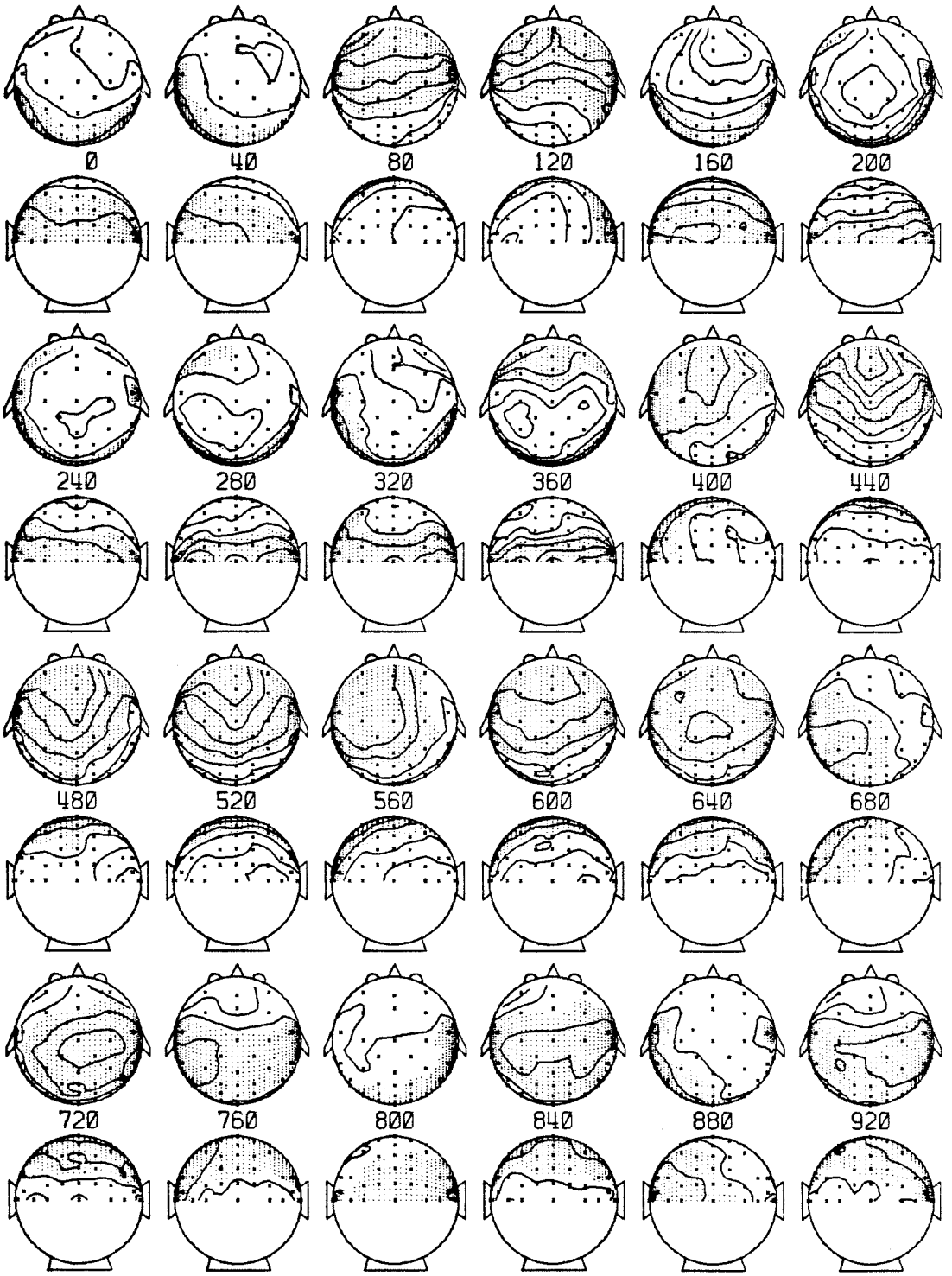

Figure 6-12. Equipotential maps for S1 for the RARE condition. For explanation see Figure 6-9. N = 45.

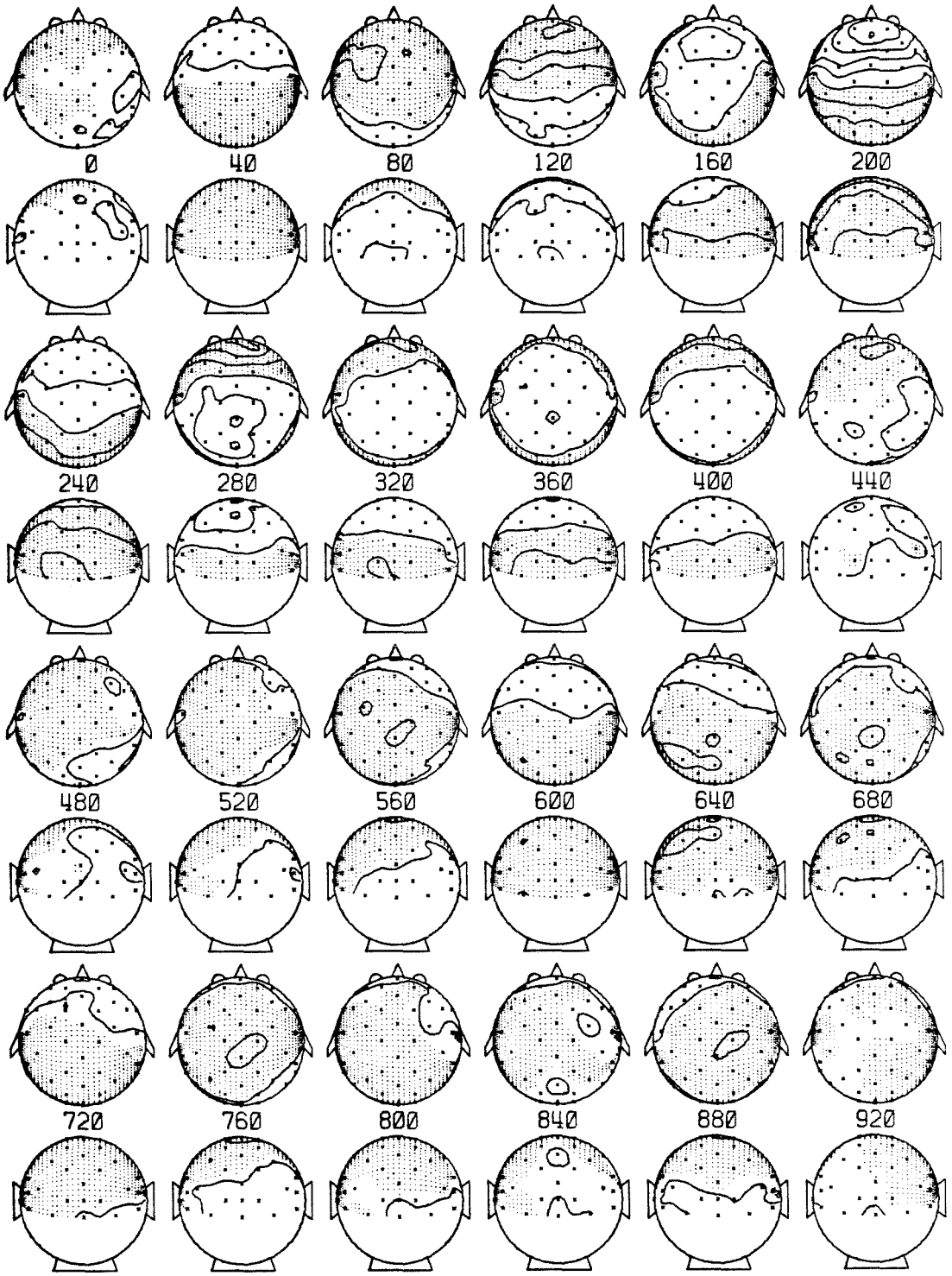

Figure 6-13. Equipotential maps for S2 for the RARE condition. For explanation see Figure 6-9. N = 144.

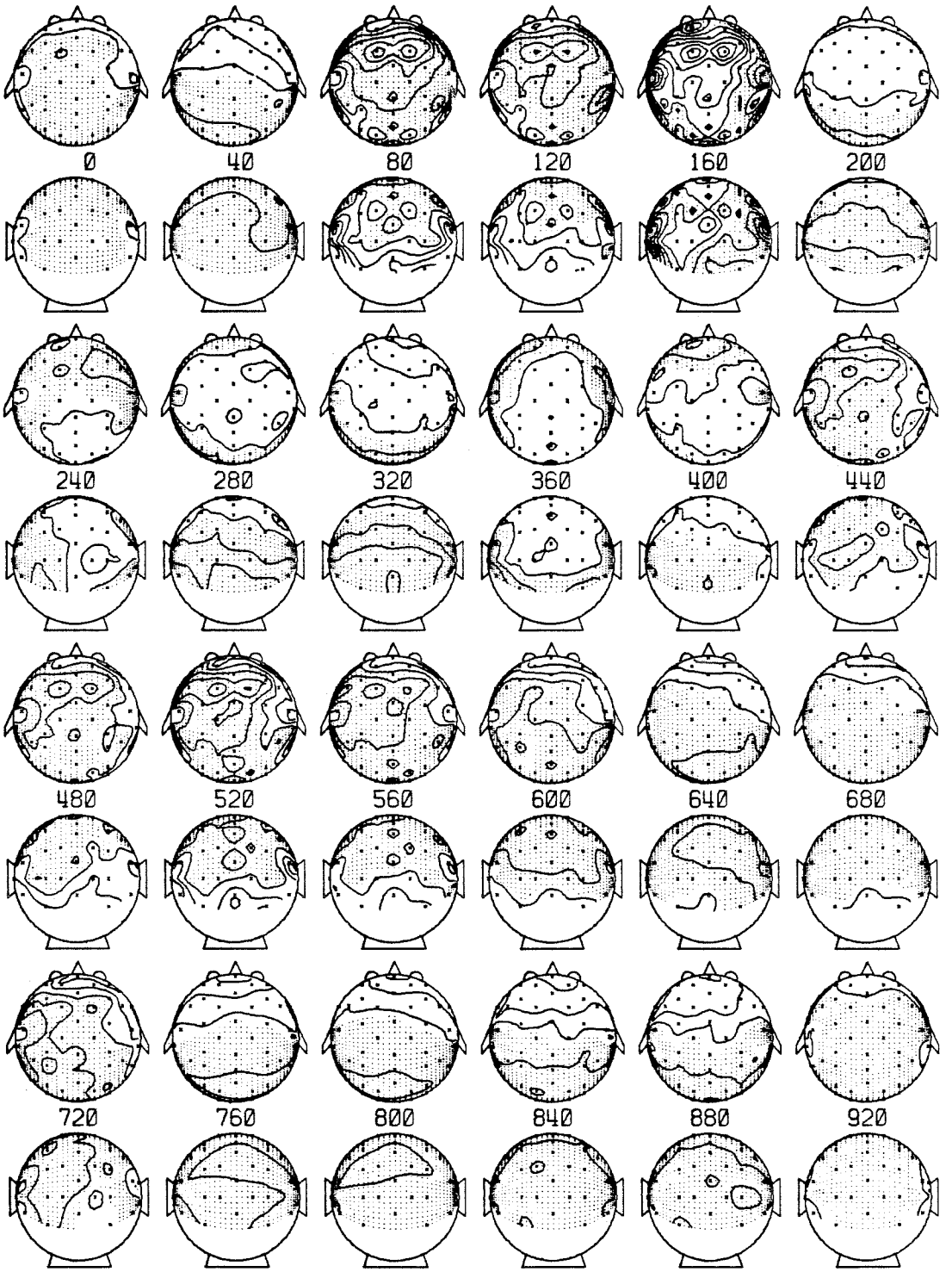

Figure 6-14. Equipotential maps for S3 for the RARE condition. For explanation see Figure 6-9. N = 160.

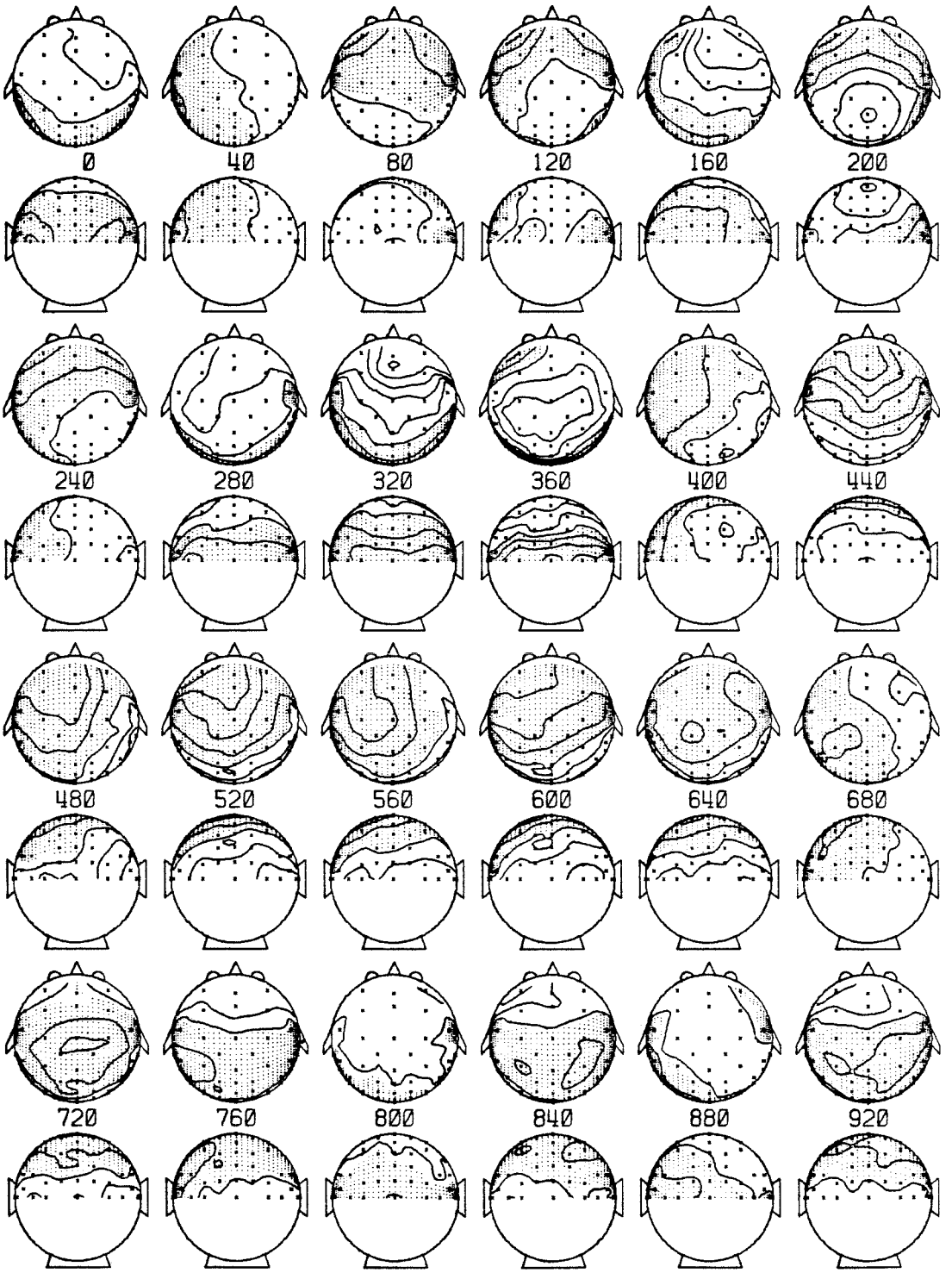

Figure 6-15. Equipotential maps for S1 for the DIFF condition. For explanation see Figure 6-9. N = 45.

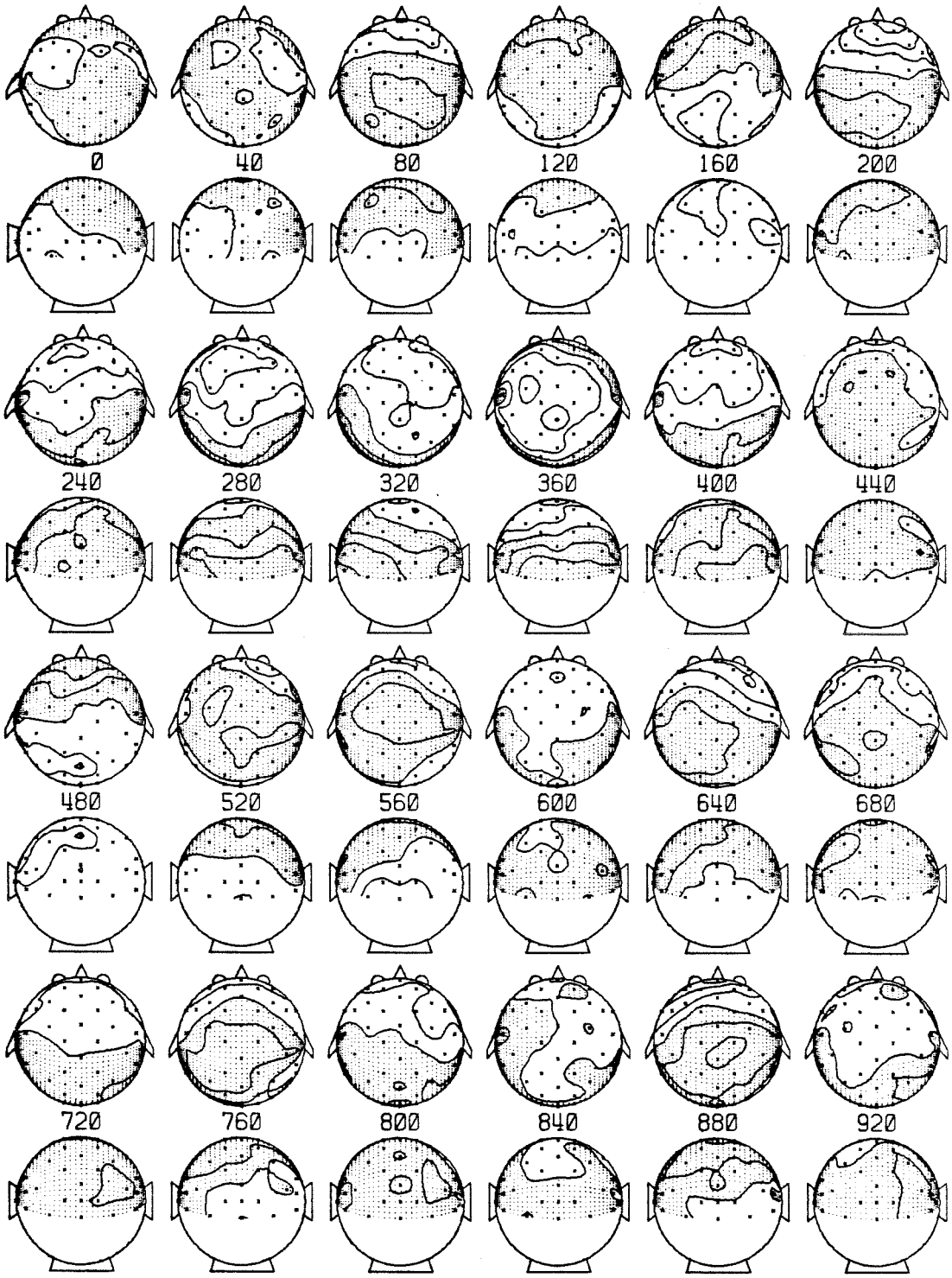

Figure 6-16. Equipotential maps for S2 for the DIFF condition. For explanation see Figure 6-9. N = 144.

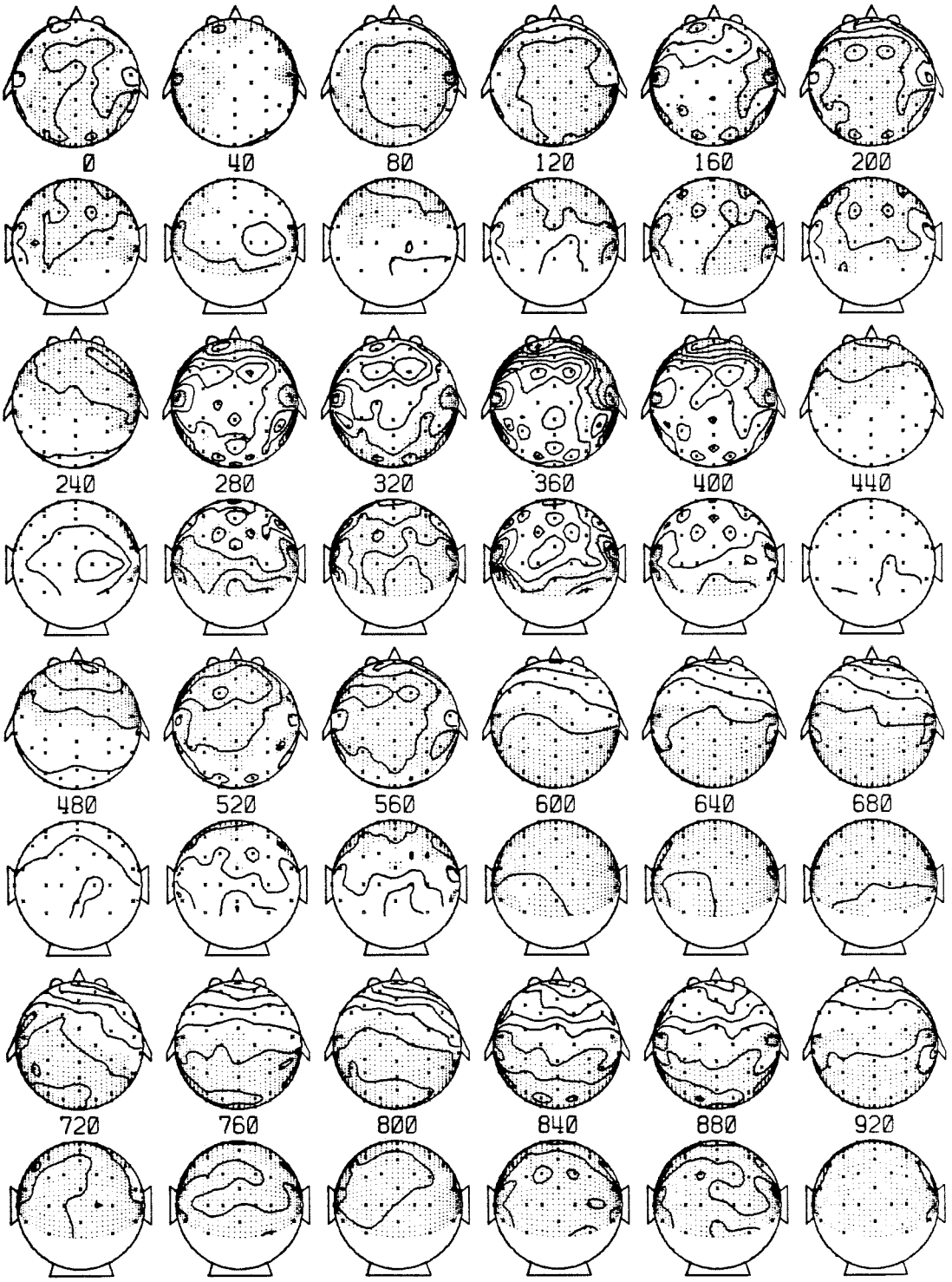

Figure 6-17. Equipotential maps for S3 for the DIFF condition. For explanation see Figure 6-9. N = 160.

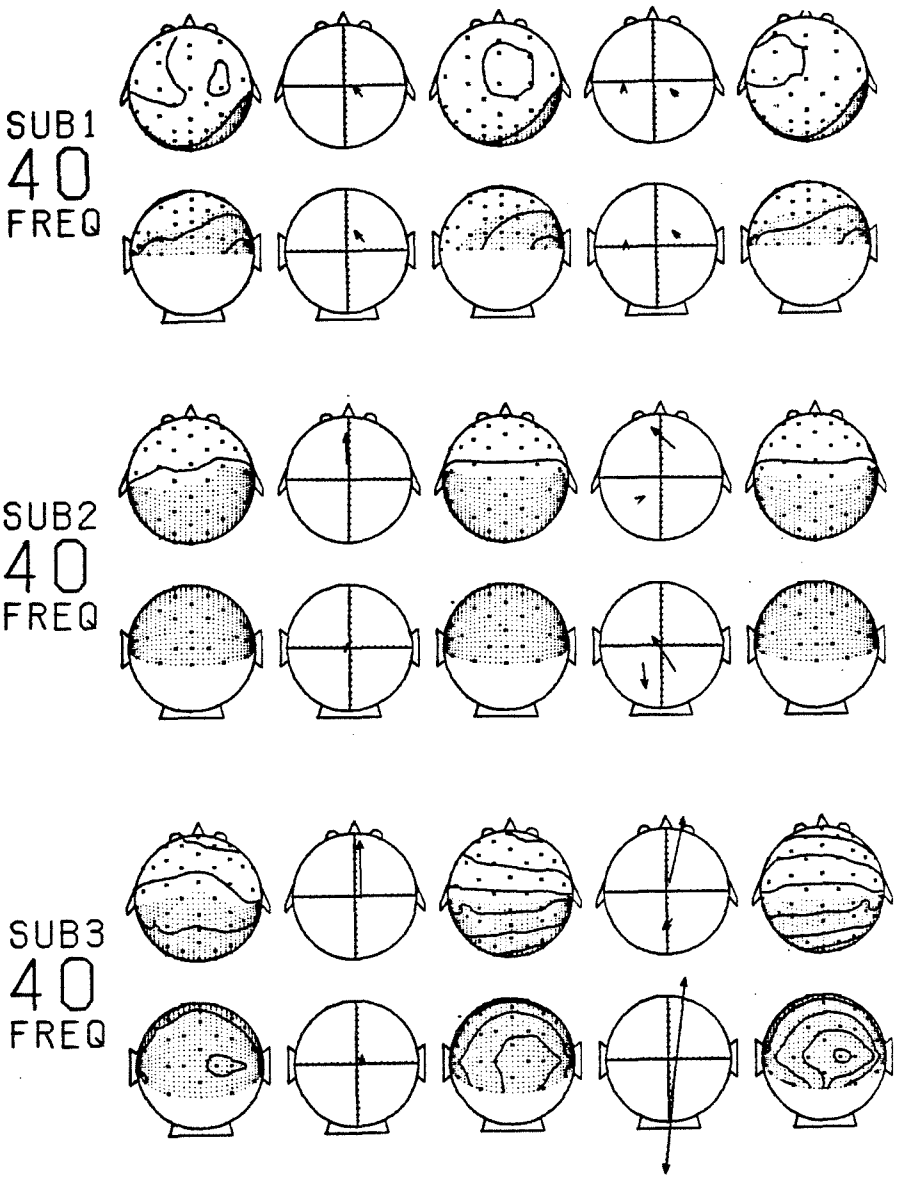

Figure 6-18. Comparisons of experimental data and dipole model fits for three subjects for the FP40 peak of the FREQ condition. Each map is normalized to produce ten contour lines for the maximum field power of each subject under this condition. The first column is the experimental data map. The second column shows the parameters of the best fitting single equivalent dipole. The third column is the map that results from the single dipole fit. The fourth column shows the parameters of the best fitting two-dipole fit. The fifth column is the map that results from the two-dipole fit. Each dipole is represented by an arrow with its base at the center of the dipole and pointing in the positive direction. The length of the arrow represents the amplitude of the dipole moment. Dipole lengths are normalized for each subject to fit reasonably on the page.

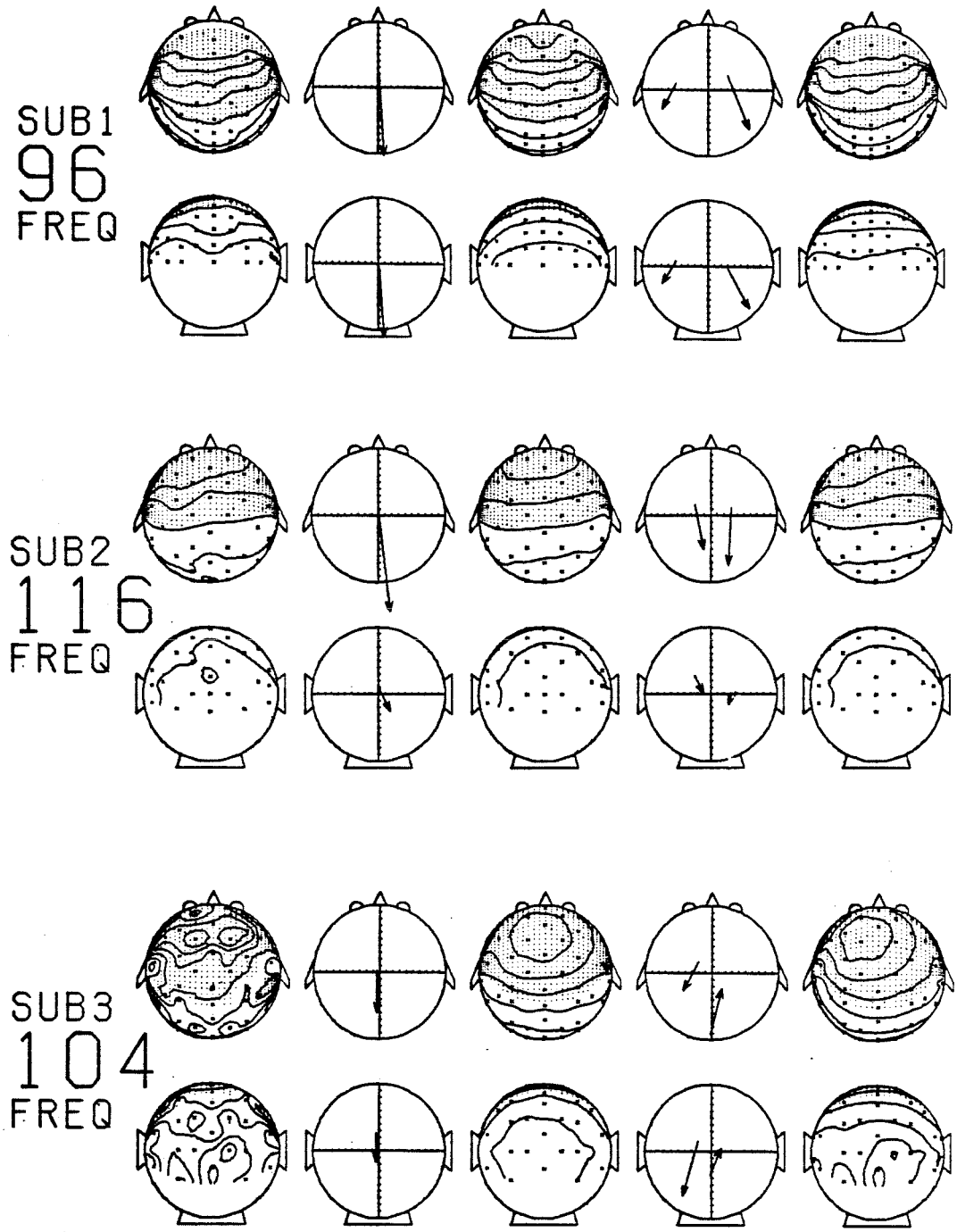

Figure 6-19. Comparisons of experimental data and dipole model fits for three subjects for the FP100 peak of the FREQ condition. For explanation see Figure 6-18. Each subject's peak time is indicated in ms.

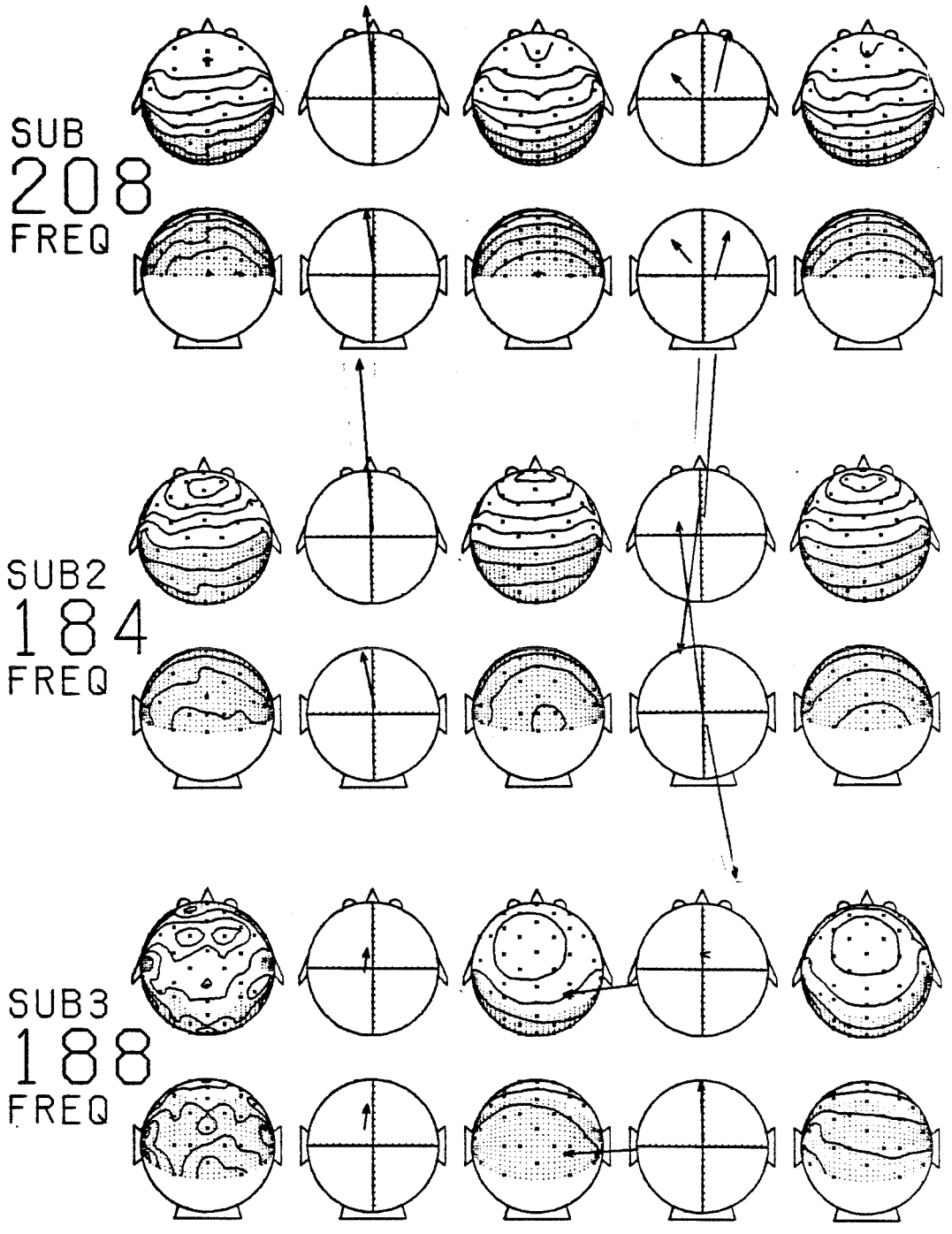

Figure 6-20. Comparisons of experimental data and dipole model fits for three subjects for the FP200 peak of the FREQ condition. For explanation see Figure 6-18. Each subject's peak time is indicated in ms.

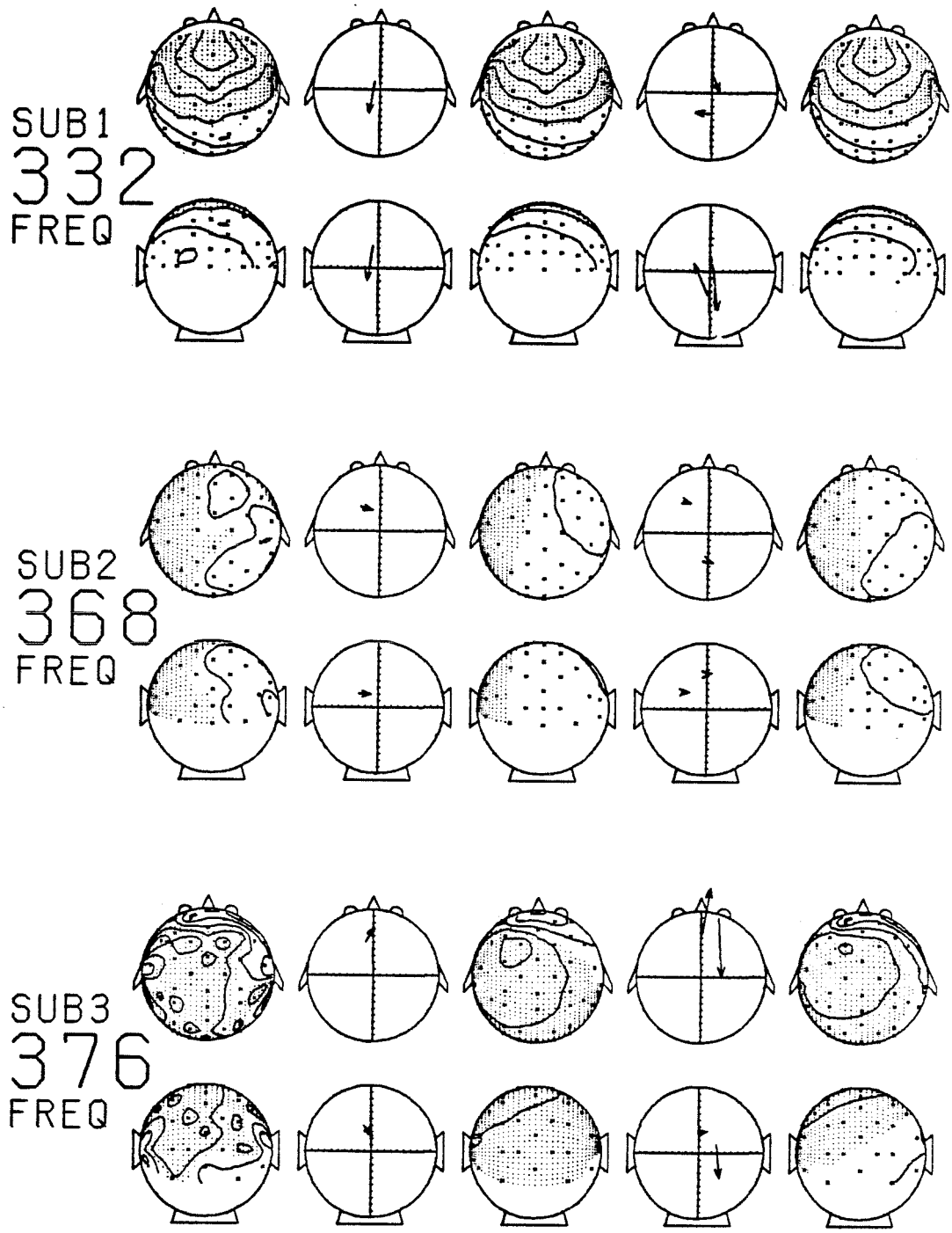

Figure 6-21. Comparisons of experimental data and dipole model fits for three subjects for the FP350 peak of the FREQ condition. For explanation see Figure 6-18. Each subject's peak time is indicated in ms.

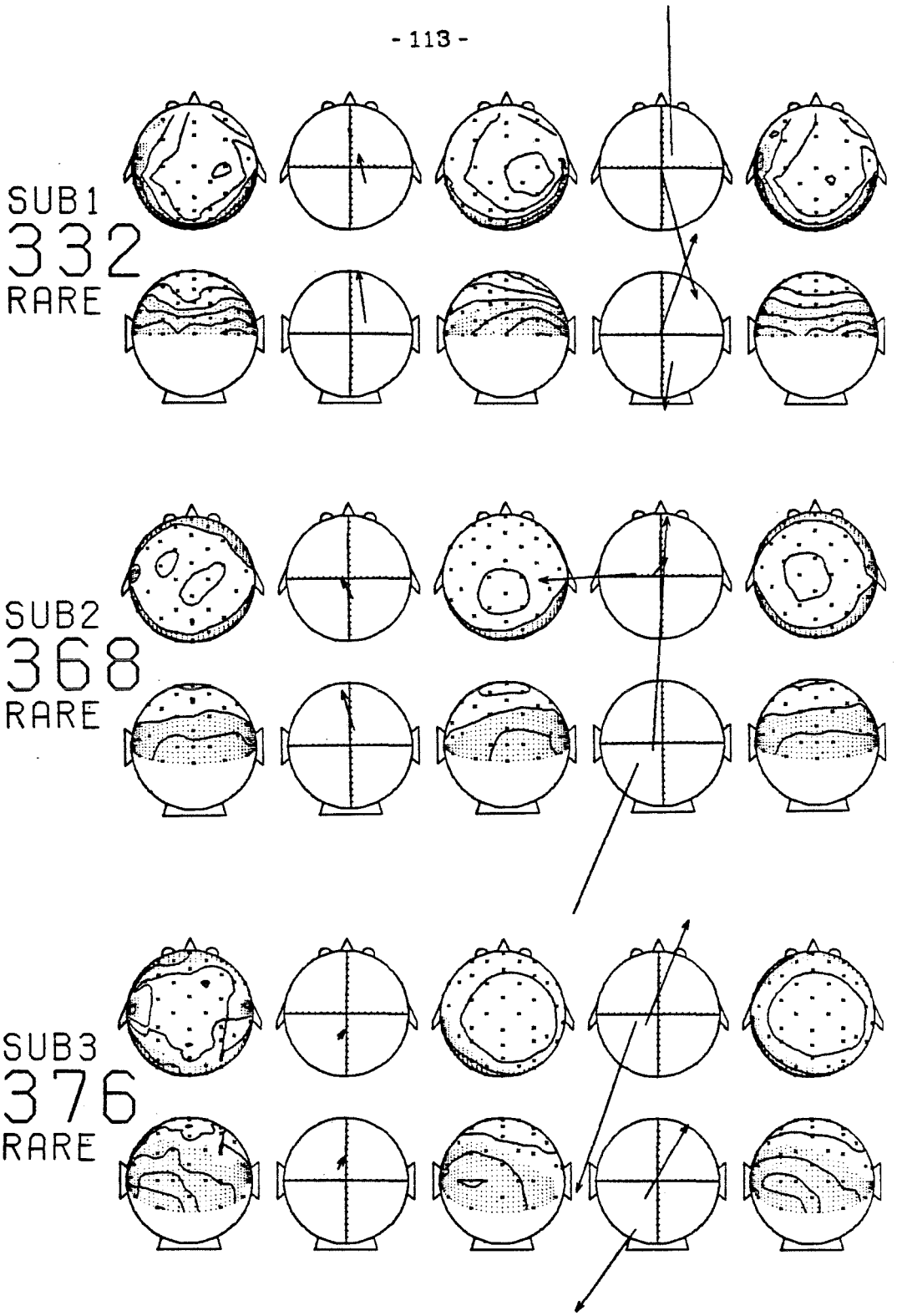

Figure 6-22. Comparisons of experimental data and dipole model fits for three subjects for the FP350 peak of the RARE condition. For explanation see Figure 6-18. Each subject's peak time is indicated in ms.

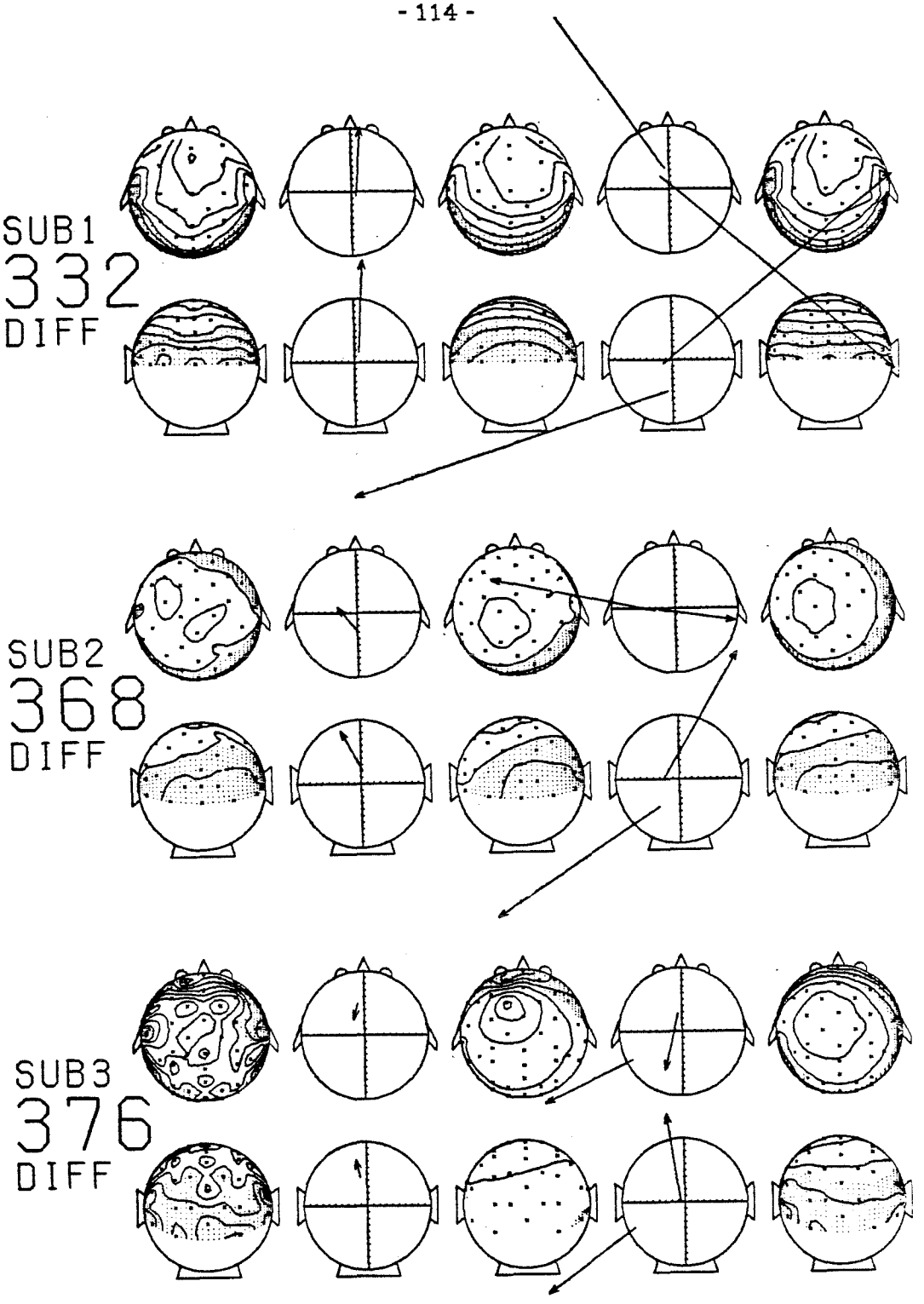

Figure 6-23. Comparisons of experimental data and dipole model fits for three subjects for the FP350 peak of the DIFF condition. For explanation see Figure 6-18. Each subject's peak time is indicated in ms.

7. DISCUSSION

In this chapter I will compare my results to those of other researchers and point out the similarities and differences. I will discuss the results of the source localizations in relation to brain physiology and anatomy. I will suggest improvements in procedure and further experimental work. Lastly, I will discuss the usefulness of the techniques presented in this thesis to cognitive psychophysiology.

7.1 AEP Comparisons

To compare the aEPs I have recorded to those of others, many reports have to be sifted. P300-like responses are usually recorded in response to one of three different tasks. The first is a guessing task such as used by Sutton et al. [1965] and recently by Karis et al. [1983]. The second is a signal detection task such as used by Debecker and Desmedt [1966] and Begleiter et al. [1983]. The third and most popular is the odd-ball discrimination task used here and by many other workers from Ritter and Vaughan [1969] to Wickens et al. [1983].

Those who have their subjects perform the odd-ball task use a variety of stimulus modalities, stimulus attributes, recording sites, amplifier bandpass and filtering, referencing methods, averaging, and component definitions. The reader is referred to the following for experiments most similar to the ones described here: Ritter et al. [1972], Simson et al. [1977a], Goodin et al. [1978], and Fitzgerald and Picton [1981]. The work of Goodin et al., in particular, was chosen as a model for this experiment. They used tones of 1000 and 2000 Hz, with a probability ratio of .15/.85, and calculated the DIFF potential. They also ran a control experiment in which the subject ignored all the tones and read a book. Their DIFF potential was calculated from the RARE tone responses when attending to the tones and when ignoring them. However, examination of their

waveforms indicates that the RARE response minus the FREQ response would have given the same DIFF potential.

Electrode 3 of S1 is the closest to the vertex as defined in the 10-20 system of electrode placement [Jasper 1957]. The aEP recorded from it closely resembles the DIFF waveform recorded at the vertex in Goodin's Figure 1, with a P160, an N210, and a P310 corresponding to their P165, N200, and P300. Of course, S1's data has been calculated with respect to an average reference, but the zero-potential line runs near the mastoids in most of his responses; hence his data will correspond with the mastoid reference used by Goodin. S2's electrode 39 is near his vertex, but his data cannot be said to resemble that in Goodin's Figure 1. However, S2 does fall in the range of the 15 subjects presented in Goodin's Figure 2. The data for S3 fit that of Goodin's typical subject as well as S1 does, with his near-vertex electrodes 35 and 36 where a P150, N200, and P300 are evident.

7.2 Subject Comparisons and Controls

The three subjects for these experiments show a lot of similarities in their field potential distributions at the four power-peak times selected. In terms of source localization they do not compare as closely. Part of the reason for this is the putative noise associated with S3's data. Aside from this, S1 was presented with louder tones than the other two subjects. This could have led to stronger auditory cortical sources for S1. Stronger sources would most certainly result in more easily separated peak distributions on the two sides of the head, based on a greater signal/noise. This in turn would make two-dipole source localizations more reliable. In fact, S1 is the only subject who shows reasonable bilateral sources for all three of the exogenous auditory aEP components at 40, 100, and 200 ms.

It has been well established in the ERP literature that an easy discrimination will give a higher amplitude P300 than a difficult discrimination. Having louder tones made the odd-ball task easier for S1. Accordingly, S1 has the highest relative DIFF FP350 of the three subjects. It is also possible that because of the lower stimulus intensities, the odd-ball task became more of a signal detection task for S2 and S3. In signal detection tasks all stimuli elicit a P300-type response. If this were the case it could partially explain the smaller FP350 DIFF responses of S2 and S3.

Though S2 and S3 were run under very similar conditions, they show very dissimilar field-power curves, while all three subjects show topographical differences for various times between the power peaks selected for study here. Major differences between the subjects occurred in the latter half of the DIFF responses. S1 had a broad peak in the 400-650 ms interval, S2 had virtually nothing, and S3 had a broad peak in the final 650-920 ms interval. One might speculate that the broad peak could be related to the mental counting of the odd-ball stimuli. In S1 it occurs earlier because the tone is louder and easier to detect and recognize. But examination of the equipotential maps shows that the topographies are quite different for these two subjects, indicating different source configurations.

Certain controls discussed in Chapter 4 were not accomplished. Tone reversal was done only for S2, and these results have been added together here. The condition in which the tones were ignored was not run, either. One or both of these should be done in further studies of this type to control the exogenous responses and the attentional state of the subject. Recordings of purely exogenous responses would need to be done to ascertain better what parts of the FREQ response were endogenous. Eye movement and muscle contractions should be studied separately to identify their probable sources.

7.3 Use of Power Curves and Spatial Rate-of-Change

The use of spatial field power curves to define components is a necessary evil. It allows the summary and comparison of a large number of channels across subjects. It is a measure of the strength and complexity of a field pattern but is not very well correlated with the latter. All orientation information about the field pattern is lost. Many different source configurations can produce the same field power curve, so it also suffers from non-uniqueness. Thus it should only be used with the greatest caution and only as a first step in analysis.

Field patterns can rotate and change complexity quite rapidly, yet not show any change in their spatial power. It can be argued that a lot of the information content in topographical data is contained in the time periods of rapid change. To quantify periods of such change another statistic was reported by Darcey et al. [1980b] as the sum-of-squares of the time derivative of all the voltages.

The spatial rate-of-change still suffers from the same problems of the field power in that it loses all orientation and most complexity information, and is non-unique. It is useful for just what it does: provide a summary of the time course of the change in field power over all the electrodes. Many other simplifications of the vast amount of information contained in multi-channel recordings could be devised, including specific measures of complexity, orientation, etc., but anything more complex than these two would probably be a waste of time. With just a little more effort a physically realistic summary of the data can be made, namely equivalent source modeling.

7.4 Difference Calculations

There is no doubt that calculating a DIFF waveform is useful in delineating changes that would otherwise be obscure. The experimental procedures of differential amplification and average referencing are used for this reason. They

can be safely applied based on sound physical principles of linearity and superposition applied over the spatial dimension. The DIFF potentials used here, though, are calculated across the dimension of experimental manipulation, and are thus valid only if linearity and superposition hold over that dimension. Certainly they hold in biophysical terms since the neurophysiology and neuroanatomy should be constant over the time frame of most experiments, assuming as we do that Poisson's equation holds. The main question is if the mental processes that change with cognitive activity or brain state are linear and obey some form of superposition.

It is one thing to use a DIFF potential as an aid in describing change, but another thing entirely to base quantitative analysis on it. I would say that a DIFF potential is always valid, and that validity criteria should rather be applied to any further analysis based on the DIFF potential. How can we determine the validity of a DIFF analysis or, alternatively, how can we determine if the changes in response to experimental manipulation obey linear superposition? In some cases it may be possible to elicit the same phenomenon without using a DIFF potential. An emitted P300 occurs following an omitted stimulus in a repetitive train. This type of P300 is very similar to the P300 response defined by subtraction [Simson et al. 1976, Ruchkin and Sutton 1978, and Ford and Hillyard 1981], including the presence of an N200 and sometimes the P165 described by Goodin et al. [1978, 1983].

In general, though, analysis of the DIFF potential cannot be used to prove anything about the underlying causes of EP changes, just as ESM cannot be used to prove anything absolutely about the sources of scalp electromagnetic activity. But it can be used quite profitably to formulate and test hypotheses about the underlying causes, especially in conjunction with ESM. A case in point is the FP350 component considered in this thesis. By calculating the DIFF potential I

uncovered a large power peak at around 350 ms (for S1 and S3 anyway). I then make the hypothesis that this field power arises from a new mental process or source configuration that follows the RARE response but is partially obscured by activity that occurs in both the FREQ and RARE responses. ESM quantitatively embodies this hypothesis, and the results of source localization can be checked for self-consistency and agreement with the original hypothesis.

7.5 Topography Comparisons

True topographical studies have been few and far between in the past. Vaughan and Ritter [1970] used 12 electrodes in two linear arrays to record auditory aEPs. Based on this rather sparse data they hand-drew isopotential contours on a cartoon of the side of the head from which they recorded. The two contour maps thus generated for their AI (P200) and AII (P300) components match my maps for the FP200 and FP350 components.

Goff [1978] recorded auditory aEPs using about 20 electrodes placed according to the 10-20 system and schematized the resultant topography. He used a higher bandpass and enough repetitions to delineate many middle (10-100 ms) components, so the FP40 component described here is not directly comparable. Goff plots both a P115 and an N115 component that might correspond to my FP100, but it is hard to compare because he plots positive and negative voltages on separate heads. His last figure, taken from Hillyard et al. [1976], shows the topography of a P200 and two types of P300. These conform to my FP200 and FP350 quite well.

More recently, Wolpaw and Wood [1982] recorded from 20 electrodes on one side of the head and drew machine-calculated isopotential contours based on auditory aEPs. The topography of the 100 ms map in their Figure 6 indicates more detail than can be seen in my maps on the side of the head, though the

topography on the top of the head is similar to that which I found. In a companion paper, Wood and Wolpaw [1982] present a variety of maps that cover the range from 20 to 250 ms. My FP40 map matches their 31 and 56 ms maps. My FP100 map matches their 88 ms map. My FP200 map matches their 170 ms map.

Simson et al. [1976, 1977a] specifically sought to discover the scalp topographies of two types of P300. In the first paper they report the results of a missing stimulus task which produces an emitted P300 that they call the MSP for missing stimulus potential. It actually has both an N200 and a P300 in it. For both auditory and visual stimuli they find that the P300 is similar, with the vertex positive. My auditory FP350 maps match their P300 maps. They claim that the N200 part of the MSP is different for auditory and visual tasks. I can only compare my auditory DIFF FP200 to their auditory MSP N200. Their grand average subject shows a frontal-vertex positive spatial peak for the N200 that shifts backwards to an occipital-vertex position. For S1, the DIFF FP212 is occipital-vertex and shifts forward to a frontal-vertex position at FP332. Thus the activity for S1 shifts in the opposite direction from Simson's average subject. S2, however, follows Simson's subjects by shifting from a frontal FP196 to a top FP368. S3 behaves as does S2 within the limits of his noise. Only actual source localization can resolve the anomalous behavior of S1's spatial peak shift. Maps for the seven individual subjects in Simson's study do show quite a bit of variability in the rostral-caudal location of spatial peaks

In Simson et al.'s other paper [1977b] they compare the DIFF potentials from auditory and visual odd-ball tasks to the MSP of their first paper. They find that the MSP N200 is very similar in topography to the DIFF N200, and that the MSP P300 is very similar in topography to the DIFF P300. This experiment is the closest in task and analysis to this thesis that I can find in the literature.

Simson's auditory N100 and P200 also match the topography of my FP100 and FP200.

7.6 ESM Results Comparison

7.6.1 Actual ESM

Various authors have speculated on the neural generators of exogenous auditory and endogenous ERP components, but this thesis represents the first reported attempt to apply numerical optimization methods to source localizations of the endogenous components. Most previous attempts involved EEG, visual EPs, or somatosensory EPs. Wood [1982] reported single-dipole fits to auditory aEPs in the 90-170 ms range. The dipole fits in his Figure 6 compare favorably with my source localizations in the second column of my Figure 6-11 and 6-12. His dipole fits for times between 100 and 200 ms do not agree with mine. This is most likely because Wood recorded only on one side of the head while I used a montage that covered the whole upper half of the head. The necessity of using as wide a coverage as possible was first pointed out by Schneider [1972].

7.6.2 ESM Based Topographic Arguments

For many years it was assumed that the auditory vertex potentials, so named because of their vertex maxima, originated in parietal association cortex, as did the vertex potentials in the visual and somatosensory modalities. This was a naive assumption, but fit the idea that all modalities projected to the parietal area. Vaughan and Ritter [1970] showed that their auditory topographic results were consistent with bilateral dipole sources in primary auditory cortex for the P200 component. The resulting field pattern appeared like a single midline source because of the way the bilateral sources summed. Similarly, they showed that the P300 distribution could be explained by bilateral extended

cortical surface layers in parieto-temporal association area. They based these results on 14 electrodes in two linear arrays on one side of the head. They did not use any type of optimization method to find the best fit to their data.

In later work [Simson et al. 1976, 1977a] they stuck to the same basic interpretation, suggesting that the N100 originates in a "small supratemporal generator" while the P200 is "generated on the lateral surface of the superior temporal gyrus." These interpretations are supported by intracranial work and comparisons to animal models. The emitted or the DIFF N200, they suggest, corresponds to the joint activity of sources in auditory cortex in the supratemporal plane and auditory association cortex on the lateral surface of the superior temporal gyrus. They suggest that the emitted or difference P300 arises from the inferior parietal lobule. These suggestions are all evidently based on visually inspecting the topographic aEP results with no forward or inverse dipole calculations whatsoever. In a recent review [Vaughan 1982] a similar interpretation is reiterated.

Wood and Wolpaw [1982] have done the most extensive topographic studies to date on the auditory aEP, covering the interval from 20 to 250 ms. In their paper they rightly point out the limitations of traditional aEP and spatial peak component definitions and note their lack of correlation with scalp topography. They summarize the auditory aEP in terms of stability and change in the topography over eight sub-intervals. Comparing their verbal descriptions of topology in each of these intervals to S1, I find substantial agreement between my results and theirs. Any differences could probably be explained by the fact that Wood and Wolpaw recorded on only one side of the head.

Wood and Wolpaw also quickly review equivalent source modeling and correctly make the following observation about the technique: "Hypothesized

sources can be rejected if they conflict with empirical scalp distributions, but competing hypotheses that account equally well for empirical distributions must be evaluated using other data (e.g., intracranial recordings, lesion effects, animal studies, etc.)." They go on to say that the topology in the 20-60 ms region is consistent with bilateral auditory cortical generators. My FP40 source localizations support this contention for S1, at least. As mentioned earlier, more realistic head and dipole models might also support it for S2 and S3.

My data are also consistent with bilateral sources in auditory cortex for S1 and S2 at 100 ms and S1 at 200 ms. As with the 40 ms component, more realistic sources would probably result from using better modeling techniques. With accurate anatomical data, as might be obtained from CT scans or ultrasound, it is conceivable that ESM techniques could be used to differentiate relative contributions of closely spaced cortical generators, such as those of primary/secondary auditory cortex.

To summarize this section on the neural generators of the auditory and odd-ball responses, it is clear that the scalp distributions of potential that I measured on my three subjects match those of previous experimenters, within the limits of variability of referencing, electrode placements, and stimulus parameters. The source locations that were calculated here are in accord with previous qualitative and quantitative source-location estimates. My addition to this literature has been to present the fullest distributions so far of auditory and odd-ball responses, and to attempt one- and two-dipole model fits to a large portion of this data. My results do not as yet conclusively decide between single and multiple sources for these phenomena.

7.6.3 Intracranial Comparisons

Proper intracranial recording done over a large region of the brain can

establish the true location of neural and glial electrical activity. Most everyone agrees on this point, but not on the proper way to interpret intracranial recordings. Unlike what many seem to believe, recording inside the head is almost identical to recording on the surface. Volume conduction still holds throughout the head and referencing problems still arise. Many hang their highest hopes on locating the polarity reversal that indicates passing from one side of a dipole sheet to the other. But if the reference is improperly placed, both ends of a dipole can appear of the same polarity. This is evidently what happens when Goff et al. [1980] performs his intracranial probes around auditory cortex and detects no reversal. On this basis he later states that intracranial recording data does not select between the old associational cortex origin of vertex potentials and the current theories of Vaughan and Ritter or Wood and Wolpaw, involving bilateral sources in auditory cortex.

Polarity reversals can be properly detected if the reference is allowed to travel close to the active electrode, thus measuring the local potential gradients near the dipole. Recordings done in this manner or data re-calculated differentially in this manner would definitely help decide between conflicting hypotheses of the origin of the aEPs discussed here. Theoretically, measuring the second spatial derivative is the best play. One of Maxwell's equations tells us this should be zero everywhere except at the source.

A definitive intracranial study of P300 in epileptic patients was reported by Wood et al. [1980]. Scalp and intracranial recordings were made simultaneously during auditory and somatosensory odd-ball tasks. P300 activity was observed on the scalp and in depth for most of the subjects. With a linked-ear reference, maximum P300 amplitude occurred deep in the brain. Simple polarity inversion was not found, but then the referencing problem was not dealt with properly. The depth-P300 was independent of stimulus modality as was the scalp-P300.

Overall, these results cast doubt on a purely cortical origin of P300-like activity.

7.6.4 Lesion Comparisons

Lesion studies can provide another independent source of information about the neural generators of aEPs. The major problem encountered is the exact specification of the ablated or damaged area. A recent study by Knight et al. [1980] used CT scans to delineate brain damaged areas. It was found that frontal cortex lesions had no effect on aEP parameters, except perhaps the removal of a small inhibitory gating. Temporal-parietal lesions had a marked effect on the N100 component but no effect on the P200 component. This result supports the consensus of hypotheses for the origin of the auditory aEP.

7.6.5 Animal Models

Animal models have been instrumental in suggesting hypotheses for the origin of analogous human EPs, notably in the auditory modality [Arrezo et al. 1975]. Animal models for some of the endogenous ERP components have been discovered in recent years. Pirch [1980ab] records CNV and slow-wave components in rats. Endogenous responses have also been reported in the cat [Paller et al. 1982] and monkey [Neville and Foote 1981]. Arthur and Starr [1984] reported a P300-like response during an odd-ball task, performed by two monkeys, that has features in common with the human P300. Further work with this animal model may bring to light useful information on the neural generators of this and other endogenous components.

7.6.6 Magnetic Results

Two reports of magnetic measurements of evoked fields are relevant to the work presented here. Romani et al. [1982] were able to demonstrate that certain steady-state auditory responses could be modeled by a current dipole in auditory cortex. Their experiment was performed in the frequency domain, so

latency comparisons are not possible. Using a simplified localization method they estimated the depth of the associated dipole based on the location of the two field extrema found over the surface of the head. They discovered that the estimated magnetic source locations varied in depth with the frequency of the tone, thus indicating the existence of a tonotopic mapping in human auditory cortex.

EP evidence for a tonotopic mapping in humans has been lacking, presumably because of the summation effects of the bilateral sources in auditory cortex. With proper two-dipole ESM, such a mapping could be found using EP techniques to collaborate the EF findings. The bilateral magnetic sources do seem to have a tighter field pattern, both theoretically and empirically [Cohen and Cuffin 1983], and thus do not summate to a single broad vertex field analogous to the vertex potential.

The magnetic field associated with the visual odd-ball task has recently been reported by Okada et al. [1983]. They estimate a current source deep in the brain to be the cause of their M300, which they place in the hippocampus or amygdala. The dipole representing their M300 is directed upward toward the vertex, just as is the source I calculate for the FP350 component.

7.6.7 Summary of Neural Origins

The prevailing consensus for the source of exogenous evoked potentials in the time range considered here is auditory cortex. Topographic examination and limited dipole ESM support this consensus, including the one- and two-dipole source localizations done for this thesis. Lesion studies, intracranial recordings, primate studies, and magnetic field measurements also support this interpretation. Properly interpreted intracranial studies and further detailed ESM will undoubtedly refine our knowledge of these sources.

The notion that auditory vertex potentials actually originate at the vertex has been pretty much discounted. Now the notion that the P300 originates in associational cortex is being brought into question. Intracranial and magnetic studies have indicated the probable involvement of deep sources, perhaps in addition to cortical sources, in the electrogenesis of the odd-ball P300 and its relatives. The ESM that was done here does not yet help differentiate between different hypotheses of P300 origin, but then not very many hypotheses have been tested. With more data collection, some further controls, estimates of variance, and realistic models, ESM will definitely be able to make a contribution toward understanding these types of brain responses.

7.7 ESM Improvements

Many improvements are possible for ESM. Most have already been used or suggested previously by the small group of people most involved with ESM. In the following I will discuss what are reasonable improvements to make for the next stage of application to the type of experiments performed in this thesis.

7.7.1 Better Head Models

A necessary improvement for the head model is the use of multiple shells to simulate the scalp, skull, and brain coverings. Corrections can be applied to the homogeneous source localizations reported here to map them to their proper locations in an inhomogeneous model, but it is still better to actually perform the inhomogeneous source calculations if the computing resources are available. A further improvement would involve the actual estimation of head parameters such as electrical conductivity and scalp and skull thickness for individual subjects for inclusion in their model Ary et al. [1981c].

A problem encountered in the present experiments involves the mapping between electrodes on the plexiglas helmet and the spherical computer model.

The helmets were originally laid out for a good fit of a sphere to the back of the head for use in visual experiments. This produces a skewed mapping for frontal electrode positions from subject head to model sphere. In terms of source localization, calculated dipoles that depend strongly on data gathered from frontal regions should be placed more eccentrically and further back on the head. To correct this problem properly I would suggest measuring all the electrode positions on the helmets in an appropriate coordinate system and then fitting a sphere to these locations in a least-squares sense. Then I would find the radial projection of each electrode onto this sphere and use the resulting location as the coordinates for that electrode. This is probably the best that can be done without switching to a non-spherical head model.

7.7.2 Better Source Models

Better source models have been suggested and used by Darcey [1979] and Sidman et al. [1978]. Extended dipole sheets in the form of pieces of cortex, namely spherical caps and annular sectors, may give more realistic results in some cases. Given some knowledge of an individual's brain anatomy, configurations of dipoles can be designed to fit any arbitrary geometry that would be encountered. Non-dipolar source models are also possible.

7.7.3 Accounting for Variance

No analysis of the variance of this data was attempted, mainly because of the lack of a sufficient sample base. When enough data are collected to be able to judge the variance accurately, the errors in dipole fitting can be estimated and measures of the accuracy and reliability of the fits made. Obviously, the number of model parameters can be increased up to the number of measurement sites and the data fitted exactly. But given a finite variance in the data, many fewer parameters are usually sufficient to account for it. Increasing

the number of parameters should properly be stopped as soon as all of the variance in the data has been accounted for.

7.7.4 Using ESM to Subtract Noise

For various reasons already discussed, S3's data was contaminated with noise that was most obvious in the spatial domain. Some results of source localizations were presented in the last chapter indicating that some of the noise could be ascribed to electromyographic activity near the ears, to eye-movements, and to putative occipital alpha generators. Figure 7-1 shows the results of three-dipole fits to some of S3's data. For the FP104 peak, one dipole corresponds to a possible EMG source near the ear, one to possible EOG activity near the eyes, and one to possible auditory cortical activity. For the FP188 peak, a midbrain source and two central sources are indicated, though the central ones appear spurious. For the FP376 peak an ear source is again indicated, as well as a midbrain one. Four- and five-dipole fits may very well be able to account for ear, eye, and occipital noise sources, with two left over for the bilateral auditory cortex. To confirm any of these results would necessitate proper experimental controls where each noise source was purposefully activated, both singly and in combination. And it goes without saying that the amplifier gains would have to be properly stabilized and calibrated.

Some of the earliest optimal sources calculated were for ongoing EEG [Schneider 1972]. With more work ESM could become a useful tool for the study of biological noise sources in aEPs and for modeling single trial EPs. In the latter case, the sources of the ongoing activity could be modeled and subtracted out, leaving something close to the true single-trial evoked potential.

7.8 Use of ESM in Cognitive Psychophysiology

While the results of ESM applied to the auditory and odd-ball responses described here do not yet provide definitive information to choose between competing hypotheses of the origins of these responses, a little further study should provide that information. A next step would be to study various aspects of the odd-ball response in depth. The effects of all the variables discussed in Chapter 4 under controls need to be studied with ESM, including manipulations of probability, intensity, pitch, detectability, discriminability, and modality. The odd-ball P300 should be compared to the signal-detection P300 and the guessing P300. Other endogenous responses could then be studied with ESM, most especially the attention-related N100, since with source characterization there is some hope of separating it from the strong exogenous N100.

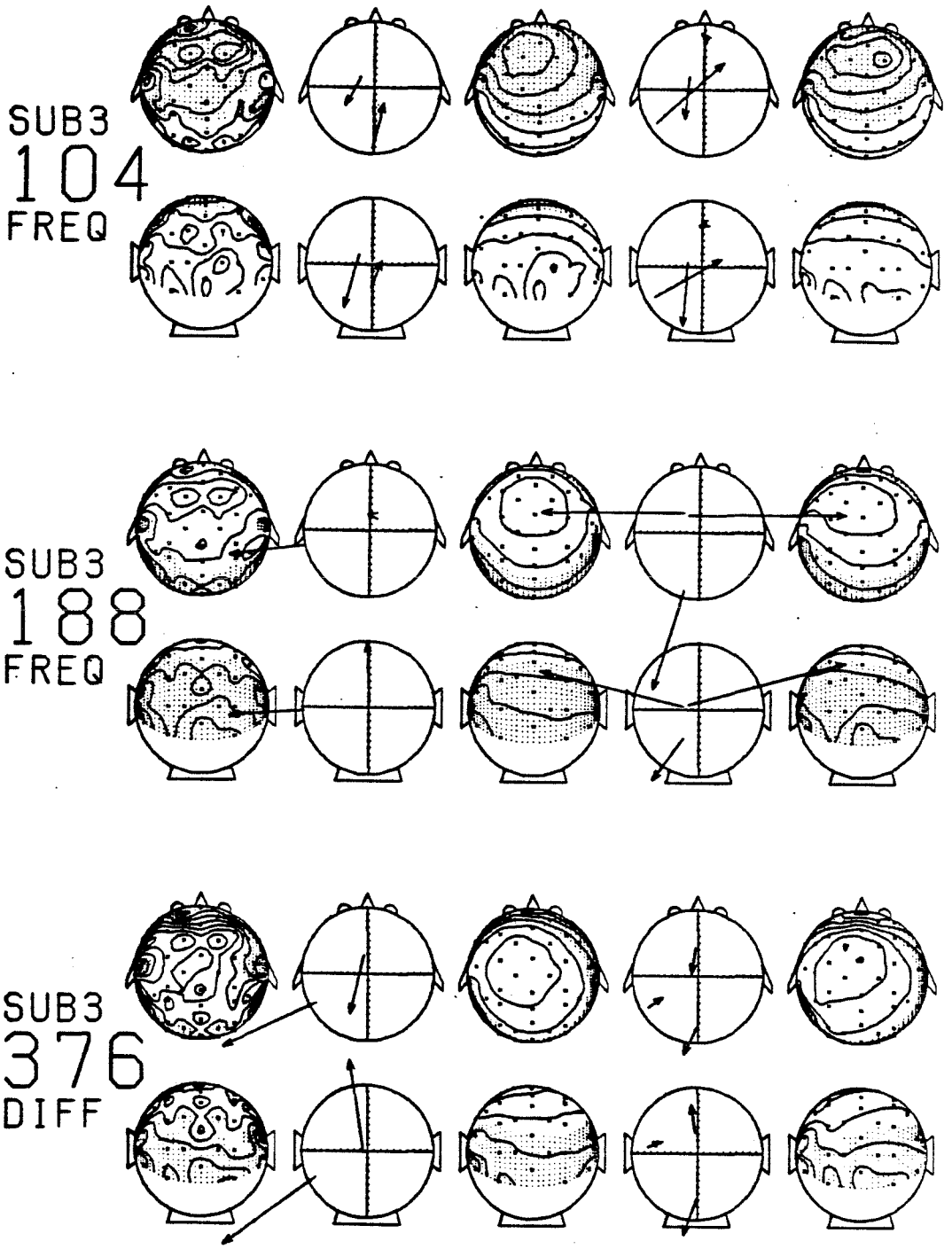

Figure 7-1. Comparisons of experimental data and dipole model fits for S3 for selected peaks. For explanation see Figure 6-18.

[1] Allison, T.; Matsumiya, Y.; Goff, G.D. and Goff, W.R. **1977.** The Scalp Topography of Human Visual Evoked Potentials. *EEG J. 42:* 185-197.

[2] Arezzo, J.; Pickoff, A. and Vaughan, H.G., Jr. **1975.** The Source and Intracerebral Distribution of Auditory Evoked Potentials in the Alert Rhesus Monkey. *Brain Res. Bull. 90:* 57-73.

[3] Arthur, D. Lee and Starr, Arnold. **1984.** Task-Relevant Late Positive Component of the Auditory Event-Related Potential in Monkeys Resembles P300 in Humans. *Science 223:* 186-188.

[4] Ary, James. P. **1976.** The Effect of Color on the Localization of the Sources of the Human Visual Evoked Response. *Ph.D. Dissertation.* Ohio State University.

[5] Ary, J.P.; Darcey, T.M. and Fender, D.H. **1981a.** A Method for Locating Scalp Electrodes in Spherical Coordinates. *IEEE Trans. Biomed. Engng. 28(12):* 834-836.

[6] Ary, James P.; Darcey, Terrance M. and Fender, Derek H. **1981b.** Locating Electrical Sources in the Human Brain. In: *IEEE 1981 Frontiers of Engineering in Health Care.* 182-186.

[7] Ary, James. P.; Klein, Stanley and Fender, Derek H. **1981c.** Location of Sources of Evoked Scalp Potentials: Corrections for Skull and Scalp Thicknesses. *IEEE Trans. Biomed. Engng. 28(6):* 447-452.

[8] Asimov, Isaac **1951.** *The Foundation Trilogy - The Second Foundation.* Doubleday & Company. 107-108.

[9] Barth, Daniel S.; Sutherling, William; Engle, Jerome Jr. and Beatty, Jackson. **1982.** Neuromagnetic Localization of Epileptiform Spike Activity in the Human Brain. *Science 218:* 891-894.

[10] Begleiter, H.; Porjesz, B.; Chou, C.L. and Aunon, J.I. **1983.** P3 and Stimulus Incentive Value. *Psychophysiol. 20(1):* 95-101.

[11] Bickford, Reginald G.; Jacobson, James L. and Cody, D. Thane R. **1961.** Nature of Average Evoked Potentials to Sound and Other Stimuli in Man. *Ann. N.Y. Acad. Science:* 204-223.

[12] Brazier, Mary A.B. **1949.** A Study of the Electrical Fields at the Surface of the Head. *EEG J. Suppl. 2:* 38-52.

[13] Brenner, D.; Williamson, S.J. and Kaufman, L. **1975.** Visually Evoked Magnetic Fields of the Human Brain. *Science 190:* 480-482.

[14] Brenner, D.; Lipton, J.; Kaufman, L. and Williamson, S.J. **1978.** Somatically Evoked Magnetic Fields of the Human Brain. *Science 199:* 81-83.

[15] Buchsbaum, M.S.; Rigal, F.; Coppola, R.; Cappelletti, J.; King, C. and Johnson, J. **1982.** A New System for Gray-Level Surface Distribution Maps of Electrical Activity. *EEG J. 53:* 237-242.

[16] Buchwald, Jennifer S. **1983.** Generators of the Auditory Brain-Stem Evoked Responses. In: Ernest J. Moore, *Bases of Auditory Brain-Stem Evoked Responses.* Grune and Stratton. 157-195.

[17] Chapman, Robert M. **1969.** Discussion of Eye Movements, CNV, and AEP. In: E. Donchin and F. Rigal, *Averaged Evoked Potentials: Methods, Results, and Evaluations. NASA SP-191.* Government Printing Office. 177-180.

[18] Clynes, M. and Kohn, M. **1960.** The Use of the Mnemotron for Biological Data Storage, Reproduction, and for an Average Transient Computer. In: *4th Annual Meeting of the Biophysics Society.*

[19] Cohen, David **1968.** Magnetoencephalography: Evidence of Magnetic Fields Produced by Alpha-Rhythm Currents. *Science 161:* 784-786.

[20] Cohen, David and Cuffin, B. Neil **1983.** Demonstration of Useful Differences Between Magnetoencephalogram and Electroencephalogram. *EEG J. 56:* 38-51.

[21] Darcey, Terrance Michael **1979.** Methods for Localization of Electrical Sources in the Human Brain and Applications to the Visual System. *Ph.D. Dissertation.* California Institute of Technology.

[22] Darcey, T.M.; Wieser, H.G.; Meles, H.P.; Skrandies, W. and Lehmann, D. **1979.** Intracerebral and Scalp Fields Evoked by Visual Stimulation. In: *Fall 1979 Meeting of the Swiss EEG Society.*

[23] Darcey, T. M.; Ary, J. P. and Fender, D. H. **1980a.** Methods for the Localization of Electrical Sources in the Human Brain. In: *Motivation, Motor and Sensory Processes of the Brain, Progress in Brain Research, Vol. 54.* 128-134.

[24] Darcey, T. M.; Ary, J. P. and Fender, D. H. **1980b.** Spatio-Temporal Visually Evoked Scalp Potentials in Response to Partial-Field Patterned Stimulation. *EEG J. 50:* 348-355.

[25] Dawson, G.D. **1947.** Cerebral Responses to Electrical Stimulation of Peripheral Nerve in Man. *J. Neuro. Neurosurg. Psych. 10:* 134-140.

[26] Dawson, G.D. **1951.** A Summation Technique for Detecting Small Signals in a Large Irregular Background. *J. Physiol. 115:* 2-3.

[27] Debecker, J. and Desmedt, J. E. **1966.** Rate of Intermodality Switching Disclosed by Sensory Evoked Potentials Averaged During Signal Detection Tasks. In: *Proc. of the Physiol. Soc.* 52P-53P.

[28] Donchin, Emanuel **1966.** A Multivariate Approach to the Analysis of Average Evoked Potentials. *IEEE Trans. Biomed. Engng. 13(3):* 131-139.

[29] Donchin, Emanuel; Tueting, Patricia; Ritter, Walter; Kutas, Marta and Heffley, Earle **1975.** On the Independence of the CNV and the P300 Components of the Human Averaged Evoked Potential. *EEG J. 38:* 449-461.

[30] Donchin, Emanuel; Ritter, Walter and McCallum, W. Cheyne **1978.** Cognitive Psychophysiology: The Endogenous Components of the ERP. In: E. Callaway, P. Tueting and S. H. Koslow, *Event-Related Brain Potentials in Man.* Academic Press. 349-411.

[31] Donchin, Emanuel **1979.** Event-Related Brain Potentials: A Tool in the Study of Human Information Processing. In: Henri Begleiter, *Evoked Brain Potentials and Behavior* Plenum Press, New York. 13-88.

[32] Dubinsky, Janet and Barlow, John S. **1980.** A Simple Dot-Density Topogram for EEG. *EEG J.* 48: 473-477.

[33] Duffy, Frank H.; Burchfiel, James L. and Lombroso, Cesare T. **1979.** Brain Electrical Activity Mapping (BEAM): A Method for Extending the Clinical Utility of EEG and Evoked Potential Data. *Ann. Neurol. 5(4):* 309-321.

[34] Duncan-Johnson, C.C. and Donchin, E. **1977.** On Quantifying Surprise: The Variation in Event-Related Potentials with Subjective Probability. *Psychophysiol. 14:* 456-467.

[35] Estrin, Thelma and Uzgalis, Robert **1969.** Computerized Display of Spatio-Temporal EEG Patterns. *IEEE Trans. Biomed. Engng. 16(3):* 192-196.

[36] Fender, D.H. and Santoro, T.P. **1977.** Spatiotemporal Mapping of Scalp Potentials. *J. Op. Soc. Am. 67(11):* 1489-1494.

[37] Feynman, Richard P.; Leighton, Robert B. and Sands, Matthew **1964.** Electrostatics. *The Feynman Lectures on Physics*, Chapter 4. Addison-Wesley Publishing Company.

[38] Fitzgerald, Peter G. and Picton, Terence W. **1981.** Temporal and Sequential Probability in Evoked Potential Studies. *Can. J. Psychol. 35(2):* 188-200.

[39] Ford, Judith M.; Roth, Walton T.; Dirks, Stanley J. and Kopell, Bert S. **1973.** Evoked Potential Correlates of Signal Recognition Between and Within Modalities. *Science 181:* 465-466.

[40] Ford, Judith M. and Hillyard, Steven A. **1981.** Event-Related Potentials (ERPs) to Interruptions of a Steady Rhythm. *Psychophysiol. 18(3):* 322-330.

[41] Goff, William R. **1978.** The Scalp Distribution of Auditory Evoked Potentials. In: *Evoked Electrical Activity in the Auditory Nervous System.* Academic Press. 505-524.

[42] Goff, W. R.; Williamson, P. D.; VanGilder, J. C.; Allison, T. and Fisher, T. C. **1980.** Neural Origins of Long Latency Evoked Potentials Recorded from the Depth and from the Cortical Surface of the Brain in Man. In: J. E. Desmedt, *Clinical Uses of Cerebral, Brainstem and Spinal Somatosensory Evoked Potentials. Prog. clin. Neurophysiol., Vol. 7.* 126-145.

[43] Goodin, Douglas S.; Squires, Kenneth C.; Henderson, Beverley H. and Starr, Arnold **1978.** An Early Event-Related Cortical Potential. *Psychophysiol. 15(4):* 360-365.

[44] Goodin, Douglas; Squires, Kenneth C. and Starr, Arnold **1983.** Variations in Early and Late Event-Related Components of the Auditory Evoked Potential with Task Difficulty. *EEG J. 55:* 680-686.

[45] Helmholtz, H. 1853. Ueber einige Gesetze der Vertheilung elektrischer Strome in korperlichen Leitern mit Anwendung auf die thierisch-elektrischen Versuche. *Ann. der Physik. Ser. 2 29:* 211-233.

[46] Henderson, C.J.; Butler, S.R. and Glass, A. **1975.** The Localization of Equivalent Dipoles of EEG Sources by the Application of Electrical Field Theory. *EEG J. 39:* 117-130.

[47] Herning, Ronald I.; Hunt, Johanna S. and Jones, Reese T. **1983.** Event-Related Potentials During Speech Perception. In: *23rd Annual Meeting of the Society for Psychophysiological Research.*

[48] Hillyard, Steven A.; Hink, Robert F.; Schwent, Vincent L. and Picton, Terence W. **1973.** Electrical Signs of Selective Attention in the Human Brain. *Science 182:* 177-179.

[49] Hillyard, S.A.; Courchesne, E.; Krausz, H.I. and Picton, T.W. **1976.** Scalp Topography of the P3 Wave in Different Auditory Decision Tasks. In: W. C.

McCallum and J. R. Knott, *The Responsive Brain*. Wright. 81-87.

[50] Hillyard, Steven A. **1981.** Selective Auditory Attention and Early Event-Related Potentials: A Rejoinder. *Can. J. Psychol. 35(2):* 159-174.

[51] Hillyard, Steven A. and Kutas, Marta **1983.** Electrophysiology of Cognitive Processing. *Ann. Rev. Psychol. 34:* 33-61.

[52] Hosek, Ronald S.; Sances, Anthony Jr.; Jodat, Ronald W. and Larson, Sanford J. **1978.** The Contributions of Intracerebral Currents to the EEG and Evoked Potentials. *IEEE Trans. Biomed. Engng. 25(5):* 405-413.

[53] Hughes, J.R.; Hendrik, D.E.; Cohen, J.; Duffy, F.H.; Mayman, C.I.; Scholl, M.L. and Cuffin, B.N. **1976.** Relationship of the Magnetoencephalogram to the Electroencephalogram. Normal Wake and Sleep Activity. *EEG J. 40:* 261-278.

[54] Hunt, Johanna S.; Herning, Ronald I. and Jones, Reese T. **1983.** Extracting Components from Event Related Potential: The Nonlinear Modeling Approach. In: *23rd Annual Meeting of the Society for Psychophysiological Research.*

[55] Jasper, Herbert H. **1957.** The Ten Twenty Electrode System of the International Federation. *EEG J.* 370-375.

[56] Jeffreys, D.A. **1971.** Cortical Source Locations of Pattern-Related Visual Evoked Potentials Recorded from the Human Scalp. *Nature 229:* 502-504.

[57] Jeffreys, D.A. and Axford, J.G. **1972a.** Source Locations of Pattern-Specific Components of Human Visual Evoked Potentials. I. Component of Striate Cortical Origin. *Exp. Brain Res. 16:* 1-21.

[58] Jeffreys, D.A. and Axford, J.G. **1972b.** Source Locations of Pattern-Specific Components of Human Visual Evoked Potentials. II. Component of Extrastriate Cortical Origin. *Exp. Brain Res. 16:* 22-40.

[59] Karis, Demetrios; Chesney, Gregory L. and Donchin, Emanuel **1983.** "...'twas ten to one; And yet we ventured...": P300 and Decision Making. *Psychophysiol. 20(3):* 260-268.

[60] Kavanagh, Robert N. **1972.** Localization of Sources of Human Evoked Responses. *Ph.D. Dissertation.* California Institute of Technology.

[61] Kavanagh, Robert N.; Darcey, Terrance M. and Fender, Derek H. **1976.** The Dimensionality of the Human Visual Evoked Scalp Potential. *EEG J. 40:* 633-644.

[62] Kavanagh, Robert N.; Darcey, Terrance M.; Lehmann, Dietrich and Fender, Derek H. **1978.** Evaluation of Methods for Three-Dimensional Localization of Electrical Sources in the Human Brain. *IEEE Trans. Biomed. Engng. 25(5):* 421-429.

[63] Knight, Robert T.; Hillyard, Steven A.; Woods, David L. and Neville, Helen J. **1980.** The Effects of Frontal and Temporal-Parietal Lesions on the Auditory Evoked Potential in Man. *EEG J. 50:* 112-124.

[64] Kuffler, Stephen W. and Nicholls, John G. **1976.** Physiology of Neuroglial Cells. In: *From Neuron to Brain, A Cellular Approach to the Function of the Nervous System.* Sinauer Associates. 377-401.

[65] Kutas, Marta; McCarthy, Gregory and Donchin, Emanuel **1977.** Augmenting Mental Chronometry: The P300 as a Measure of Stimulus Evaluation time.

Science 197: 792-795.

[66] Kutas, Marta and Hillyard, Steven A. **1980a.** Reading Between the Lines: Event-Related Brain Potentials During Natural Sentence Processing. *Brain and Language 11:* 354-373.

[67] Kutas, Marta and Hillyard, Steven A. **1980b.** Reading Senseless Sentences: Brain Potentials Reflect Semantic Incongruity. *Science 207:* 203-205.

[68] Kutas, Marta and Hillyard, Steven A. **1980c.** Event-Related Brain Potentials to Semantically Inappropriate and Surprisingly Large Words. *Biol. Psych. 11:* 99-116.

[69] Lehmann, Dietrich **1971.** Multichannel Topography of Human Alpha EEG Fields. *EEG J. 31:* 439-449.

[70] Lehmann, D. and Skrandies, W. **1980.** Reference-free Identification of Components of Checkerboard-Evoked Multichannel Potential Fields. *EEG J. 48:* 609-621.

[71] Marquardt, Donald W. **1963.** An Algorithm for Least-Squares Estimation of Nonlinear Parameters. *J. Soc. Indust. Appl. Math. 11(2):* 431-441.

[72] McGillem, Clare D. and Aunon, Jorge I. **1977.** Measurements of Signal Components in Single Visually Evoked Brain Potentials. *IEEE Trans. Biomed. Engng. 24(3):* 232-241.

[73] Nakamura, Zenju and Biersdorf, William R. **1971.** Localization of the Human Visual Evoked Response: Early Components Specific to Visual Stimulation. *Am. J. Ophth. 72(5):* 988-997.

[74] Nelder, J. A. and Mead, R. **1965.** A Simplex Method for Function Minimization. *The Computer Journal 7:* 308-313.

[75] Neville, H.J. and Foote, S. **1981.** *Neurosci. Res. Bull. 20:* 242-242.

[76] Okada, Y.C.; Kaufman, L. and Williamson, S.J. **1983.** Hippocampal Formation as a Source of the Magnetic Field Correlated with Endogenous Slow Potentials. *EEG J.*

[77] Paicer, P. L.; Larson, S. J. and Sances, A. Jr. **1967.** Theoretical Evaluation of Cerebral Evoked Potentials. In: *20th Annual Conference on Engineering in Medicine and Biology,Boston, Massachusetts.*

[78] Paller, K.A.; Zola-Morgan, S.; Squires, L.R. and Hillyard, S.A. **1982.** *Soc. Nero. Abst. 8:* 975-975.

[79] Petsche, H.; Prohaska, O.; Rappelsberger, P.; Vollmer, R. and Kaiser, A. **1974.** Cortical Seizure Patterns in Multidimensional View: The Information Content of Equipotential Maps. *Epilepsia 15:* 439-463.

[80] Pirch, James H. **1980a.** Correlation Between Steady Potential Baseline and Event-Related Slow Potential Magnitude in the Rat. *Int. J. Neurosci. 11:* 25-33.

[81] Pirch, James H. **1980b.** Event-Related Slow Potentials in Rat Cortex During a Reaction Time Task: Cortical Area Differences. *Brain Res. Bull. 5:* 199-201.

[82] Plonsey, Robert **1969.** Volume Conductor Fields. *Bioelectric Phenomena*, Chapter 5. McGraw-Hill, New York. 203-275.

[83] Plonsey, Robert **1974.** The Active Fiber in a Volume Conductor. *IEEE Trans. Biomed. Engng. 21(5):* 371-381.

[84] Posner, Michael I. and Boies, Stephen J. **1971.** Components of Attention. *Psychol Rev. 78(5):* 391-408.

[85] Powell, M.J.D. **1964.** An Efficient Method for Finding the Minimum of a Function of Several Variables Without Calculating Derivatives. *Comp. J. 7:* 155-162.

[86] Rall, Wilfrid and Shepherd, Gordon M. **1968.** Theoretical Reconstruction of Field Potentials and Dendrodendritic Synaptic Interactions in Olfactory Bulb. *J. Neurophysiol. 31:* 884-915.

[87] Reite, Martin; Zimmerman, John T. and Zimmerman, James E. **1981.** Magnetic Auditory Evoked Fields: Interhemispheric Asymmetry. *EEG J. 51:* 388-392.

[88] Rémond, A. **1961.** Integrative and Topological Analysis of the EEG. *EEG J. S20:* 64-67.

[89] Ritter, Walter and Vaughan, H. G. Jr. **1969.** Averaged Evoked Responses in Vigilance and Discrimination: A Reassessment. *Science 164:* 326-328.

[90] Ritter, Walter; Simson, Richard and Vaughan, Herbert G. Jr. **1972.** Association Cortex Potentials and Reaction Time in Auditory Discrimination. *EEG J. 33:* 547-555.

[91] Romani, Gian Luca; Williamson, Samuel J. and Kaufman, Lloyd **1982.** Tonotopic Organization of the Human Auditory Cortex. *Science 216:* 1339-1340.

[92] Ruchkin, Daniel S. **1965.** An Analysis of Average Response Computations Based Upon Aperiodic Stimuli. *IEEE Trans. Biomed. Engng.* 87-94.

[93] Ruchkin, Daniel S. **1974.** Comparison of Statistical Errors of the Median and Average Evoked Responses. *IEEE Trans. Biomed. Engng. (1):* 54-56.

[94] Ruchkin, D. S. and Sutton, S. **1978.** Emitted P300 Potentials and Temporal Uncertainty. *EEG J. 45:* 268-277.

[95] Rush, Stanley and Driscoll, Daniel A. **1968.** Current Distribution in the Brain from Surface Electrodes. *Anesth. Analges. 47(6):* 717-723.

[96] Ryding, Erik **1980.** A Mathematical Model for Localization of the Source of Cortical Evoked Potentials. *EEG J. 48:* 312-317.

[97] Schneider, Michel R. **1972.** A Multistage Process for Computing Virtual Dipolar Sources of EEG Discharges from Surface Information. *IEEE Trans. Biomed. Engng. 19(1):* 1-12.

[98] Sencaj, Randy and Aunon, Jorge. **1979.** Dipole Localization of Potentials Elicited by Visual Pattern Stimulation. In: *IEEE Frontiers of Engineering in Health Care.* 236-240.

[99] Shaw, John C. and Roth, Martin **1955a.** Potential Distribution Analysis. I: A New Technique for the Analysis of Electrophysiological Phenomena. *EEG J. 7:* 273-284.

[100] Shaw, John C. and Roth, Martin **1955b.** Potential Distribution Analysis. II. A Theoretical Consideration of its Significance in Terms of Electrical Field Theory. *EEG J. 7:* 285-292.

[101] Sidman, R.D.; Giambalvo, V.; Allison, T. and Bergey, P. **1978.** A Method for Localization of Sources of Human Cerebral Potentials Evoked by Sensory Stimuli. *Sens. Proc. 2:* 116-129.

[102] Sidman, Robert D. **1979.** Finding the Extended Sources of Evoked Cerebral Potentials: An Application to the N55 Component of the Somatosensory Evoked Potential. In: *IEEE Frontiers of Engineering in Health Care.* 233-235.

[103] Simson, Richard; Vaughan, Herbert G. Jr. and Ritter, Walter **1976.** The Scalp Topography of Potentials Associated with Missing Visual or Auditory Stimuli. *EEG J. 40:* 33-42.

[104] Simson, Richard; Vaughan, Herbert G. Jr. and Ritter, Walter **1977a.** The Scalp Topography of Potentials in Auditory and Visual Discrimination Tasks. *EEG J. 42:* 528-535.

[105] Simson, Richard; Vaughan, Herbert G. Jr. and Ritter, Walter **1977b.** The Scalp Topography of Potentials in Auditory and Visual Go/Nogo Tasks. *EEG J. 43:* 864-875.

[106] Smith, D.B.; Lell, M.E.; Sidman, R.D. and Mavor, H. **1973.** Nasopharyngeal Phase Reversal of Cerebral Evoked Potentials and Theoretical Dipole Implications. *EEG J. 34:* 654-658.

[107] Squires, N.K.; Squires, K.C. and Hillyard, S.A. **1975.** Two Varieties of Long-Latency Positive Waves Evoked by Unpredictable Auditory Stimuli in Man. *EEG J. 38:* 387-401.

[108] Sutton, Samuel; Braren, Margery; Zubin, Joseph and John, E. R. **1965.** Evoked-Potential Correlates of Stimulus Uncertainty. *Science 150:* 1187-1188.

[109] Truex, Raymond C. and Carpenter, Malcolm B. **1969.** *Human Neuroanatomy.* Waverly Press.

[110] Vaughan, Herbert G. Jr. and Ritter, Walter **1970.** The Sources of Auditory Evoked Responses Recorded from the Human Scalp. *EEG J. 28:* 360-367.

[111] Vaughan, Herbert G. Jr. **1982.** The Neural Origins of Human Event-Related Potentials. *Ann. N.Y. Acad. Science* 125-138.

[112] Walter, Donald O. **1971.** Two Approximations to the Median Evoked Response. *EEG J. 30:* 246-247.

[113] Walter, W. Grey; Cooper, R.; Aldridge, V. J.; McCallum, W. C. and Winter, A. L. **1964.** Contingent Negative Variation: An Electric Sign of Sensorimotor Association and Expectancy in the Human Brain. *Nature 203:* 380-384.

[114] Wickens, Christopher; Kramer, Arthur; Vanasse, Linda and Donchin, Emanuel **1983.** Performance of Concurrent Tasks: A Psychophysiological Analysis of the Reciprocity of Information-Processing Resources. *Science 221:* 1080-1082.

[115] Wilkus, R.J.; Kalk, D.F.; Mars, N.J.I.; Lopes da Silva, F.H. and Chatrian, G.E. **1981.** Automated Isopotential Contour Plotting of EEG Epileptiform Discharges. In: M. Dam, L. Gram and J. K. Perry, *Advances in Epileptology: XIIth Epilepsy International Symposium.* Raven Press, New York. 379-386.

[116] Wilson, Frank N. and Bayley, Robert H. **1950.** The Electric Field of an Eccentric Dipole in a Homogeneous Spherical Conducting Medium.

Circulation 1: 84-92.

[117] Witwer, Jeffrey Garth; Trezek, George J. and Jewett, Don L. **1972.** The Effect of Media Inhomogeneities Upon Intracranial Electrical Fields. *IEEE Trans. Biomed. Engng. 19(5):* 352-362.

[118] Wolpaw, Jonathan R. and Wood, Charles C. **1982.** Scalp Distribution of Human Auditory Evoked Potentials. I. Evaluation of Reference Electrode Sites. *EEG J. 54:* 15-24.

[119] Wood, Charles C.; Allison, Truett; Goff, William R.; Williamson, Peter D. and Spencer, Dennis D. **1980.** On the Neural Origin of P300 in Man. In: H. H. Kornhuber and L. Deeke, *Motivation, Motor and Sensory Processes of the Brain Electrical Potentials, Behavior and Clinical Use.* Elsevier. 51-56.

[120] Wood, Charles C. and Allison, Truett **1981.** Interpretation of Evoked Potentials: A Neurophysiological Perspective. *Can. J. Psychol. 35(2):* 113-135.

[121] Wood, Charles C. **1982.** Application of Dipole Localization Methods to Source Identification of Human Evoked Potentials. *Ann. N.Y. Acad. Science:* 139-155.

[122] Wood, Charles C. and Wolpaw, Jonathan R. **1982.** Scalp Distribution of Human Auditory Evoked Potentials. II. Evidence for Overlapping Sources and Involvement of Auditory Cortex. *EEG J. 54:* 25-38.

[123] Wood, Charles C. **1983.** Preconference Workshop on ERPs. In: *23rd Annual Meeting of the Society for Psychophysiological Research.*

APPENDIX A: Raw EEG

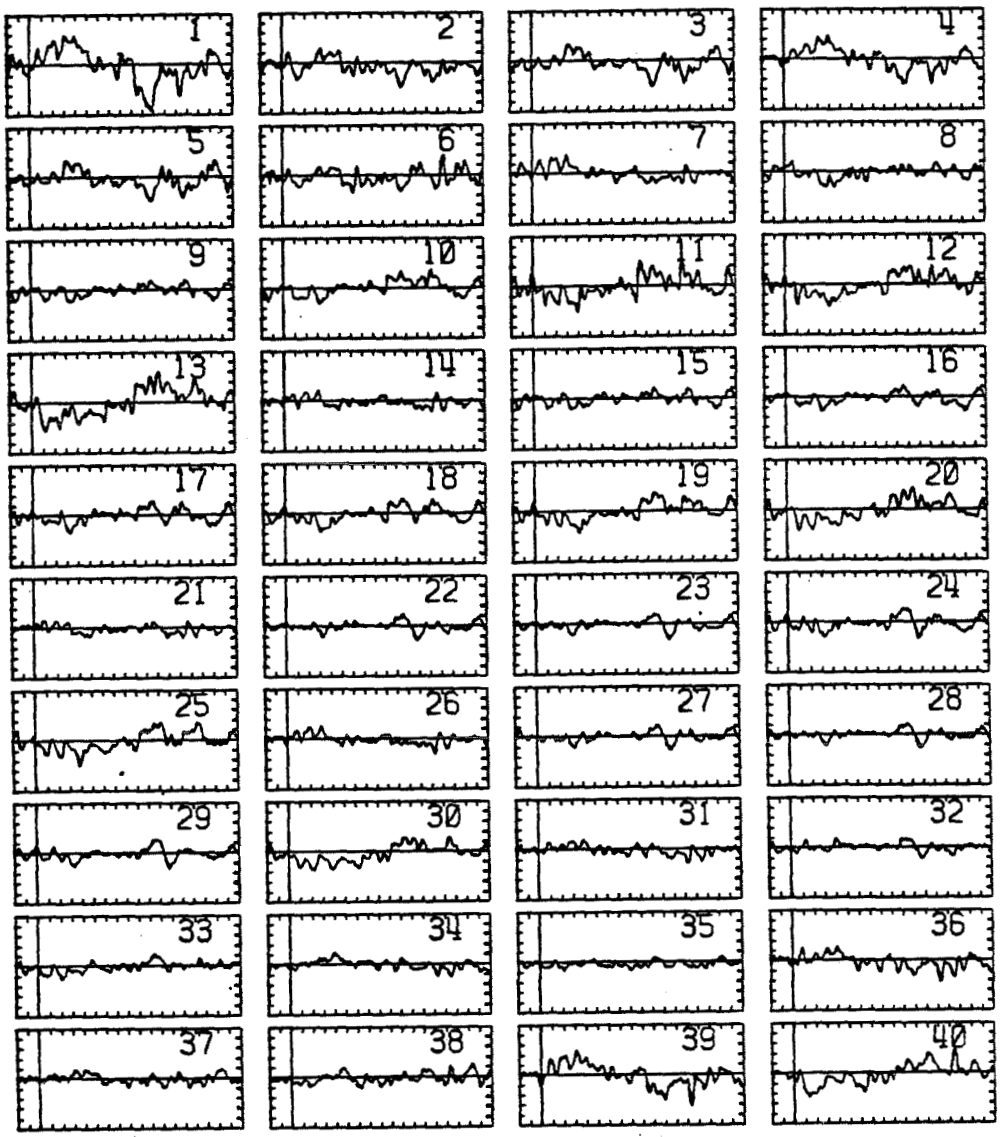

S1 Raw EEG

horizontal scale: 51 ms/div, vertical scale: 10 uV/div

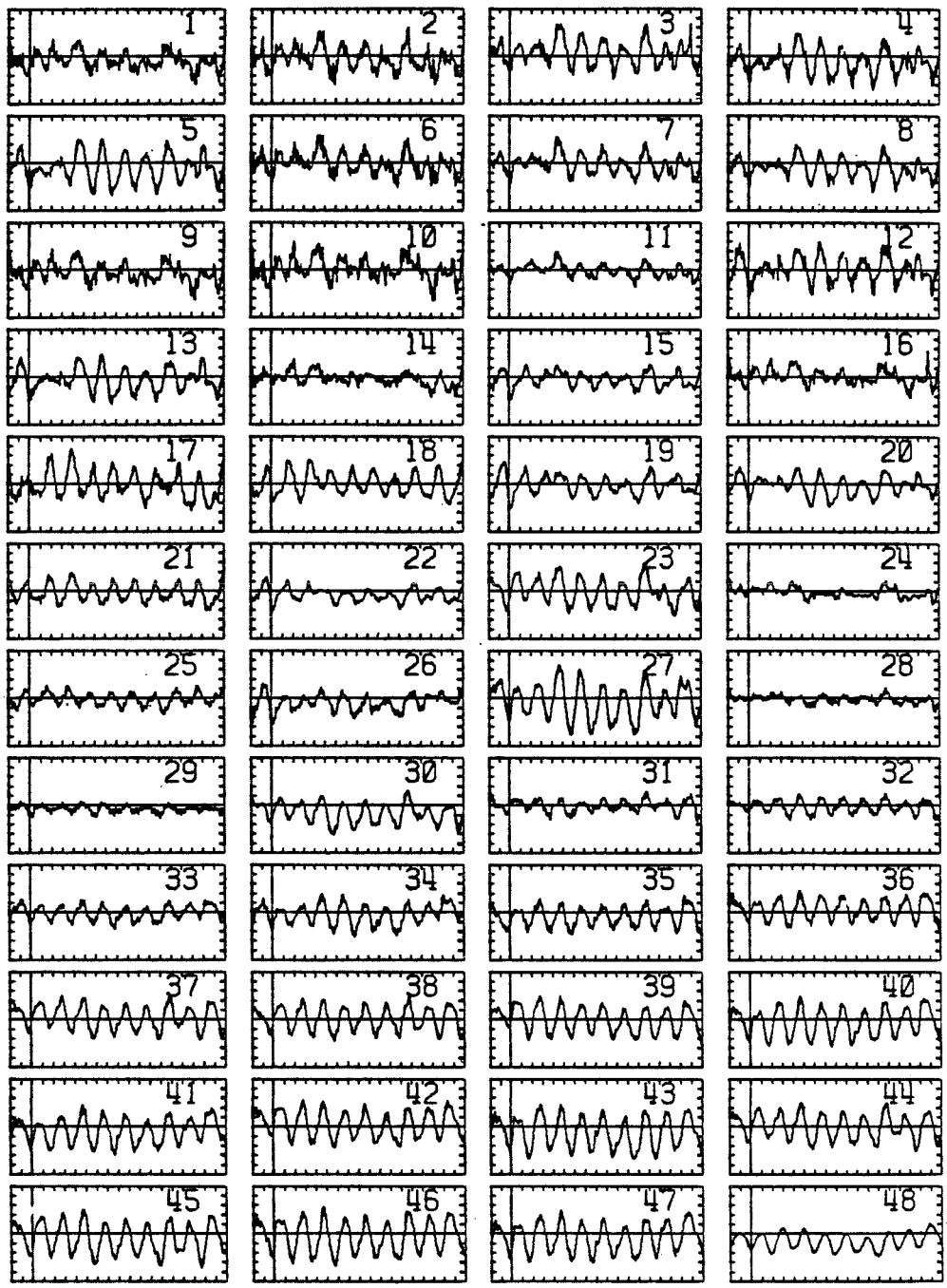

S2 Raw EEG

horizontal scale: 51 ms/div, vertical scale: 10 uV/div

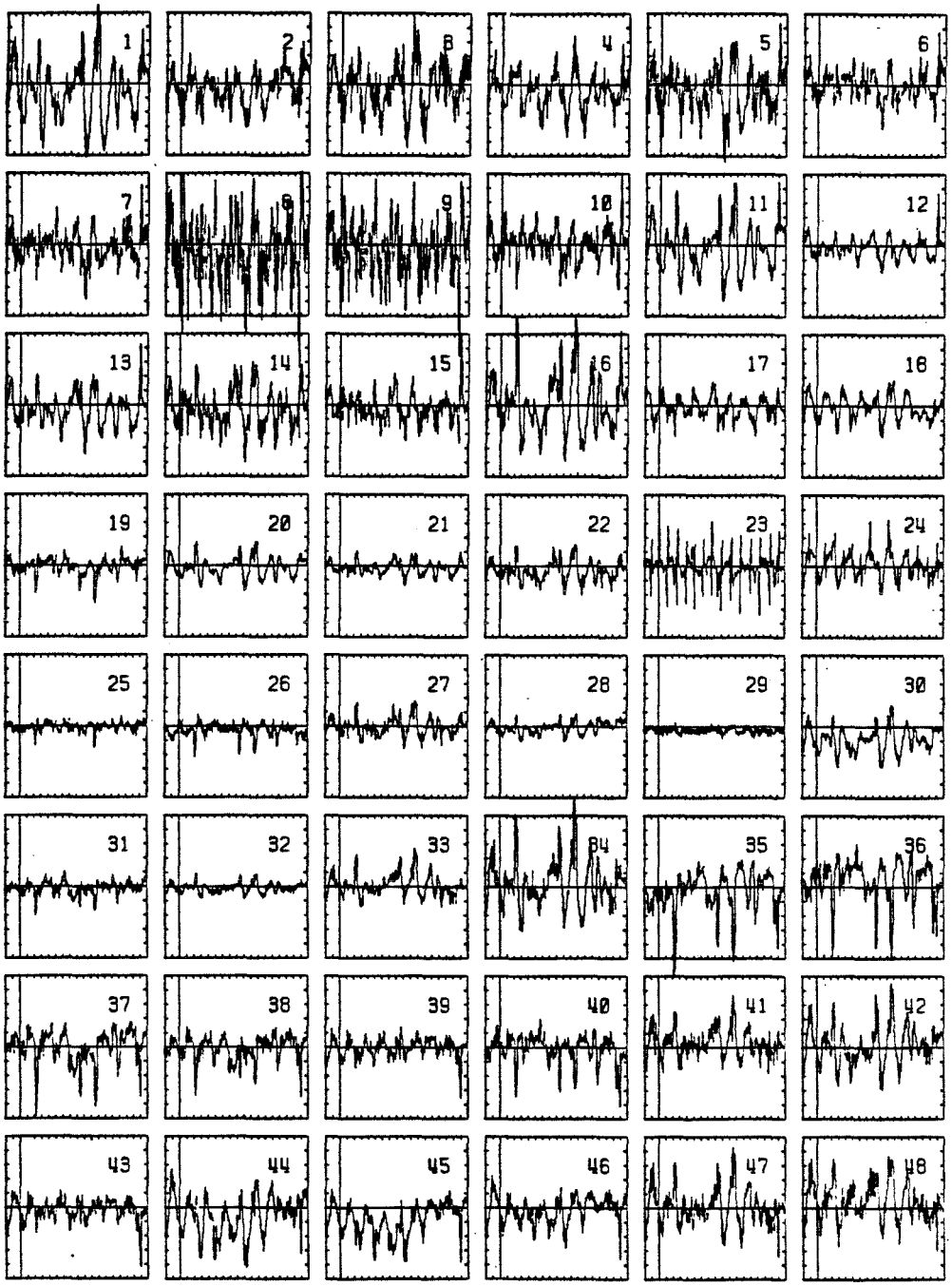

S3 Raw EEG

horizontal scale: 51 ms/div, vertical scale: 10 uV/div

APPENDIX B: AVERAGE EVOKED POTENTIALS

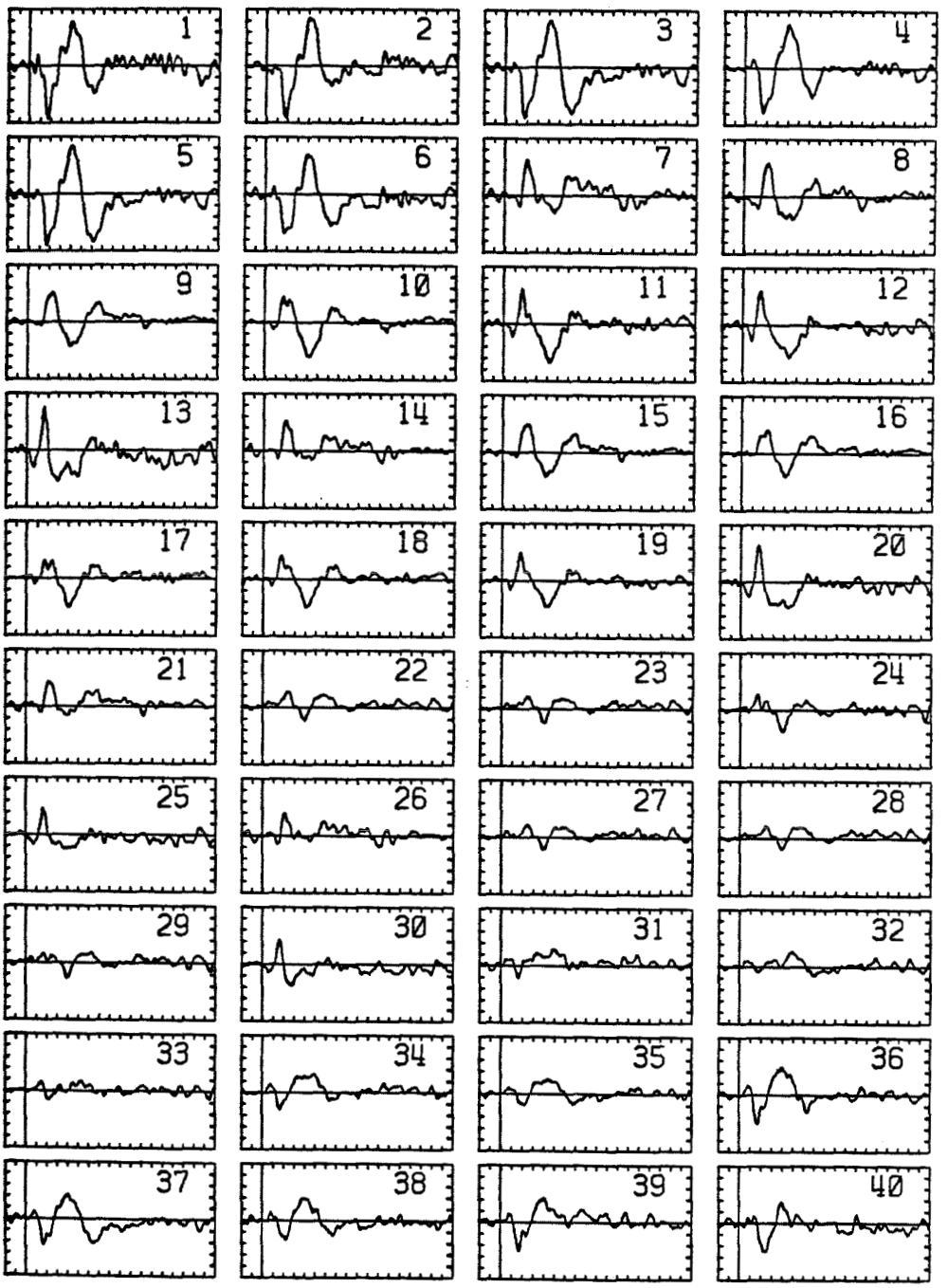

S1 FREQ aEPs

horizontal scale: 51 ms/div, vertical scale: 1.0 uV/div

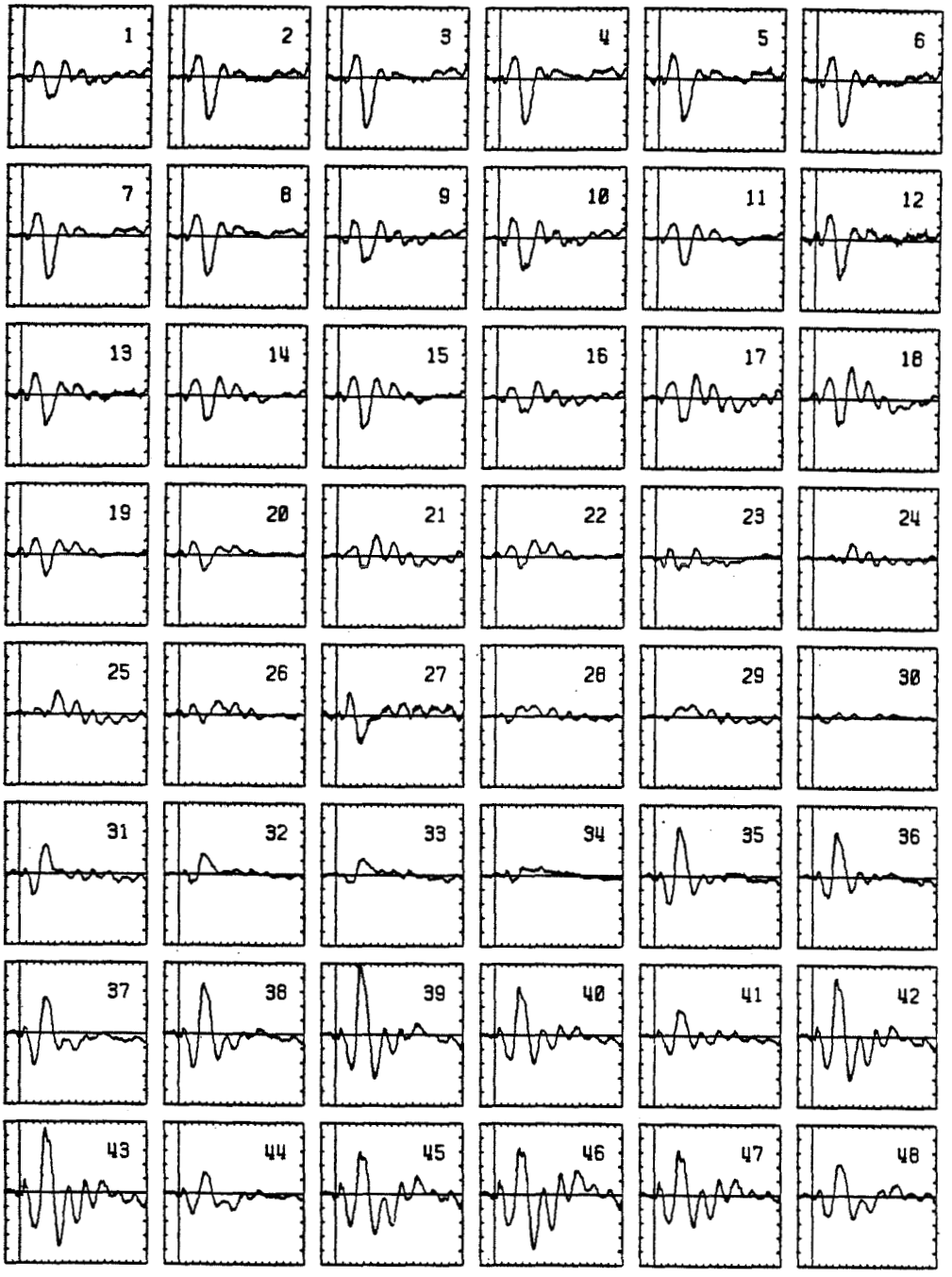

S2 FREQ aEPs

horizontal scale: 51 ms/div, vertical scale: 1.0 uV/div

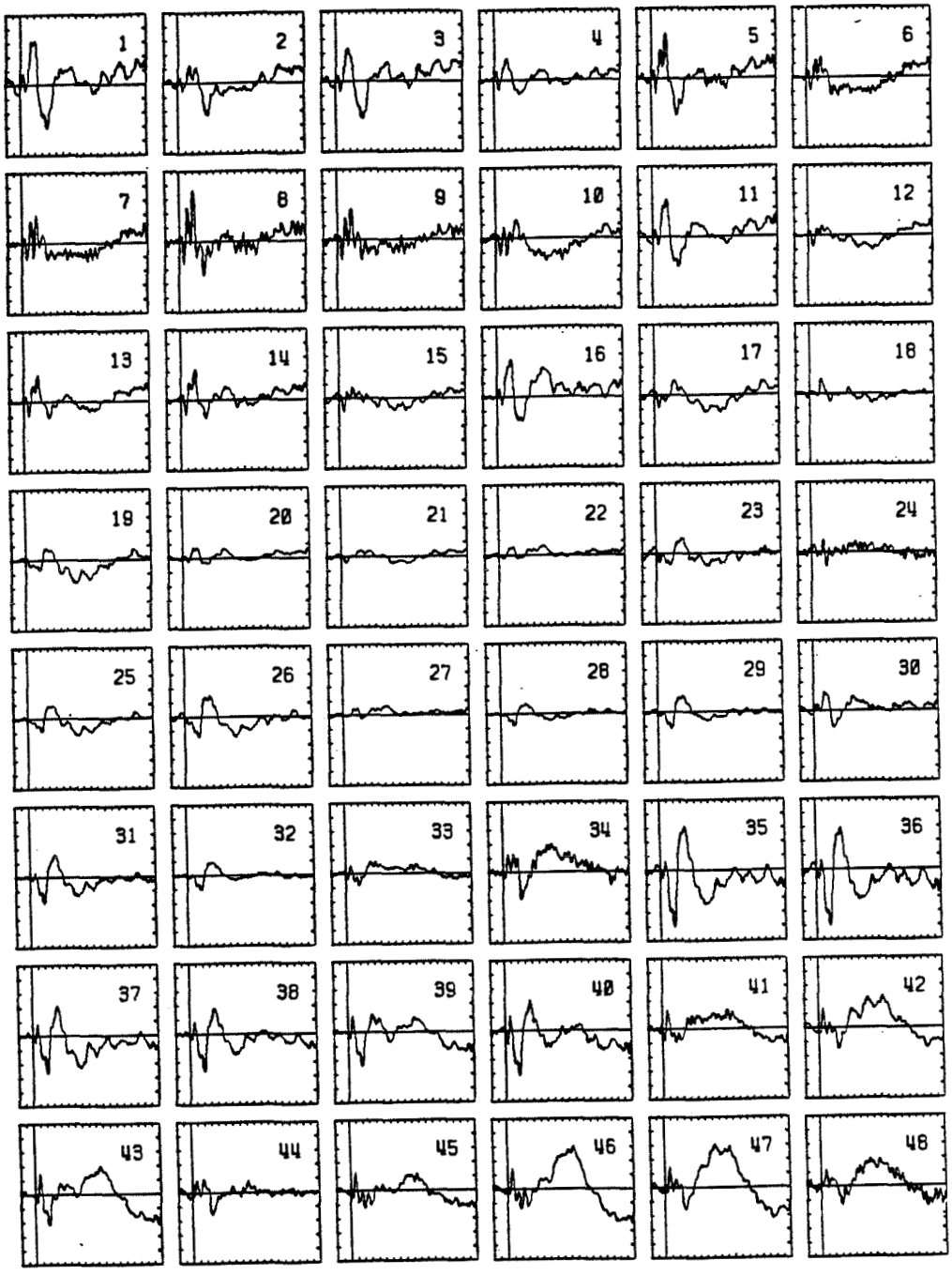

S3 FREQ aEPs

horizontal scale: 51 ms/div, vertical scale: 1.0 uV/div

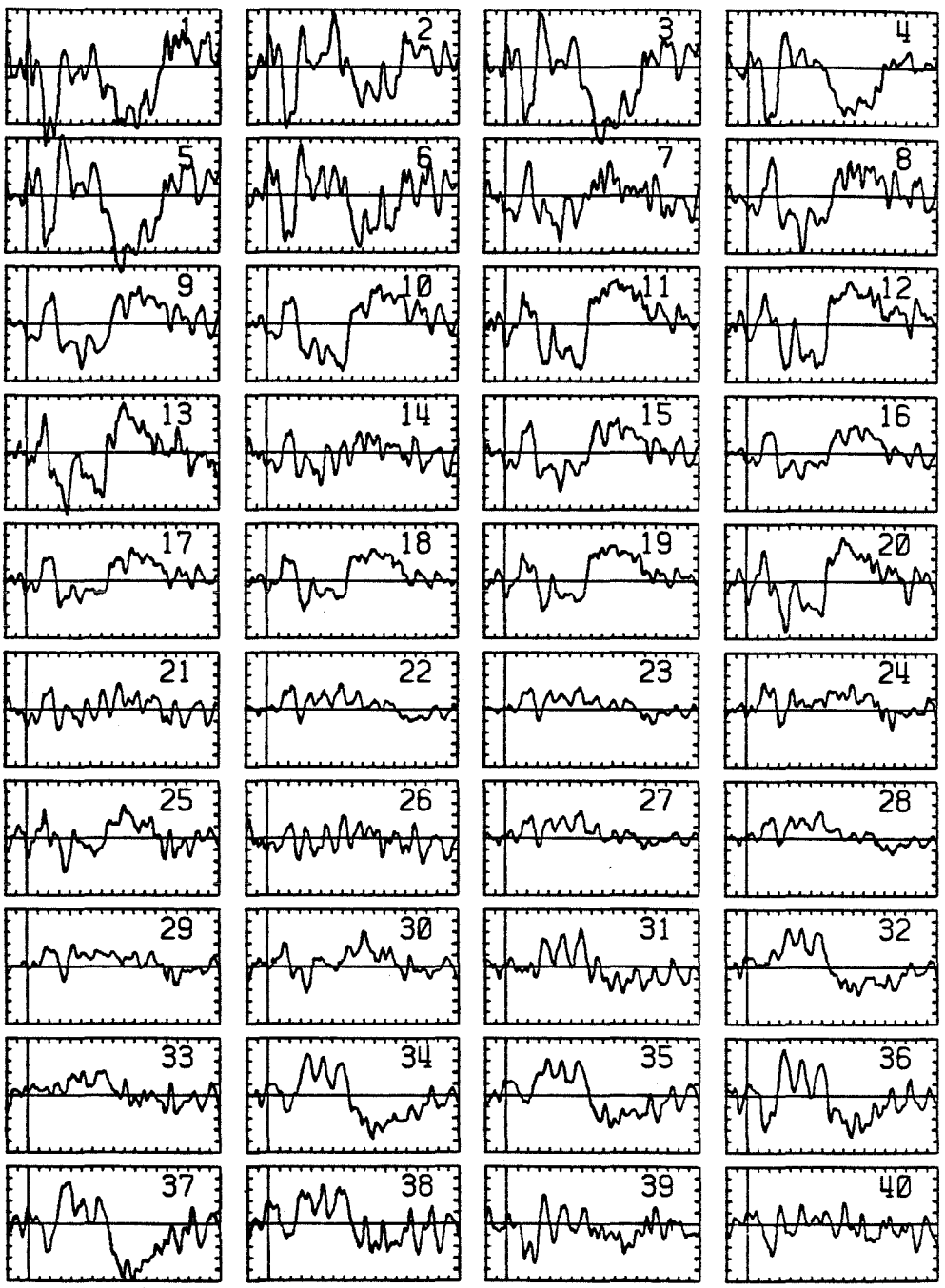

S1 RARE aEPs

horizontal scale: 51 ms/div, vertical scale: 1.0 uV/div

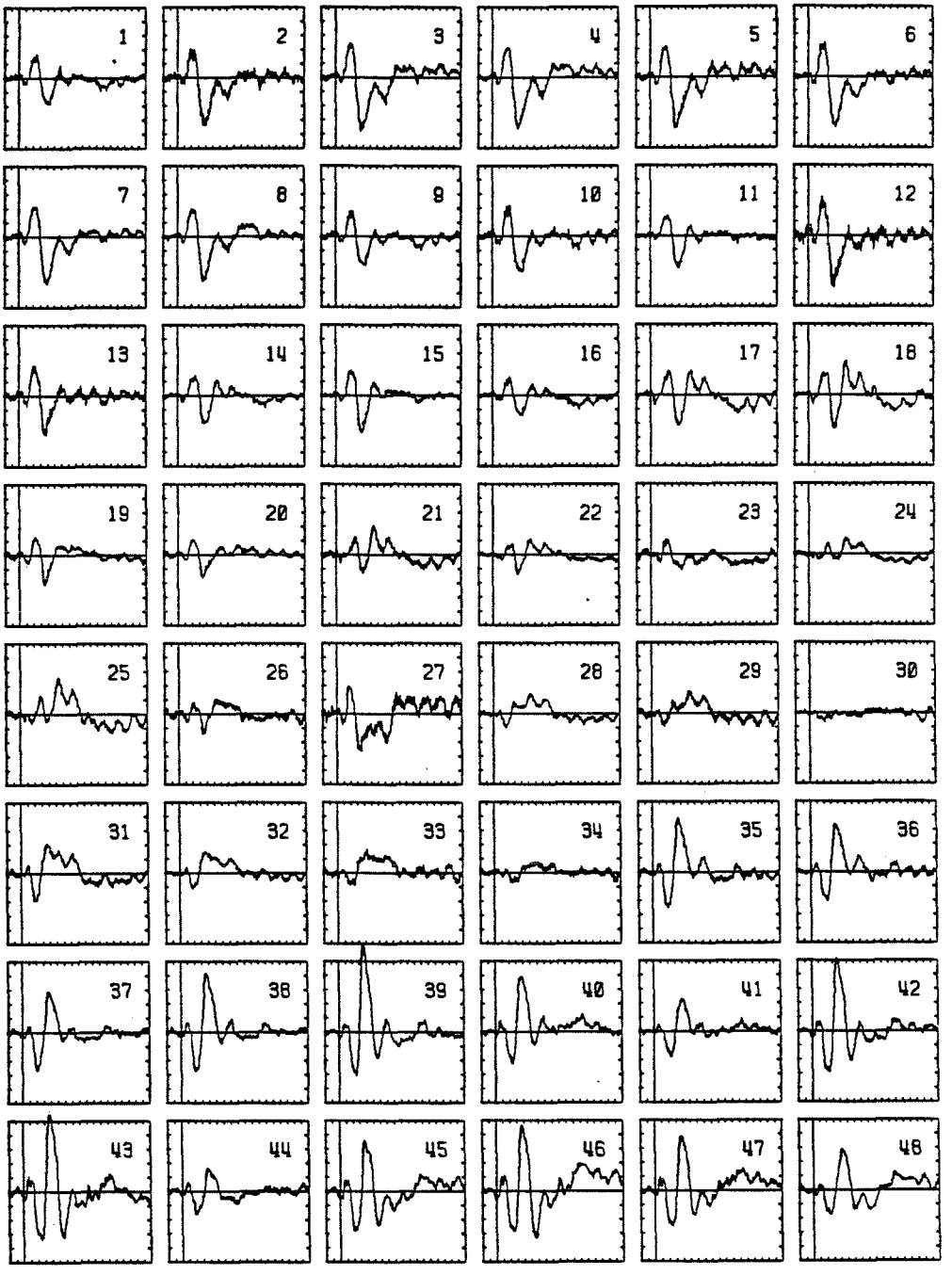

S2 RARE aEPs

horizontal scale: 51 ms/div, vertical scale: 2.0 uV/div

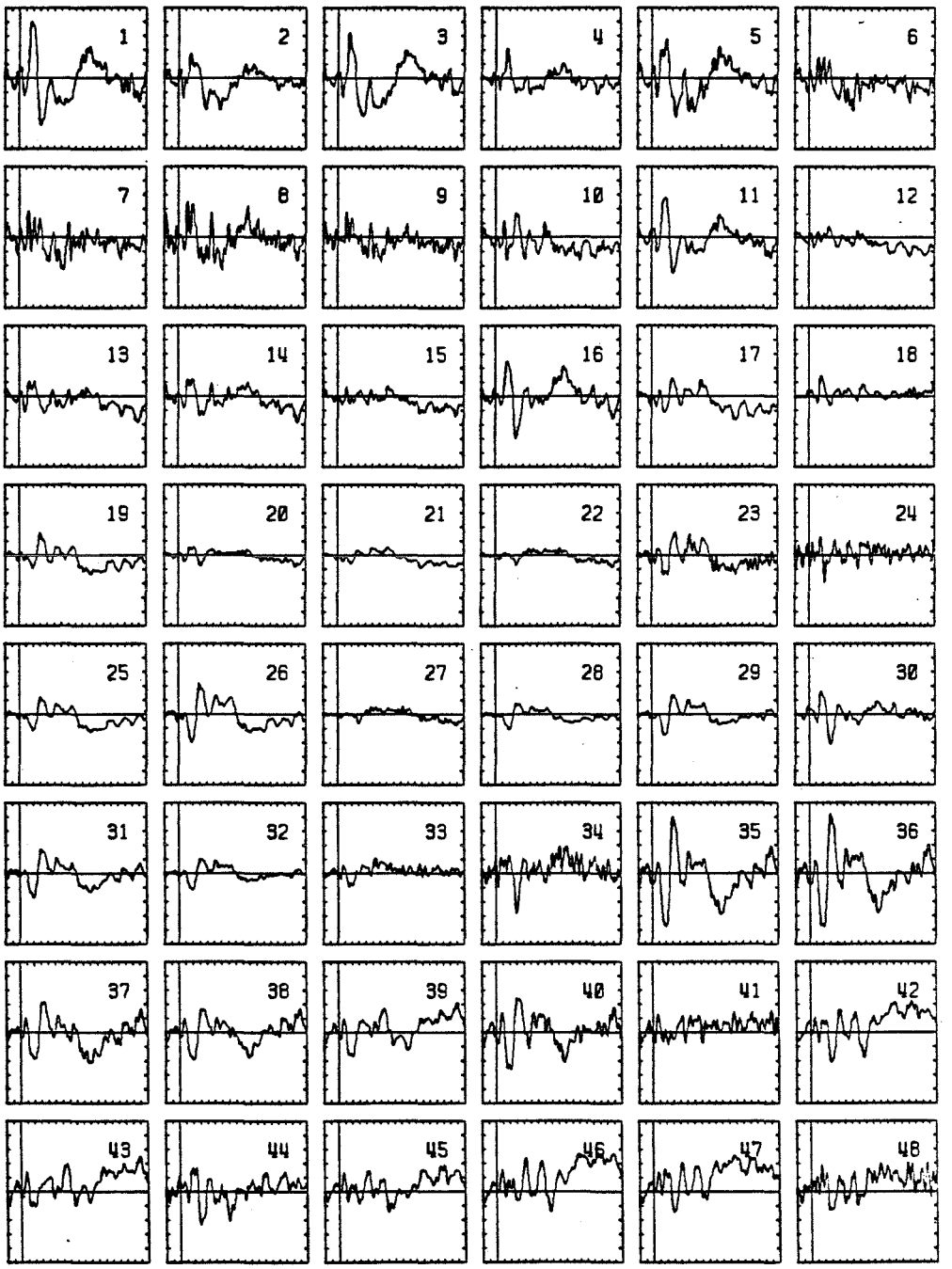

S3 RARE aEPs

horizontal scale: 51 ms/div, vertical scale: 1.0 uV/div

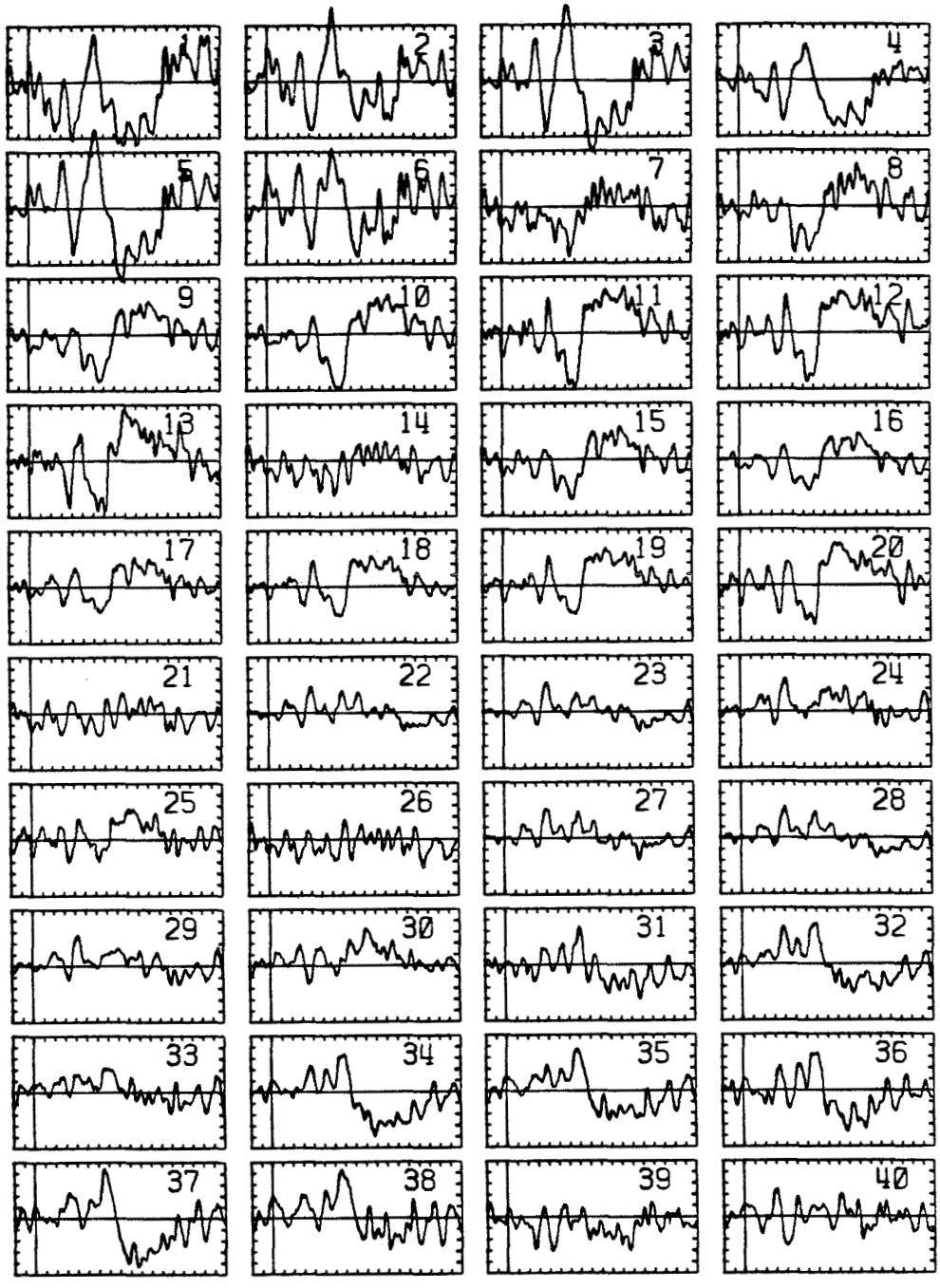

S1 DIFF aEPs

horizontal scale: 51 ms/div, vertical scale: 1.0 uV/div

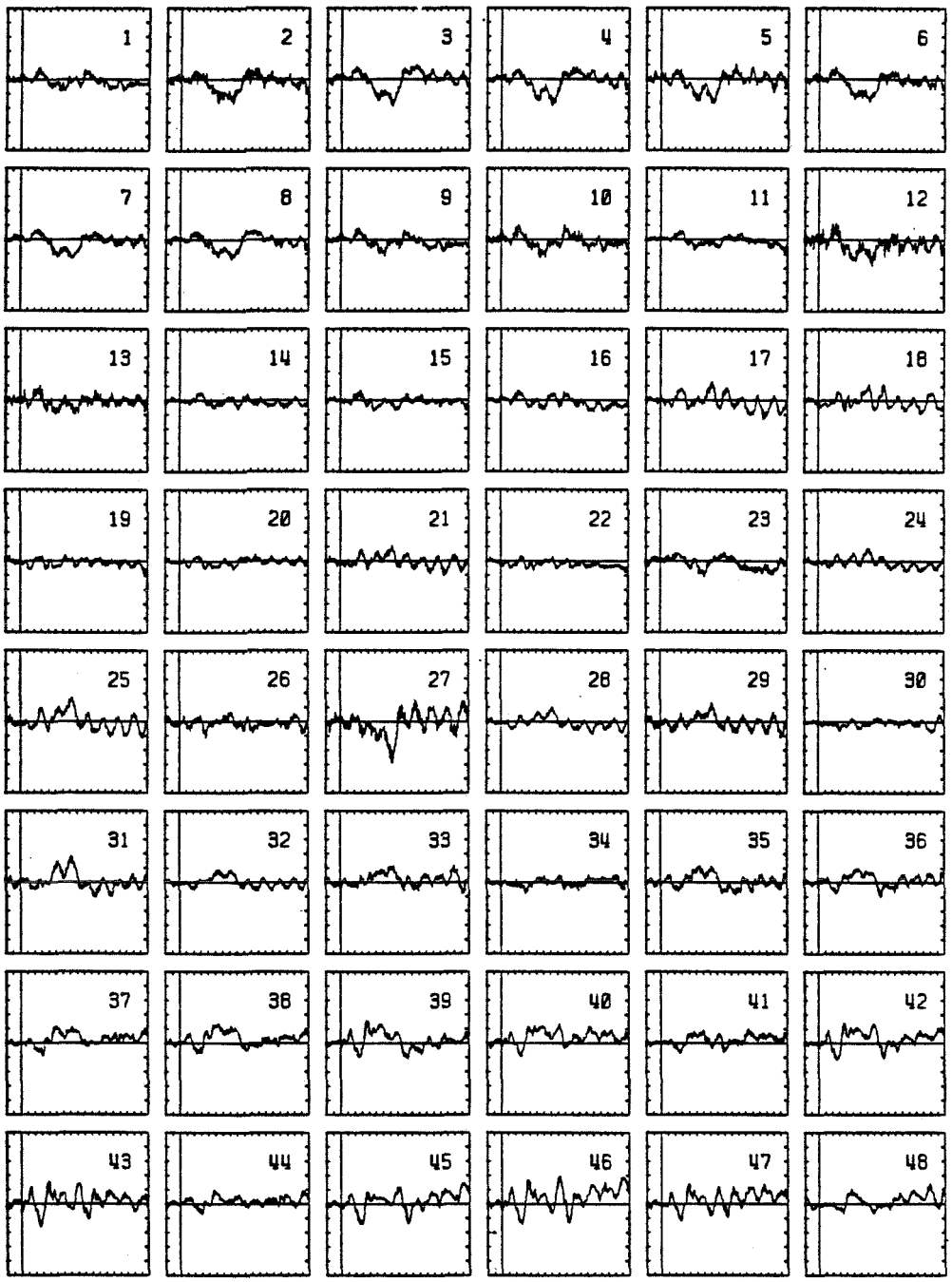

S2 DIFF aEPs

horizontal scale: 51 ms/div, vertical scale: 2.0 uV/div

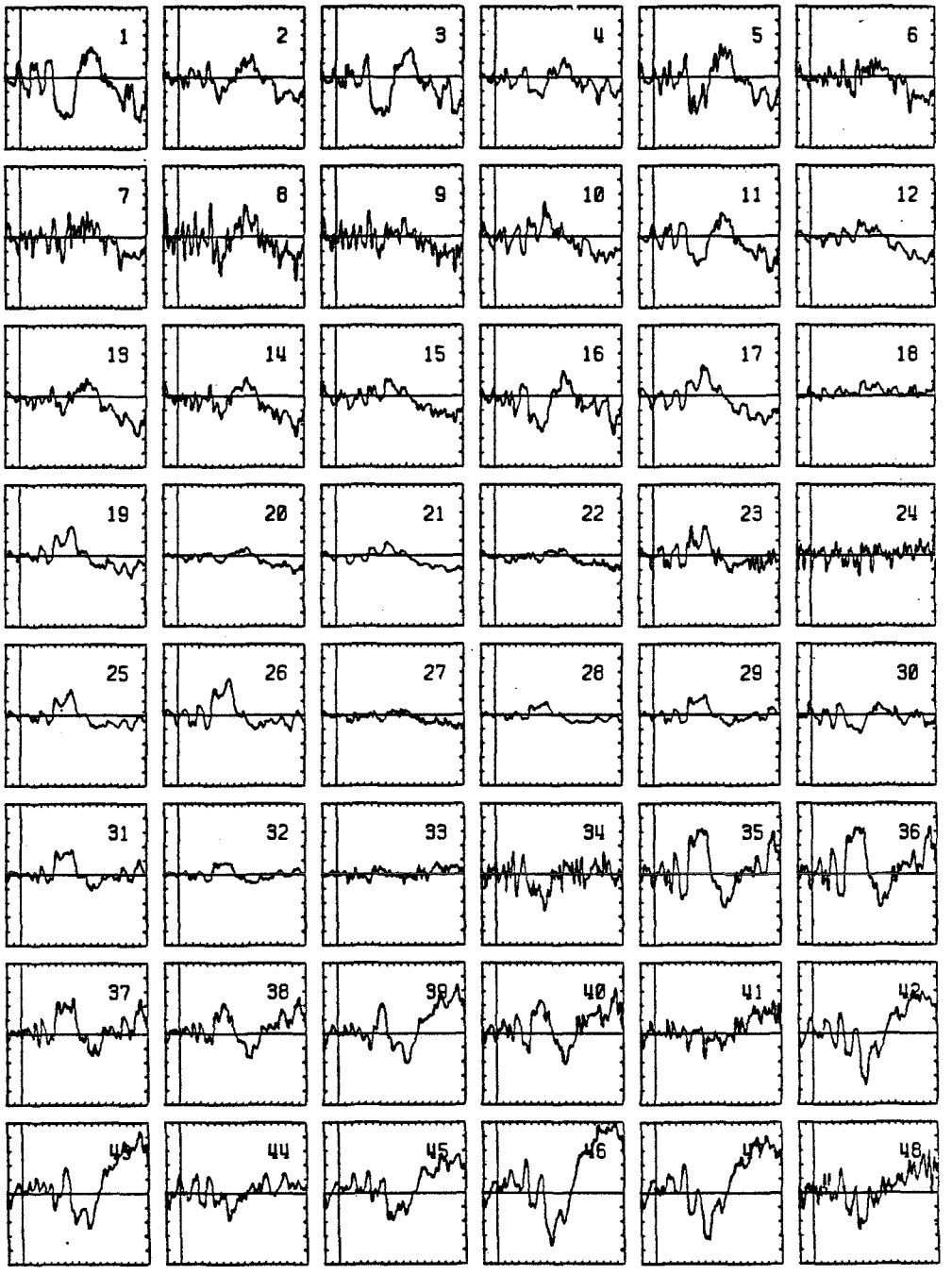

S3 DIFF aEPs

horizontal scale: 51 ms/div, vertical scale: 1.0 uV/div